Supporting Information

Water-Based Dynamic Depsipeptide Chemistry: Building Block Recycling and Oligomer Distribution Control Using Hydration-Dehydration Cycles

Martin C[‡†‡], Moran Frenkel-Pinter[‡†‡], Kelvin H. Smith[†§], Victor F. Rivera-Santana[#], Alyssa B. Sargon[†§], Kaitlin C. Jacobson[†§], Aikomari Guzman-Martinez[#], Loren Dean Williams[†‡], Luke J. Leman[†⊥], Charles L. Liotta[†‡], Martha A. Grover[†§] and Nicholas V. Hud[†‡*]

‡ Authors contributed equally

† NSF/ NASA Center for Chemical Evolution, Atlanta, Georgia 30332, United States

‡ School of Chemistry & Biochemistry, Georgia Institute of Technology, Atlanta, GA 30332, United States

§ School of Chemical & Biomolecular Engineering, Georgia Institute of Technology, Atlanta, GA 30332, United States

Department of Chemistry, University of Puerto Rico, Mayagüez, Puerto Rico 00681, United States

⊥ Department of Chemistry, The Scripps Research Institute, La Jolla, CA 92037, United States

* Corresponding Author. Contact: hud@chemistry.gatech.edu

Table of Contents

Synthetic Procedures and Analytical Methods

Materials

All reagents were purchased from Sigma Aldrich, unless otherwise stated, and were used as received. Stock solutions of building blocks were prepared using 0.2 μm filtered HPLC-grade water (VWR). Each individual building block was water-soluble up to *at least* 100 mM. All building blocks were utilized within their linear response concentration ranges for HPLC-UV integration applications. Stock solutions of buffers or additives for pH adjustment were prepared using HPLC-grade water (VWR). All dry-heating and aqueous incubation experiments were diluted to the necessary volumes and concentrations using water purified through a Milli-Q doubly distilled water system.

Base-catalyzed synthesis of dimeric *N*-(α-hydroxyacyl)-amino acid building blocks

Synthesis of each building block follows closely a previously described synthesis of *N*-(α-hydroxyacyl)-amino acids (Scheme S1).[1] For the synthesis of **gG**, **gA**, **aG**, **aA**, **gβA**, **aβA**, **gD**, **aD**, **gE**, **aE**, **dG**, **dA**, **gS**, **aS**, **fD** and **fE**, 2 mmol of methyl glycolate (for '**g**'), methyl-L-lactate (for '**a**') or methyl-L-phenyllactate (for '**f**') were mixed with 2 mmol of the amino acid ($\mathbf{X_{AA}}$) (L-stereochemistry unless otherwise noted) in 500 μL of 1,1,3,3-tetramethylguanidine and 100 μL of methanol for solvation. Similarly, building blocks with malic acid (for '**d**') were prepared using 2 mmol of (*S*)-(+)-2,2-Dimethyl-5-oxo-1,3-dioxolane-4-acetic acid (for selective coupling to the α carbonyl) plus 2 mmol of a given amino acid (Scheme S1). The solutions were stirred for 8 h at 100 °C. Crude reactions were reddish to brown in color and thick in consistency. Building blocks with ionizable side chains (*i.e.* **d**, **D**, **E**) were first purified by passage through an anion exchange column packed with 25 g of QAE Sephadex A-25 resin (GE Healthcare) with a pH 5 ammonium formate elution buffer running a gradient from 50 to 500 mM. All crude building block products were then passed through a cation exchange column packed with 15 g of Dowex 50WX8 hydrogen form (Sigma-Aldrich) charged with 0.1% formic acid solution to remove excess base. Next, products were passed through a Teledyne Isco Combiflash-Rf$^+$ flash chromatography system using a RediSep C18aq 150 g Gold column. The final round of purification involved use of a semi-preparative HPLC system. Parameters were: Waters X-Bridge BEH C18 OBD Prep Column. 5 μm xB-C_{18}130Å, 250x10mm LC column. 1 mL Injection into prewashed 1 mL loop. Solvents: **A)** 0.1% formic acid in LCMS grade water, **B)** LCMS grade acetonitrile. Flow rate: 6.60 mL/min. Gradient: 2.5 min hold 100% A, 0% B; 13 min ramp to 45% A, 55% B; 1.5 min ramp to 0% A, 100% B; 2 min hold 0% A, 100% B, 0% B; 1 min ramp to 100% A, 0 % B; 5 min hold 100% A, 0% B. Identification of the desired product was verified with ESI-MS, followed by ^{1}H and ^{13}C-NMR spectroscopy.

*Synthesis of **gX**$_{AA}$, **aX**$_{AA}$, and **fX**$_{AA}$ molecules*

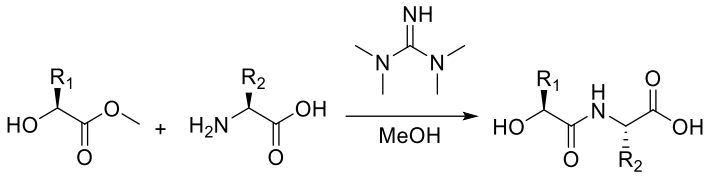

R_1 = hydroxy acid side chain, R_2 = Amino acid side chain

*Synthesis of **dX**$_{AA}$ molecules*

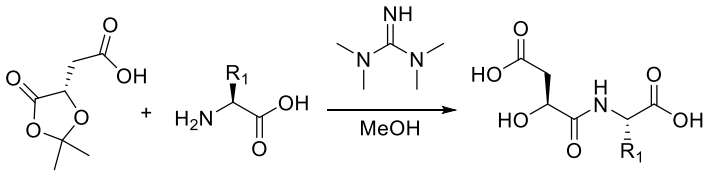

R_1 = Amino acid side chain

Scheme S1: Synthetic Scheme for Various Building Blocks Employed.

Spectral Characterization of Synthetic Building Blocks

gG - (99.0% purity) ^{1}H-NMR (700 MHz, DMSO-*d*6): δ = 7.83 (*t*, 1H, 5.1 Hz), 5.64 (br *s*, 1H), 3.83 (*s*, 2H), 3.68 (*s*, 2H, 5.5 Hz), -COOH ^{1}H resonance not observed. ^{13}C-NMR (176 MHz, DMSO-*d*6): δ = 173.54, 172.47, 63.13, 42.84. ESI-MS (m/z): calc'd for $C_4H_7NO_4$ $[M-H]^-$, 132.04, Obs'd, 132.0

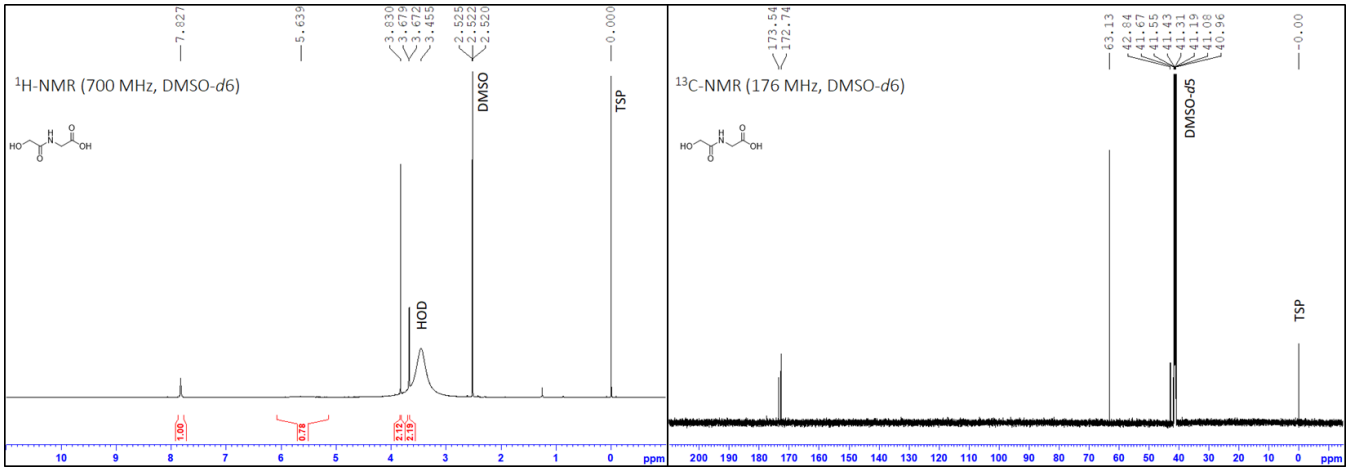

gA - (97.6% purity) ^{1}H-NMR (700 MHz, DMSO-*d*6): δ = 7.82 (*d*, 1H, 6.8 Hz), 5.59 (br *s*, 1H), 4.09 (*dq*, 1H, 7.1 Hz), 3.80 (*dd*, 2H, 19.0 Hz), 1.26 (*d*, 3H, 7.1 Hz), -COOH ^{1}H resonance not observed. ^{13}C-NMR (176 MHz, DMSO-*d*6): δ = 175.67, 172.84, 63.14, 49.55, 19.99. HRMS m/z: Calc. for $C_5H_9NO_4$: 147.0536, found 147.0519

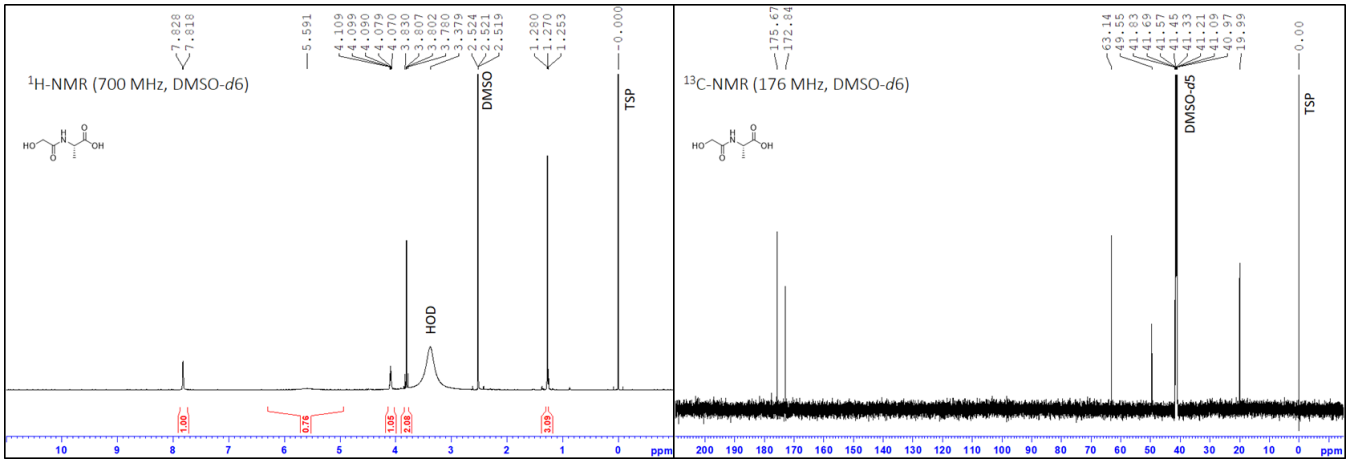

aG – (99.5% purity) ^{1}H-NMR (700 MHz, DMSO-*d*6): δ = 7.79 (*t*, 1H, 4.7 Hz), 5.62 (br *s*, 1H), 3.99 (*q*, 1H, 6.8 Hz), 3.65 (*m*, 2H), 1.22 (*d*, 3H, 6.8 Hz), -COOH ^{1}H resonance not observed. ^{13}C-NMR (176 MHz, DMSO-*d*6): δ = 176.18, 172.76, 68.96, 42.99, 22.83. ESI-MS (m/z): calc'd for $C_5H_9NO_4$ $[M-H]^-$, 146.05, Obs'd, 146.1

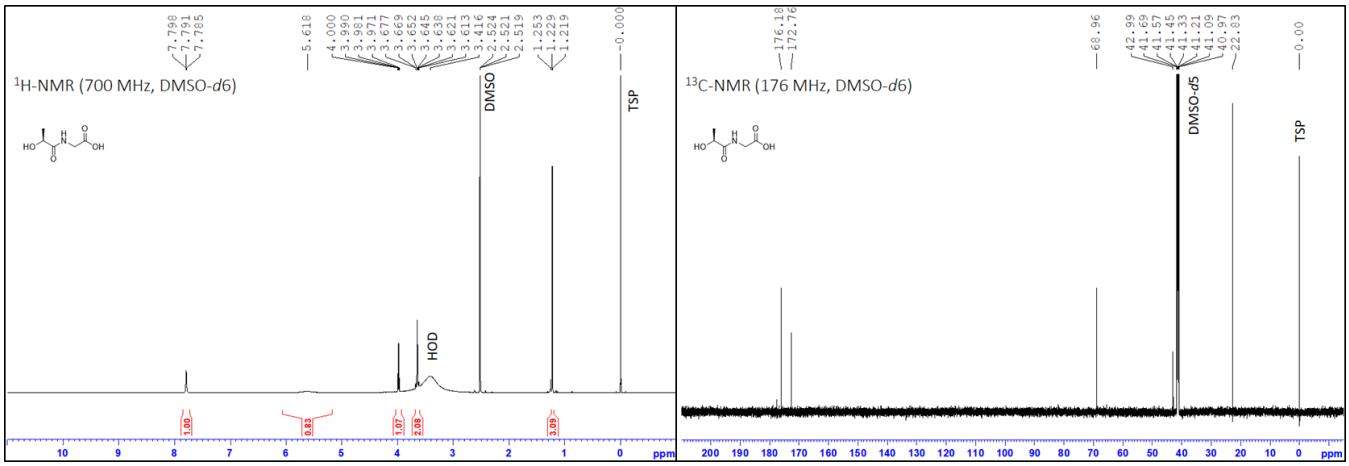

aA – (95.2% purity) ^{1}H-NMR (700 MHz, DMSO-*d*6): δ = 7.79 (*d*, 1H, 7.0 Hz), 5.59 (br *s*, 1H), 4.07 (*dq*, 1H, 6.9 Hz), 3.96 (*q*, 1H, 6.9 Hz), 1.27 (*d*, 3H, 7.1 Hz), 1.22 (*d*, 3H, 6.8 Hz). -COOH ^{1}H resonance not observed. ^{13}C-NMR (176 MHz, DMSO-*d*6): δ = 175.76, 175.58, 68.93, 49.53, 22.86, 19.92. ESI-MS (m/z): calc'd for $C_6H_{11}NO_4$ [M-H]$^-$, 160.07, Obs'd, 160.1

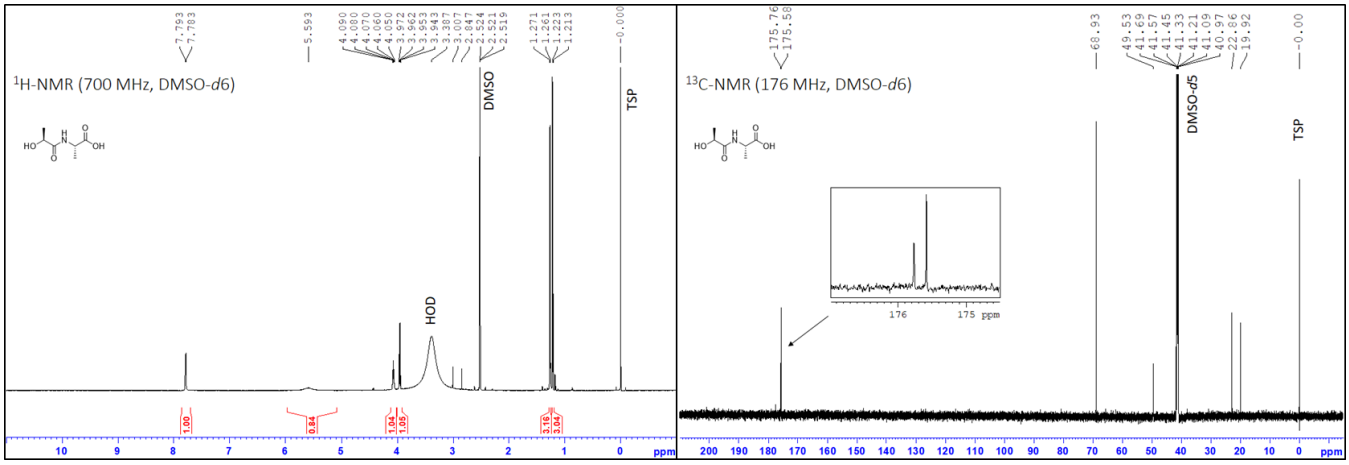

gβA – (99.5% purity) ^{1}H-NMR (700 MHz, DMSO-*d*6): δ = 7.80 (br *t*, 1H, 5.2 Hz), 3.78 (*s*, 2H), 3.29 (*q*, 2H, 6.6 Hz), 2.34 (*t* app, 2H, 6.8 Hz), -COOH ^{1}H resonance not observed. ^{13}C-NMR (176 MHz, DMSO-*d*6): δ = 175.28, 173.34, 63.19, 36.51, 36.30. ESI-MS (m/z): calc'd for $C_5H_9NO_4$ [M-H]$^-$, 146.05, Obs'd, 146.1

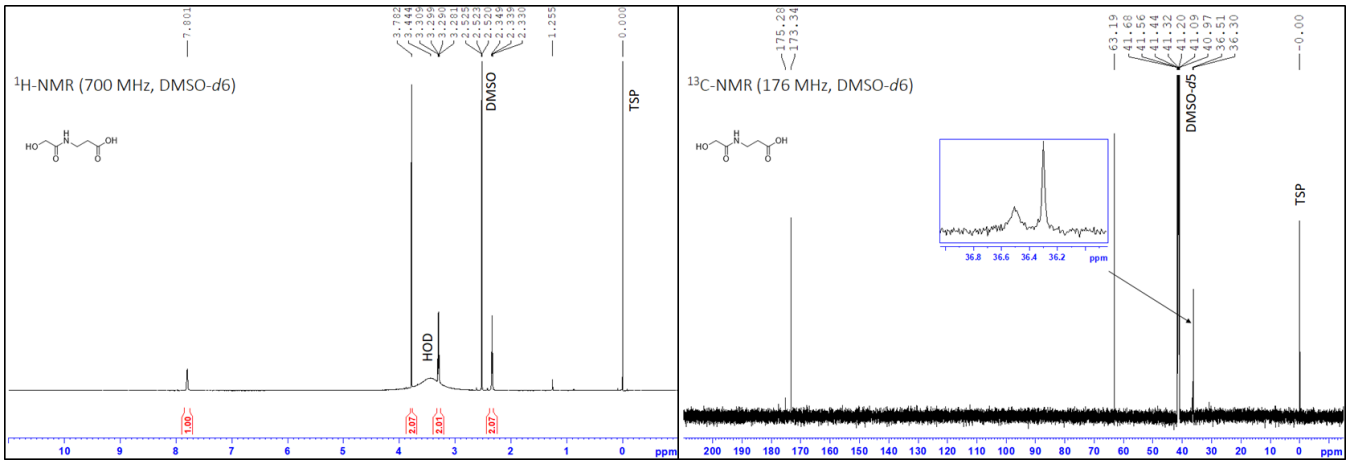

aβA – (98.4% purity) ^{1}H-NMR (700 MHz, DMSO-*d*6): δ = 7.77 (br *t*, 1H, 5.1 Hz), 5.50 (br *s*, 1H), 3.94 (*q*, 1H, 6.8 Hz), 3.26 (*m*, 2H), 2.32 (*t* app, 2H, 6.74 Hz), 1.20 (*d*, 3H, 6.8 Hz), -COOH ^{1}H resonance not observed. ^{13}C-NMR (176 MHz, DMSO-*d*6): δ = 176.02, 175.30, 69.00, 36.52, 36.42, 22.83. ESI-MS (m/z): calc'd for $C_6H_{11}NO_4$ [M-H]$^-$, 160.07, Obs'd, 160.1

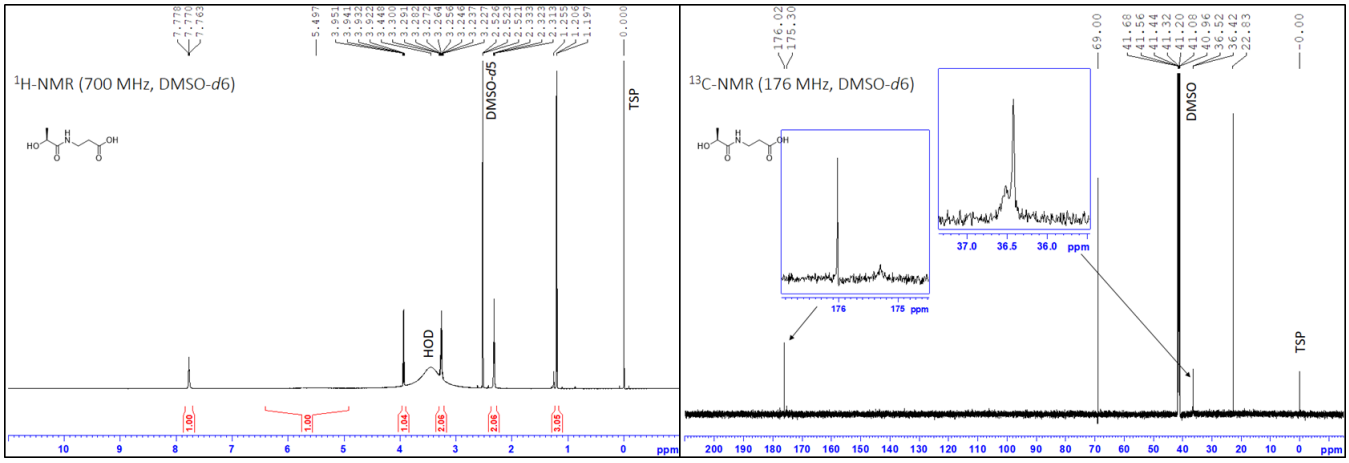

gD – (95.8% purity) ^{1}H-NMR (700 MHz, DMSO-*d*6): δ = 12.06 (br *s*, 1H), 7.86 (*d*, 1H, 5.7 Hz), 5.69 (*t*, 1H, 5.6 Hz), 4.37 (br *s*, 1H), 3.83 (*m*, 2H), 2.63 (br *m*, 2H), Not all -COOH ^{1}H resonances observed. ^{13}C-NMR (176 MHz, DMSO-*d*6): δ = 177.58, 174.02, 173.05, 63.07, 49.66, -CH_2- overlap with DMSO-*d*5 peaks. ESI-MS (m/z): calc'd for $C_6H_9NO_6$ [M-H]$^-$, 190.04, Obs'd, 190.0

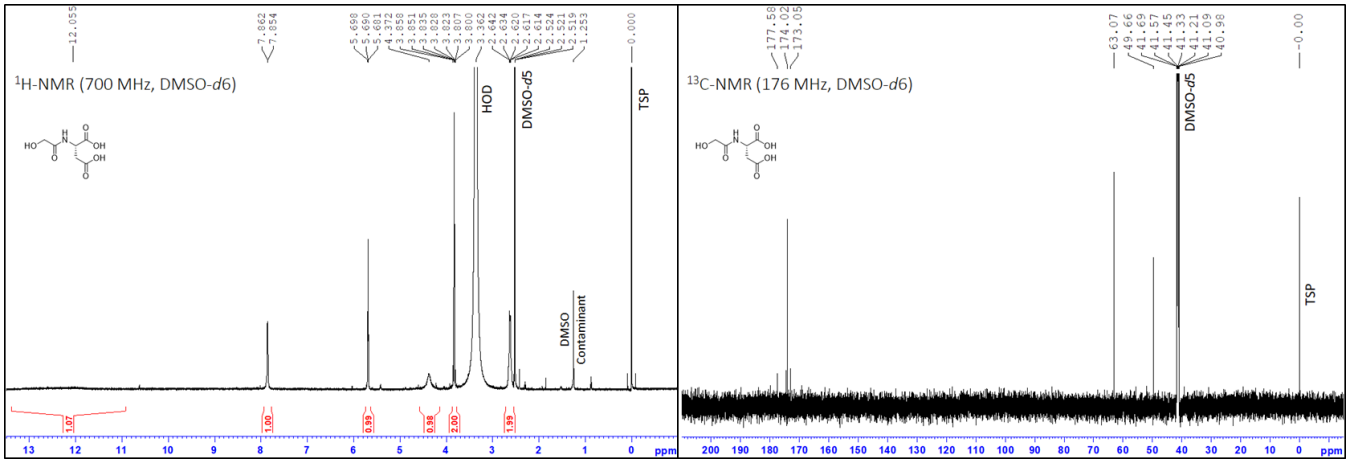

aD – (97.6% purity) ^{1}H-NMR (700 MHz, DMSO-*d*6): δ = 12.08 (br *s*, 1H, weak), 7.85 (*d*, 1H, 5.1 Hz), 5.70 (*d*, 1H, 5.0), 4.36 (br *s*, 1H), 3.98 (*quint* app, 1H, 6.5 Hz), 2.62 (br *m*, 2H), 1.22 (*d*, 3H, 6.8 Hz), Not all -COOH ^{1}H resonances observed. ^{13}C-NMR (176 MHz, DMSO-*d*6): δ = 177.57, 175.78, 173.99, 68.94, 49.69, 30.86, 22.85. ESI-MS (m/z): calc'd for $C_7H_{11}NO_6$ [M-H]$^-$, 204.06, Obs'd, 204.1

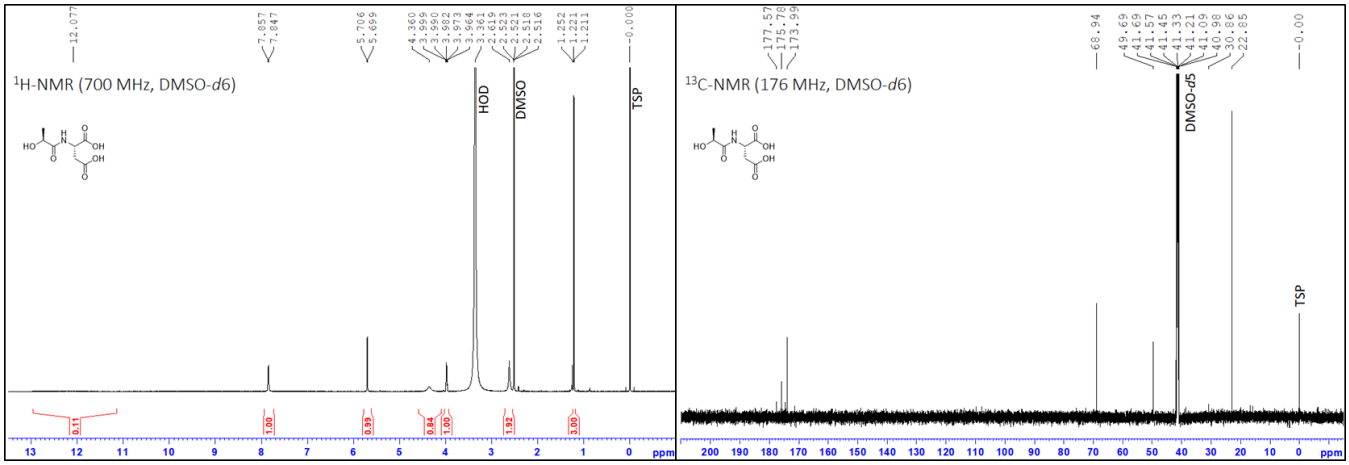

gE – (97.4% purity) ^{1}H-NMR (700 MHz, DMSO-*d*6): δ = 12.20 (br *s*, 1H, weak), 7.77 (*d*, 1H, 7.4 Hz), 5.60 (br *m*, 1H), 4.18 (*q*, 1H, 7.3), 3.82 (*m*, 2H, 15.9 & 24.1 Hz), 2.31 (*m*, 1H, 8.1 & 7.2 Hz), 2.21 (*m*, 1H, 6.8 & 8.4 Hz), 1.93 (*m*, 1H, 7.7 & 6.0), 1.82 (br *s* app, 1H), Not all -COOH ^{1}H resonances observed. ^{13}C-NMR (176 MHz, DMSO-*d*6): δ = 175.91, 174.76, 173.09, 63.12, 52.95, 33.12, 29.26. ESI-MS (m/z): calc'd for $C_7H_{11}NO_6$ [M-H]$^-$, 204.06, Obs'd, 204.1

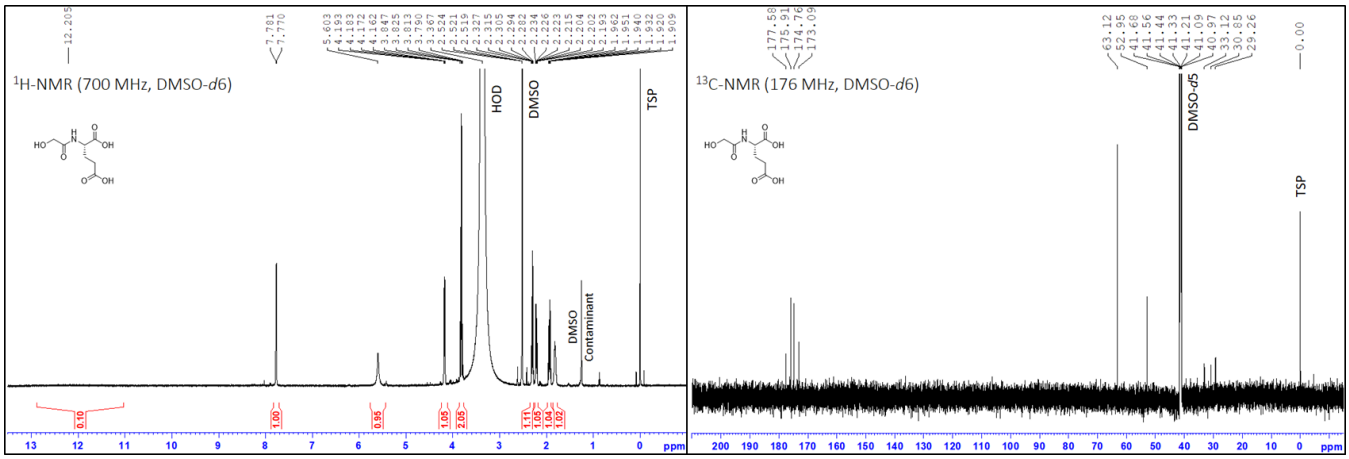

aE – (96.6% purity) ^{1}H-NMR (700 MHz, DMSO-*d*6): δ = 7.75 (*d*, 1H, 7.4 Hz), 5.61 (br *s*, 1H), 4.15 (*q*, 1H, 7.4 Hz), 3.96 (q, 1H, 6.7 Hz), 2.29 (*m*, 1H, 7.7 & 8.1 Hz), 2.21 (*m*, 1H, 6.1 & 7.7 Hz), 1.91 (*m*, 1H, 7.7 & 6.2 Hz), 1.83 (br *m*, 1H), 1.22 (*d*, 3H, 6.8 Hz), Not all -COOH ^{1}H resonances observed. ^{13}C-NMR (176 MHz, DMSO-*d*6): δ = 175.88, 175.86, 174.84, 69.01, 52.93, 33.00, 29.19, 22.96. ESI-MS (m/z): calc'd for $C_8H_{13}NO_6$ [M-H]$^-$, 218.07, Obs'd, 218.1

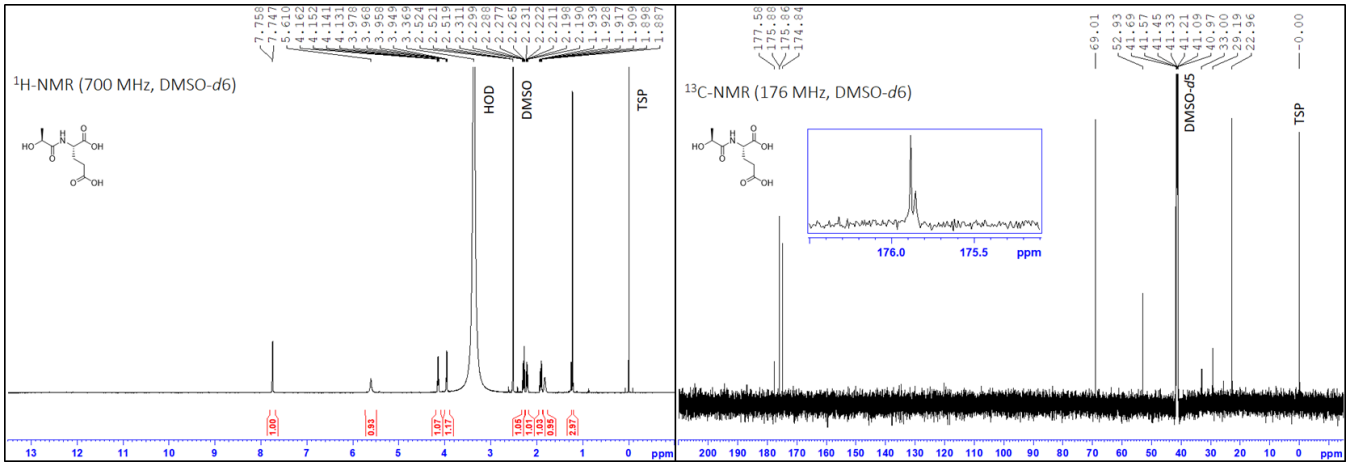

dG – (95.2% purity) ^{1}H-NMR (700 MHz, DMSO-*d*6): δ = 7.91 (*t*, 1H, 5.3 Hz), 4.24 (*dd*, 1H, 3.5 & 9.2 Hz), 3.65 (*m*, 2H, 5.4 & 17.5 & 25.5 Hz), 2.64 (*dd*, 1H, 3.5 & 15.6 Hz), 2.30 (*dd*, 1H, 8.4 & 15.6 Hz). -OH and -COOH ^{1}H resonances not observed. ^{13}C-NMR (176 MHz, DMSO-*d*6): δ = 174.75, 174.24, 172.66, 70.23, 43.12, 41.73, -CH_2- overlap with DMSO-*d*5 peaks. ESI-MS (m/z): calc'd for $C_6H_9NO_6$ [M-H]$^-$, 190.04, Obs'd, 190.0

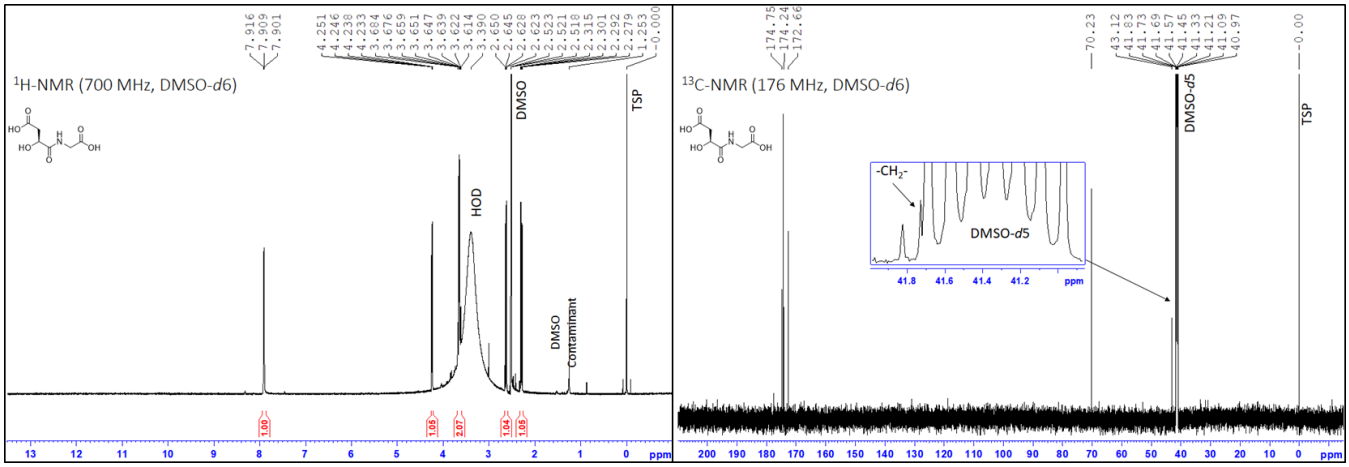

dA – (99.5% purity) ^{1}H-NMR (700 MHz, DMSO-*d*6): δ = 7.89 (*d*, 1H, 7.0 Hz), 4.21 (*dd*, 1H, 3.3 & 9.0 Hz), 4.07 (*dq*, 1H, 7.1 Hz), 2.62 (*dd*, 1H, 3.6 & 15.5 Hz), 2.31 (*dd*, 1H, 8.7 & 15.5 Hz), 1.26 (*d*, 3H, 7.1 Hz), -OH and -COOH ^{1}H resonances not observed. ^{13}C-NMR (176 MHz, DMSO-*d*6): δ = 175.69, 174.17, 174.06, 70.19, 49.72, 41.83, 19.80, -CH_2- overlap with DMSO-*d*5 peaks. ESI-MS (m/z): calc'd for $C_7H_{11}NO_6$ $[M-H]^-$, 204.06, Obs'd, 204.0

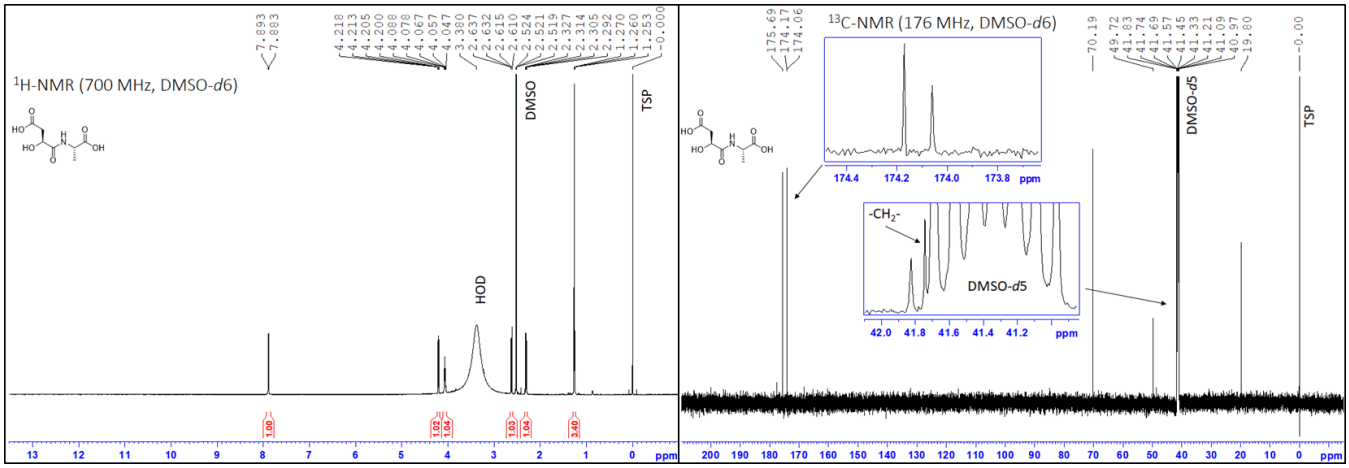

gS – (95.2% purity) ^{1}H-NMR (700 MHz, DMSO-*d*6): δ = 7.70 (*d*, 1H, 7.9 Hz), 7.14 (br *s*, 1H, weak), 5.73 (br *s*, 1H), 4.29 (*dt*, 1H, 4.0 & 7.9 Hz), 3.87 (br *s*, 2H), 3.80 (*dd*, 1H, 4.3 & 10.9 Hz), 3.65 (*dd*, 1H, 3.9 & 10.9 Hz), -COOH ^{1}H resonance not observed. ^{13}C-NMR (176 MHz, DMSO-*d*6): δ = 173.42, 173.17, 62.99, 62.85, 55.39. ESI-MS (m/z): calc'd for $C_5H_9NO_5$ $[M-H]^-$, 162.05, Obs'd, 162.0

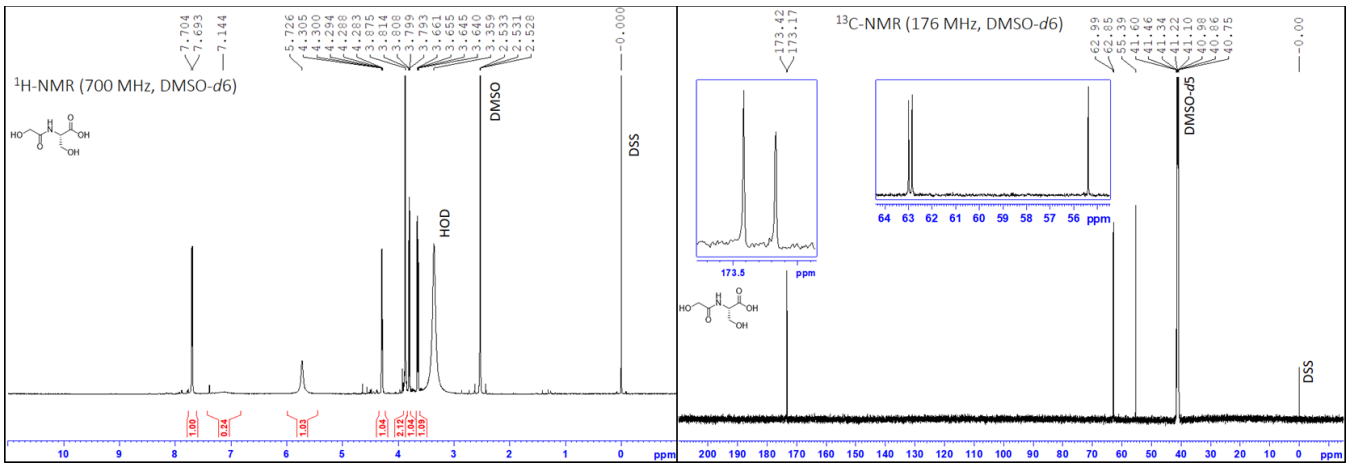

aS – (98.2% purity) ^{1}H-NMR (700 MHz, DMSO-*d*6): δ = 12.70 (br *s*, 1H, weak), 7.69 (*d*, 1H, 8.1 Hz), 5.75 (*d*, 1H, 5.0 Hz), 5.17 (br *s*, 1H, weak), 4.27 (*dt*, 1H, 3.8 & 4.0 Hz), 4.04 (*m*, 1H), 3.81 (*dd*, 1H, 4.0 & 11.0 Hz), 3.64 (*dd*, 1H, 3.8 & 11.0 Hz), 1.26 (*d*, 1H, 6.8 Hz). ^{13}C-NMR (176 MHz, DMSO-*d*6): δ = 175.85, 173.45, 68.68, 62.97, 55.42, 22.58. ESI-MS (m/z): calc'd for $C_6H_{11}NO_5$ [M-H]$^-$, 176.06, Obs'd, 176.1

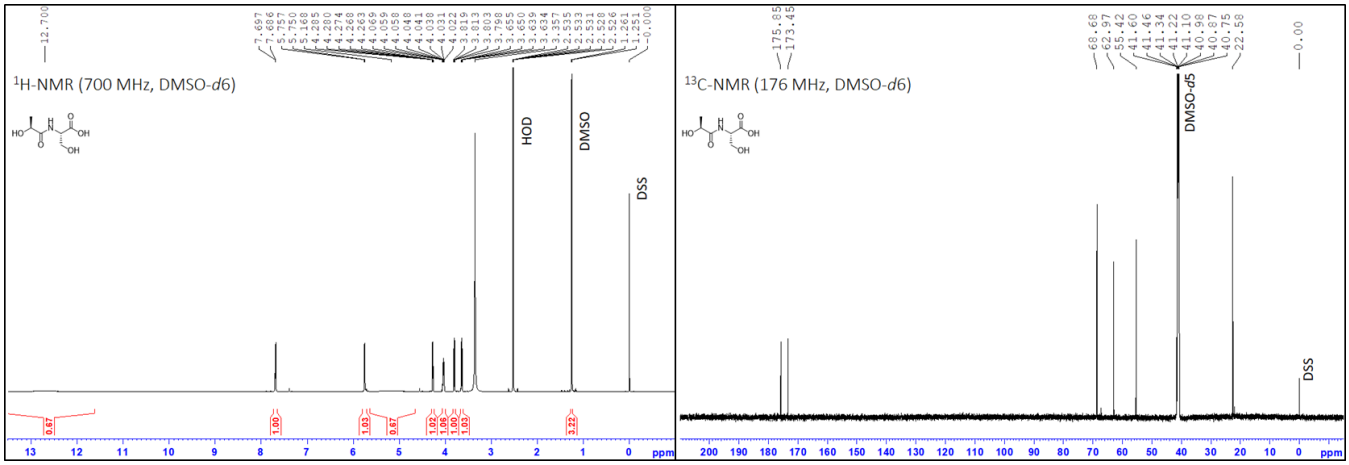

fD – (95.2% purity) ^{1}H-NMR (700 MHz, DMSO-*d*6): δ = 12.83 (br *s*, 1H), 12.45 (br *s*, 1H), 7.94 (*d*, 1H, 8.5), 7.31 – 7.18 (*m*, 5H), 5.81 (*d*, 1H, 5.85 Hz), 4.60 (*m*, 1H), 4.14 (*m*, 1H), 3.01 (*dd*, 1H, 3.5 & 13.9 Hz), 2.76 – 2.66 (*m*, 2H), 2.60 (*dd*, 1H, 5.5 & 16.9 Hz). ^{13}C-NMR (176 MHz, DMSO-*d*6): δ = 174.49, 173.84, 173.58, 139.93, 131.04, 129.49, 127.59, 73.42, 49.27, 41.91, 37.53. ESI-MS (m/z): calc'd for $C_{13}H_{15}NO_6$ [M-H]$^-$, 280.09, Obs'd, 280.1

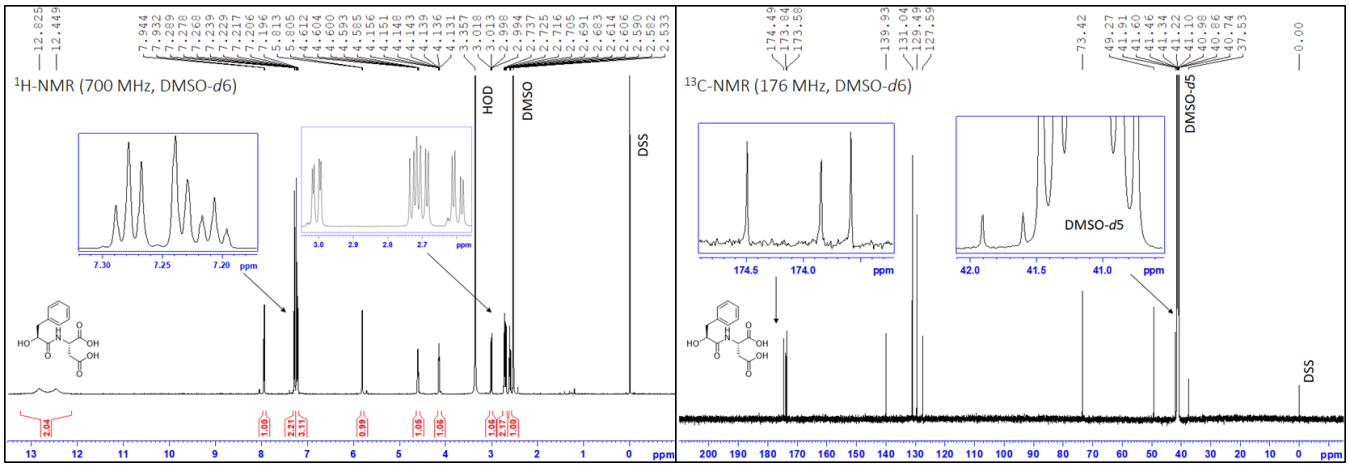

fE – (98.6% purity) ^{1}H-NMR (700 MHz, DMSO-*d*6): δ = 12.62 (br *s*, 1H), 12.32 (br *s*, 1H), 7.82 (*d*, 1H, 8.1 Hz), 7.31 – 7.18 (*m*, 5H), 5.70 (*d*, 1H, 6.1 Hz), 4.29 (*dt*, 1H, 3.9 & 4.8 Hz), 4.15 (*m*, 1H), 3.00 (*dd*, 1H, 3.7 & 13.8 Hz), 2.77 (*dd*, 1H, 8.0 & 13.8 Hz), 2.19 – 2.11 (*m*, 2H), 2.00 (*m*, 1H), 1.83 (*m*, 1H). ^{13}C-NMR (176 MHz, DMSO-*d*6): δ = 175.36, 174.85, 174.65, 139.93, 131.09, 129.48, 127.60, 73.52, 52.28, 41.91, 31.40, 27.93. ESI-MS (m/z): calc'd for $C_{14}H_{17}NO_6$ [M-H]$^-$, 294.1, Obs'd, 294.1

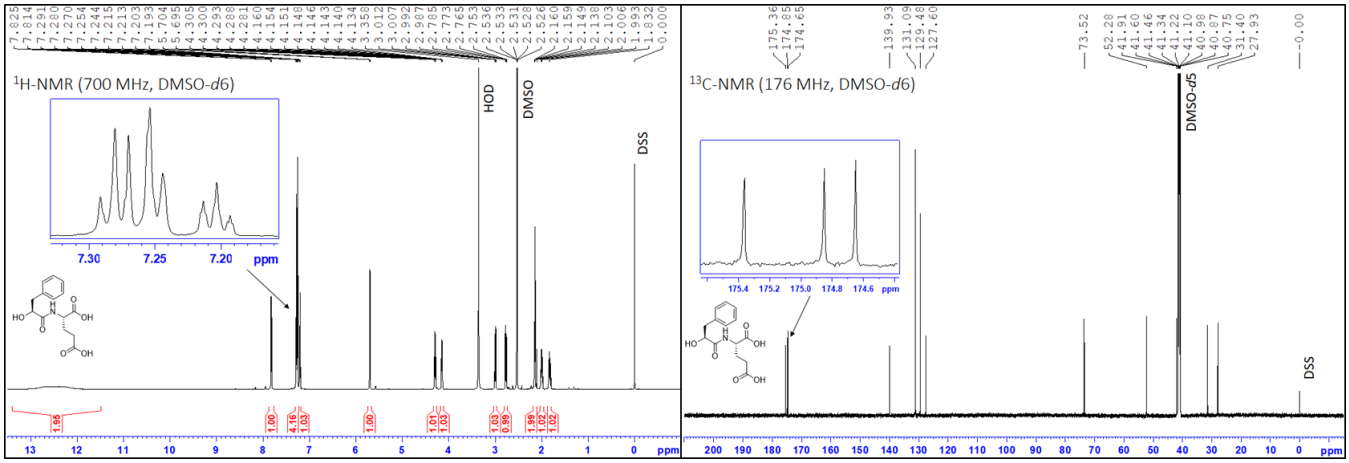

N-acyl-Peptide Synthesis

N-acyl peptides **gAG** and **gAGA**, were synthesized using solid phase peptide synthesis on Wang resin (Fisher Scientific) and employing the common Fmoc strategy. Fluorenylmethoxycarbonyl (Fmoc)-protected amino acid derivatives were purchased from Fisher Scientific. Briefly, following the first coupling to the appropriate resin with Fmoc-protected amino acid (5 eq.) in Dimethylformamide (DMF) in the presence of 10 eq. of N,N-Diisopropylethylamine (DIPEA) for 3 h, un-reacted resin was acetylated for 30 min using a solution of acetic anhydride (10 eq.) and DIPEA (20 eq.). Deprotection of the Fmoc was carried out in 30% piperidine in DMF for 10 min (2 times) and the process was repeated until all necessary amino acids were in place. For O-terminal glycolic acid, coupling with 2-(tert-butoxy)acetic acid (Enamine, EN300-104666) was performed in DMF in the presence of 10 eq. of DIPEA. The final products were released from the resin and acid-deprotected using a mixture of TFA: triethylsilane:H_2O (95 :2.5 :2.5 v/v) for 3 hours. Peptides were then purified by a Teledyne Isco CombiFlash Rf$^+$ flash chromatography system using a RediSep C18aq 150 g Gold column with a gradient of H2O and MeCN and purified peptides were analyzed by mass spectrometry. HRMS m/z: Calc. for $C_7H_{12}N_2O_5$ (**gAG**): 204.0750, found 204.0738. HRMS m/z: Calc. for $C_{10}H_{17}N_3O_6$ (**gAGA**): 275.1121, found 275.1118.

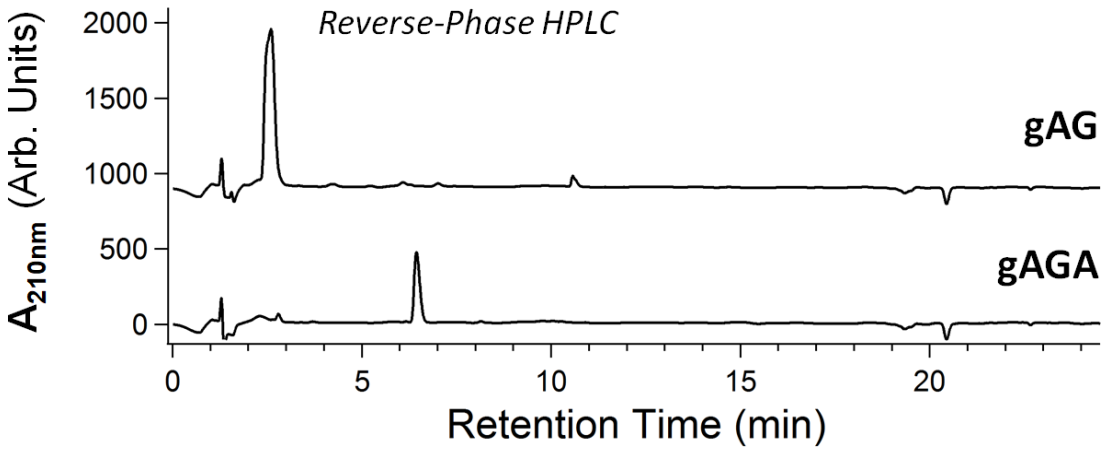

Synthesis of 3(S)-Methyl-2,5-morpholinedione (c(gA))

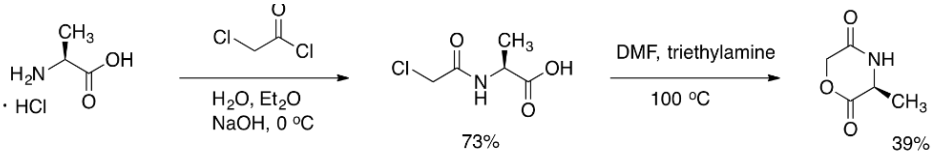

3(*S*)-Methyl-2,5-morpholinedione (**gA** morpholinedione, c(**gA**)) was prepared as described previously.[2] First, L-alanine (7.0 g, 78.6 mmol) was dissolved in 20 mL of aqueous NaOH (4 M). This solution was added to 30 mL of a 1:1 (v/v) mixture of water:diethyl ether. A solution of chloroacetyl chloride (10.0 g, 88.5 mmol) dissolved in 10 mL diethyl ether was prepared, and this was added dropwise to the amino acid solution at 0 °C over the course of 30 min, while NaOH (4 M) was simultaneously added dropwise to the mixture to keep the pH value at 11 throughout the reaction. After the addition of chloroacetyl chloride was complete and the pH stopped dropping, the mixture was allowed to warm to room temperature and stir for 1 h. The ether layer was discarded, and the aqueous layer was acidified to pH 1 and extracted with ethyl acetate (4 x 40 mL). The combined organic layers were washed with saturated NaCl solution and dried with $MgSO_4$. Evaporation of the solvent yielded N-(chloroacetyl)-L-alanine as a white crystalline solid (9.52 g, 73%). This material was used in the next step without further purification. ^{1}H-NMR (500 MHz, DMSO-d6): δ = 1.29 (d, 3H, CH_3), 4.09 (s, 2H, CH_2-Cl), 4.22 (m, 1H, NHCHCO), 8.52 (br d, 1H, NH), 12.70 (s, 1H, COOH). ^{13}C-NMR (125 MHz, DMSO-d6): δ = 17.56, 42.80, 48.31, 166.08, 174.10. ESI-MS (m/z): calcd for $C_4H_7ClNO_3$ (M^+ H^+): 166.03, found 166.0.

The 3(*S*)-methyl-2,5-morpholinedione was prepared by dissolving N-(chloroacetyl)-L-alanine (9.0 g, 54.4 mmol) and triethylamine (5.6 g, 55.0 mmol) in 200 mL of N,N-dimethylformamide (DMF). The solution was stirred at 100 °C for 6 h under nitrogen. The resulting brown mixture was allowed to stand overnight at 4 °C. After removing the crystallized triethylammonium chloride salt, the DMF was evaporated to yield a brown oil. Chloroform (50 mL) was added to the oil, resulting in precipitation of the crude morpholinedione, which was purified by recrystallizing from ethyl acetate. Yield 2.7 g (39%) colorless crystals. ^{1}H-NMR (400 MHz, DMSO-d6): δ = 1.33 (d, 3H, CH_3), 4.29 (m, ^{1}H, NHCHCO), 4.60–4.88 (dd, 2H, OCH_2CO), 8.53 (br s, ^{1}H, NH). 13C NMR (125 MHz, DMSO-d6): δ = 17.36, 48.38, 68.37, 166.67, 169.85. High resolution ESI-MS (m/z): calcd for $C_5H_7O_3N$ (M^+ H^+): 130.0499, found 130.0495.

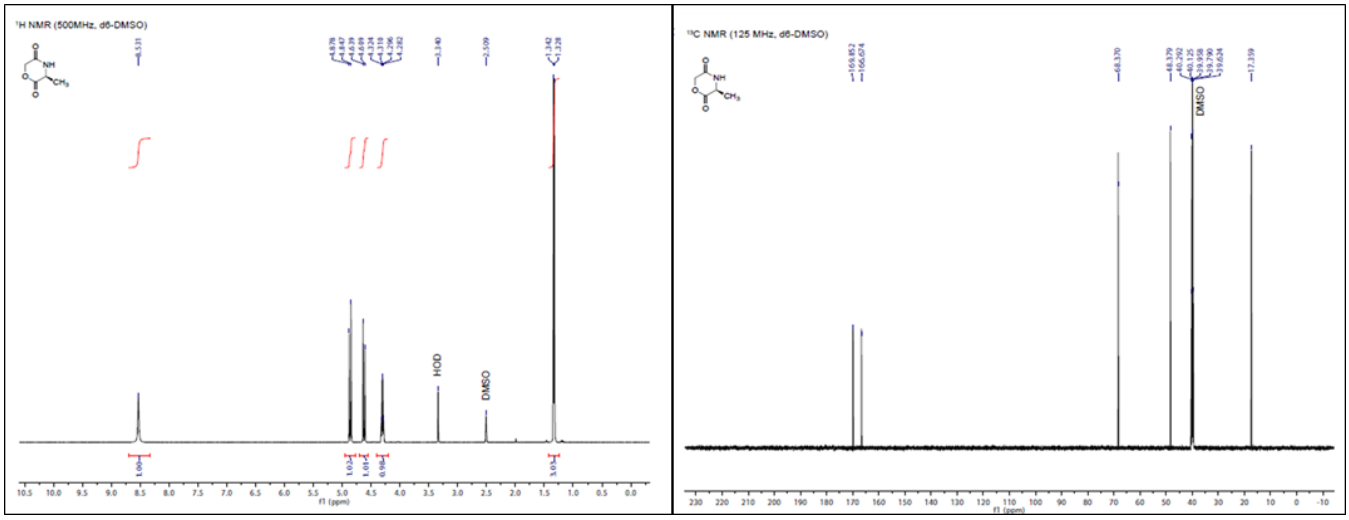

Synthesis of 2,5-morpholinedione (c(gG))

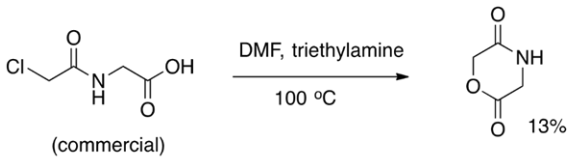

2,5-Morpholinedione (**gG** morpholinedione, c(**gG**)) was prepared as described previously.[3] N-(Chloroacetyl)-glycine (Bachem, 5.0 g, 33.0 mmol) in 50 mL of DMF. This was added dropwise under nitrogen to a stirred solution of triethylamine (3.5 g, 35.0 mmol) in 200 mL of DMF at 90 °C. The reaction was then stirred for 6 h, and was subsequently allowed to cool to room temperature. After removing the crystallized triethylammonium chloride salt, the DMF was evaporated to yield a white solid. The solid was dissolved in a minimal amount of hot isopropanol, and the insoluble material was filtered away. The solution was allowed to stand at room temperature, which yielded crystals of pure 2,5-morpholinedione. Yield 0.5 g (13%) white crystals. ^{1}H-NMR (500 MHz, DMSO-d6): δ = 4.06 (d, 2H, $NHCH_2CO$), 4.71 (s, 2H, OCH_2CO) 8.40 (br s, 1H, NH). ^{13}C-NMR (125 MHz, DMSO-d6): δ = 42.97, 68.13, 166.08, 167.11. High resolution ESI-MS (m/z): calcd for $C_4H_5O_3N$ (M+ H+): 116.0342, found 116.0388.

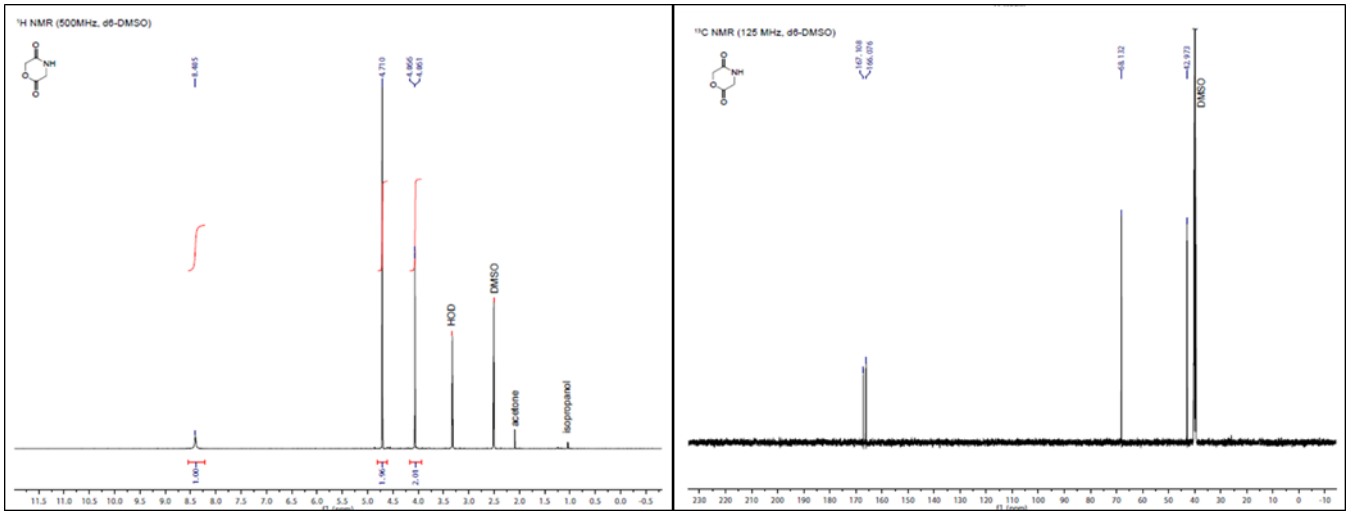

Synthesis of gAgA, (PA)AgA, and aAgG standards

Depsipeptides aAgG, gAgA, and PA-AgA were all prepared via solid-phase peptide synthesis using an Fmoc-L-Ala-glycolic acid building block.

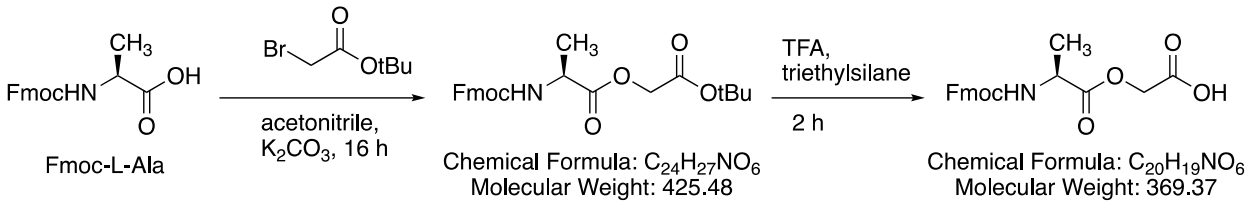

Fmoc-L-Ala-glycolic acid (or Fmoc-L-alanyl-oxyacetic acid). Fmoc-L-Ala-OH (4.67 g, 15.0 mmol) was dissolved in acetonitrile (250 mL). Next, tert-butylbromoacetate (3.07 g, 15.75 mmol) and potassium carbonate (11.2 g, 81.0 mmol) were added, each in a single portion. The suspension was stirred vigorously overnight at room temperature. TLC (10% MeOH/DCM containing a drop of conc. HCl) showed the presence of some Fmoc-L-Ala-OH remaining, so the mixture was heated for 2 h at 50 °C, after which Fmoc-L-Ala-OH was completely consumed. The mixture was filtered, and the supernatant was subjected to rotary evaporation to a clear oil that solidified to a white solid upon standing (6.17 g were obtained). Without further purification, this solid was dissolved in 20 mL of 95:5 TFA/triethylsilane. The solution was stirred for 2 h at room temperature. The solution was filtered to remove some white flocculate, and then subjected to rotary evaporation to an oil. To remove traces of TFA, toluene was added to the oil and the solution subjected to rotary evaporation, and this process was repeated. The oil was dissolved in a small volume of DCM, and hexanes was added until precipitation was observed. Rotary evaporation of the mixture yielded 4.664 g of a white solid (84% overall for 2 steps), which was used without further purification in solid phase synthesis of the depsipeptides. ^{1}H NMR (500 MHZ, DMSO-*d6*) 7.89 (t, 2H), 7.73 (t, 2H), 7.44-7.16 (m, 5H), 4.59 (q, 2H), 4.33-4.21 (m, 4H), 1.36 (d, 3H). ^{13}C NMR (126 MHZ, DMSO-*d6*) 173.0, 169.3, 156.3, 144.3, 144.2, 141.2, 129.4, 128.7, 128.1, 127.6, 125.8, 125.7, 120.6, 66.1, 61.3, 49.6, 47.1, 17.4. HRMS: $C_{20}H_{19}NO_6$, calc'd for MH^+, 370.1285; obs'd 370.1284

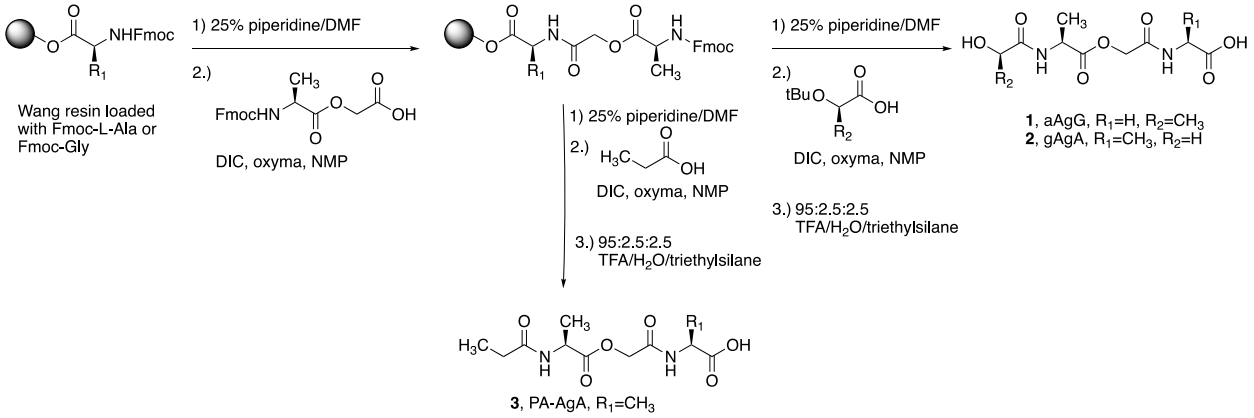

*aAgG***.** Fmoc-Gly Wang resin (0.1 g, loading 0.80 mmol/g, 0.08 mmol) was used. Deprotections of the Fmoc group involved two 5-min treatments with 25% piperidine/DMF. Coupling reactions involved 6 eq. of the acid, 6 eq. of diisopropylcarbodiimide (DIC), and 6 eq. of oxyma (ethyl cyano(hydroxyimino)acetate). Cleavage from the resin and protecting group removal involved treatment of the resin with 95:2.5:2.5 TFA/H_2O/triethylsilane for 30-60 min. The cleavage solution was subjected to rotary evaporation to an oil, to which 5 mL of water was added, and the mixture was immediately frozen and lyophilized. Purification by prep-HPLC (binary gradients of solvent A [99% H_2O, 0.9% acetonitrile, 0.1% TFA] and solvent B [90% acetonitrile, 9.9% H_2O, 0.07% TFA]) with a Thermo BioBasic C18 column (21.2 x 250 mm), followed by lyophilization afforded the depsipeptide (12 mg, 54% based on resin loading) as a clear oil. HRMS: $C_{10}H_{17}N_2O_7$, calc'd for MH^+, 277.1030; obs'd 277.1030

gAgA. Same general procedure as above, using Fmoc-L-Ala Wang resin (0.2 g, loading 0.42 mmol/g, 0.084 mmol). The depsipeptide (9 mg, 39% based on resin loading) was obtained as a clear oil. HRMS: $C_{10}H_{17}N_2O_7$, calc'd for MH^+, 277.1030; obs'd 277.1032

(PA)AgA. Same general procedure as above, using Fmoc-L-Ala Wang resin (0.2 g, loading 0.42 mmol/g, 0.084 mmol). The depsipeptide (13 mg, 57% based on resin loading) was obtained as a clear oil. HRMS: $C_{11}H_{19}N_2O_6$, calc'd for MH^+, 275.1238; obs'd 275.1234

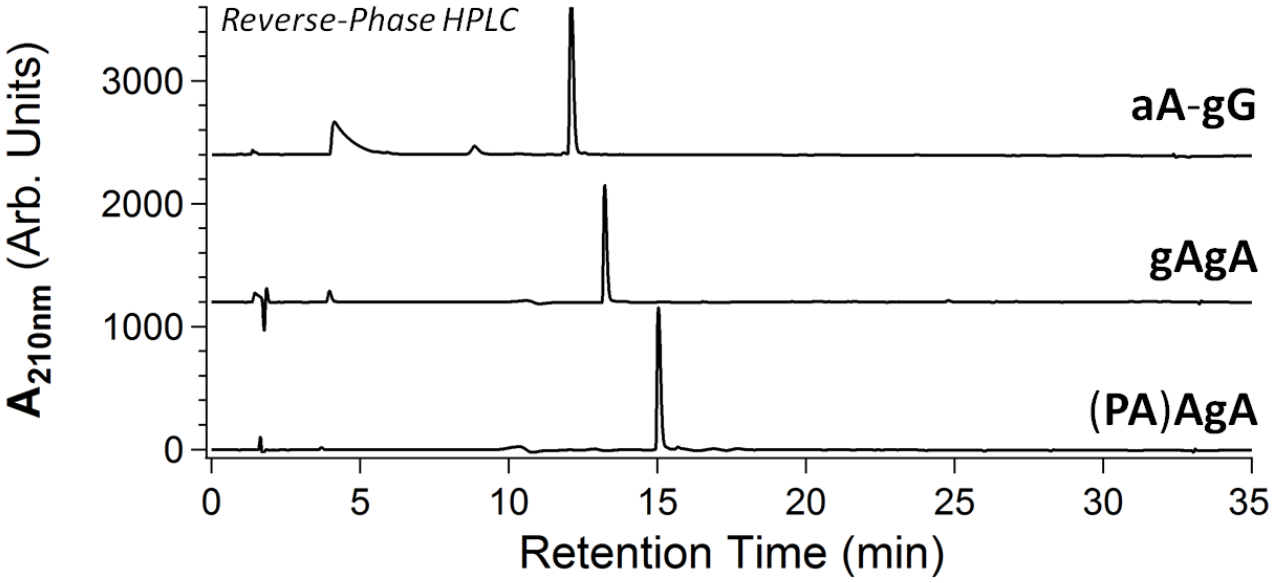

Synthesis of HO-Lac-Asp(tBu)-OtBu

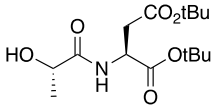

Anhydrous lactic acid (5.5 mmol, 0.495 g, Alfa-Aesar) was dissolved in ice-cold DMF (20 mL) along with HOBt hydrate (5.5 mmol, 0.842 g) and EDC (5.5 mmol, 1.054 g). To this solution was added H-Asp(tBu)-OtBu (5.0 mmol, 1.41 g, Combi-Blocks) and triethylamine (6.0 mmol, 0.84 mL). The reaction was stirred and allowed to warm to room temperature. After 16 h, the mixture was filtered and the solvent was evaporated. The residue was taken up in 100 mL DCM and then washed 2x with saturated $NaHCO_3$, 2x with saturated $KHSO_4$, and 1x with brine. The organic layer was dried over anhydrous $MgSO_4$ and evaporated to a clear oil (1.55 g, 98%) which crystallized upon standing. The product was used directly in the next step without further purification. ^{1}H NMR (500 MHz, DMSO-d6): δ 7.89-7.87 (d, 1H), 5.69-5.68 (d, 1H), 4.52-4.48 (m, 1H), 4.02-3.97 (m, 1H), 2.72-2.63 (m, 2H), 1.40 (s, 9H), 1.39 (s, 9H), 1.21-1.20 (d, 3H). ^{13}C NMR (126 MHz, DMSO-d6): δ 174.66, 170.03, 169.90, 81.54, 81.01, 67.48, 49.01, 37.58, 28.14, 28.01, 21.52. ESI-MS (m/z): $[MH]^+$ calc'd for $C_{15}H_{28}NO_6$, 318.19; found, 318.2

Synthesis of tBuO-Lac-Asp-OtBu

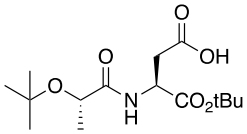

tBuO-lactic acid was prepared as described previously.[4] tBuO-lactic acid (6.0 mmol, 0.877 g) was dissolved in DMF (10 mL) along with HOBt hydrate (5.5 mmol, 0.842 g) and EDC (5.5 mmol, 1.054 g), and the mixture was allowed to stir for 30 min. Separately, H-Asp-OtBu (5.0 mmol, 0.946 g, Combi-Blocks) was mixed with bis(trimethylsilyl)-trifluoroacetamide (10 mmol, 2.574 g, Combi-Blocks) in DMF (40 mL) under Ar and allowed to stir for 30 min. The solution containing tBuO-lactic acid was then added dropwise

into the mixture containing H-Asp-OtBu, and the reaction was stirred under Ar for 16 h. Water (10 mL) was added to the reaction and allowed to stir for 1 h. The solvent was evaporated, after which the residue was taken up in 100 mL DCM and then washed 2x with saturated $NaHCO_3$, 2x with saturated $KHSO_4$, and 1x with brine. The organic layer was evaporated to a clear oil, which was purified by preparative HPLC to yield a white solid (0.612 g, 39%). ^{1}H NMR (500 MHz, DMSO-d6): δ 12.48 (br s, 1H), 7.87-7.85 (d, 1H), 4.52-4.48 (m, 1H), 4.03-3.97 (m, 1H), 2.69-2.68 (d, 2H), 1.39 (s, 9H), 1.18-1.14 (m, 12H). ^{13}C NMR (126 MHz, DMSO-d6): δ 174.11, 172.59, 170.12, 81.45, 75.04, 68.57, 48.95, 36.44, 28.03, 27.96, 21.44. ESI-MS (m/z): $[MH]^+$ calcd. for $C_{15}H_{28}NO_6$, 318.19; found, 318.3

Synthesis of HO-Lac-Asp(lac-Asp)-OH (β-(aD)$_2$)

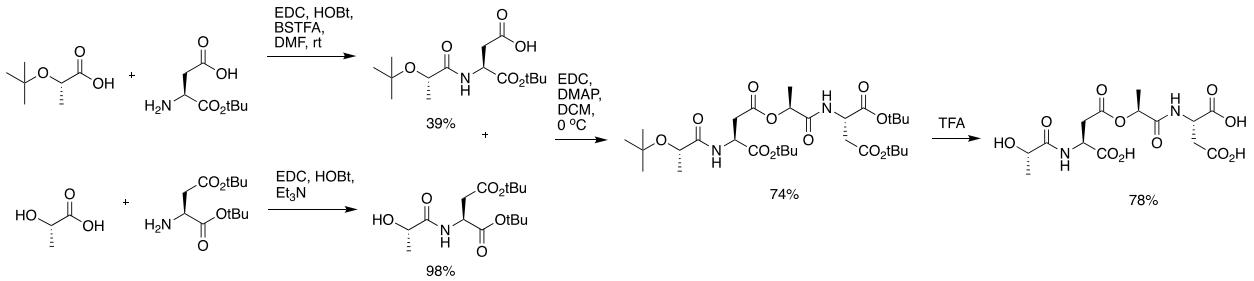

tBuO-Lac-Asp-OtBu (0.5 mmol, 0.159 g) was suspended in dry DCM (1 mL) on ice. To this was added oxyma pure (0.6 mmol, 0.086 g), DMAP (0.05 mmol, 0.006 g), and HO-Lac-Asp(tBu)-OtBu (0.55 mmol, 0.175 g). EDC (0.6 mmol, 0.115 g) was added to the mixture, and the reaction stirred at room temperature for 16 h, over which time it became a clear, yellowish solution. The reaction was diluted with DCM (10 mL) and then washed 3x with saturated $NaHCO_3$, 2x with saturated $KHSO_4$, and 1x with brine. The organic layer was dried over anhydrous $MgSO_4$ and evaporated to an oil. Purification by preparative HPLC yielded the protected depsipeptide (0.228 g, 74%), which was used directly in the next step. The protected depsipeptide was dissolved in 5 mL of 95:5 TFA/triethylsilane and allowed to stand at room temperature for 1 h. The solvent was evaporated, and preparative HPLC afforded the desired product after lyophilization as a clear, sticky oil (0.113 g, 78 %). 98.1% purity (HPLC). ^{1}H NMR (500 MHz, DMSO-d6): δ 8.31-8.29 (d, 1H), 7.97-7.95 (d, 1H), 5.04-4.99 (m, 1H), 4.64-4.52 (m, 2H), 4.01-3.97 (m, 1H), 2.91-2.83 (m, 2H), 2.74-2.70 (dd, 1H), 2.61-2.57 (dd, 1H), 1.32-1.30 (d, 3H), 1.21-1.19 (d, 3H). ^{13}C NMR (126 MHz, DMSO-d6): δ 174.85, 172.54, 172.52, 172.09, 170.14, 170.08, 70.08, 67.53, 48.91, 48.32, 36.28, 36.21, 21.44, 17.94. HRMS (m/z): $[MH]^+$ calc'd for $C_{14}H_{21}N_2O_{11}$, 393.1140; found, 393.1147; $[MNa]^+$ calc'd for $C_{14}H_{20}N_2O_{11}Na$, 415.0959; found, 415.0969.

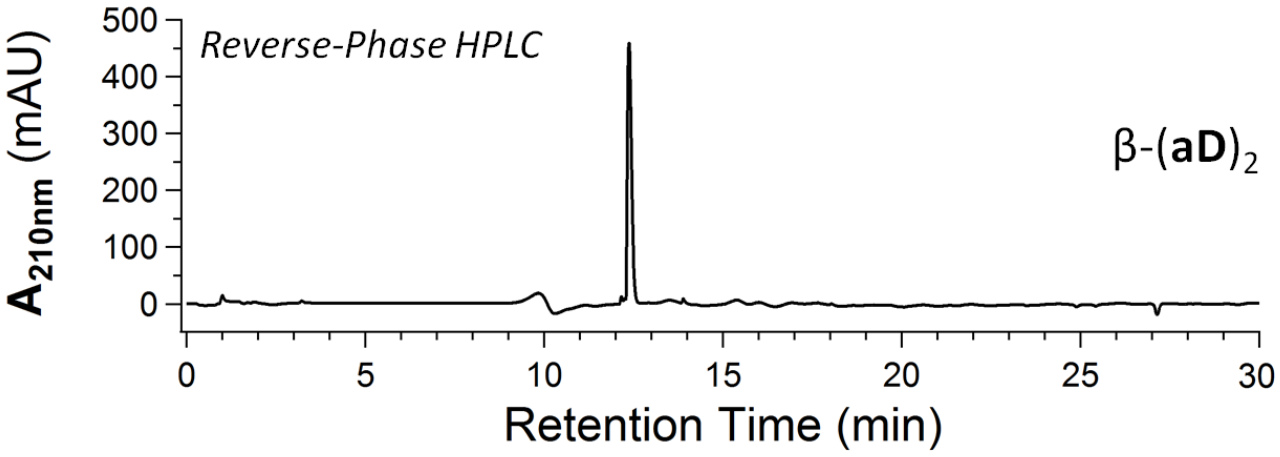

Synthesis of tBuO-Lac-Asp(OtBu)-OH

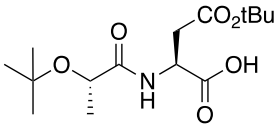

tBuO-lactic acid was prepared as described previously.[4] tBuO-lactic acid (6.0 mmol, 0.877 g) was dissolved in DMF (10 mL) along with HOBt hydrate (5.5 mmol, 0.842 g) and EDC (5.5 mmol, 1.054 g), and the mixture was allowed to stir for 30 min. Separately, H-Asp(OtBu)-OH (5.0 mmol, 0.946 g, Novabiochem) was mixed with bis(trimethylsilyl)-trifluoroacetamide (10 mmol, 2.574 g, Combi-Blocks) in DMF (40 mL) under Ar and allowed to stir for 30 min. The solution containing tBuO-lactic acid was then added dropwise into the mixture containing H-Asp(OtBu)-OH, and the reaction was stirred under Ar for 16 h. Water (10 mL) was added to the reaction and allowed to stir for 1 h. The solvent was evaporated, after which the residue was taken up in 100 mL DCM and then washed 2x with saturated $NaHCO_3$. The desired product was found to partition into the aqueous phase. The aqueous phase was acidified to pH 3 using saturated $KHSO_4$ and extracted twice with DCM. The DMC layers were combined and evaporated to a clear oil, which was purified by preparative HPLC to yield a white solid (0.807 g, 51%). ^{1}H NMR (500 MHz, DMSO-d6): δ 7.76-7.74 (m, 1H), 4.57-4.53 (m, 1H), 4.02-3.98 (m, 1H), 2.75-2.66 (m, 2H), 1.39 (s, 9H), 1.19-1.14 (m, 12H). ^{13}C NMR (126 MHz, DMSO-d6): δ 174.15, 172.51, 169.99, 80.93, 75.05, 68.63, 48.36, 37.57, 28.10, 27.90, 21.49. ESI-MS (m/z): $[MH]^+$ calc'd for $C_{15}H_{28}NO_6$, 318.19; found, 318.2.

Synthesis of (*R*)-2-chloropropanoyl-Asp(OtBu)-OtBu

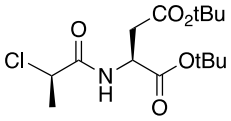

Asp(OtBu)-OtBu (3.0 mmol, 0.845 g) was dissolved in DMF (10 mL) on ice. To this solution was added triethylamine (6.0 mmol, 0.84 mL), followed by (*R*)-2-chloropropanoyl chloride (3.3 mmol, 0.32 mL). The mixture was allowed to warm to room temperature and stirred for 16 h. The reaction was filtered and solvent was evaporated, after which the residue was taken up in 100 mL DCM and then washed 2x with saturated $NaHCO_3$, 2x with saturated $KHSO_4$, and 1x with brine. The organic layer was dried over anhydrous $MgSO_4$ and evaporated to an oil, which was purified by preparative HPLC to yield a clear oil (0.861 g, 86%). ^{1}H NMR (500 MHz, DMSO-d6): δ 8.57-8.55 (d, 1H), 4.59-4.55 (q, 1H), 4.50-4.46 (m, 1H), 2.72-2.56 (dd, 2H), 1.52-1.51 (d, 3H), 1.40 (s, 18H). ^{13}C NMR (126 MHz, DMSO-d6): δ 169.69, 169.57, 169.06, 81.61, 80.97, 54.37, 49.95, 37.31, 28.13, 27.99, 21.94. ESI-MS (m/z): $[MH]^+$ calcd. for $C_{15}H_{27}ClNO_5$, 336.16; found, 336.2.

Synthesis of HO-Lac-Asp-lac-Asp-OH (α-(aD)$_2$)

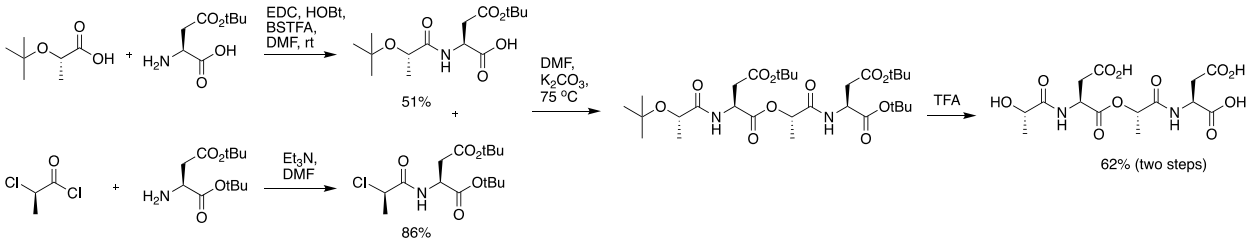

tBuO-Lac-Asp(OtBu)-OH (0.65 mmol, 0.206 g) and (*R*)-2-chloropropanoyl-Asp(OtBu)-OtBu were dissolved in DMF (2 mL), and K_2CO_3 (0.6 mmol, 0.201 g) was added. The reaction was heated to 75 °C and stirred for 24 h. The solvent was evaporated, and the protected product was isolated by preparative HPLC. Deprotection of a portion of material (300 mg) by treatment with 95:5 TFA/triethylsilane for 1 h at room temperature, followed by preparative HPLC purification, afforded the desired compound as a clear oil (118 mg, 62 % over two steps). 99.9% purity (HPLC). ^{1}H NMR (500 MHz, DMSO-d6): δ 8.24-8.22 (d, 1H), 8.16-8.14 (d, 1H),

5.03-4.99 (m, 1H), 4.64-4.60 (m, 1H), 4.55-4.51 (m, 1H), 4.02-4.00 (m, 1H), 2.87-2.83 (dd, 1H), 2.75-2.68 (m, 2H), 2.61-2.57 (dd, 1H), 1.32-1.31 (d, 3H), 1.21-1.20 (d, 3H). ^{13}C NMR (126 MHz, DMSO-d6): δ 175.29, 172.50, 172.23, 172.04, 170.55, 170.02, 70.48, 67.43, 48.91, 48.86, 36.31, 35.95, 21.41, 17.89. HRMS (m/z): $[MH]^+$ calc'd for $C_{14}H_{21}N_2O_{11}$, 393.1140; found, 393.1145; $[MNa]^+$ calc'd for $C_{14}H_{20}N_2O_{11}Na$, 415.0959; found, 415.0964.

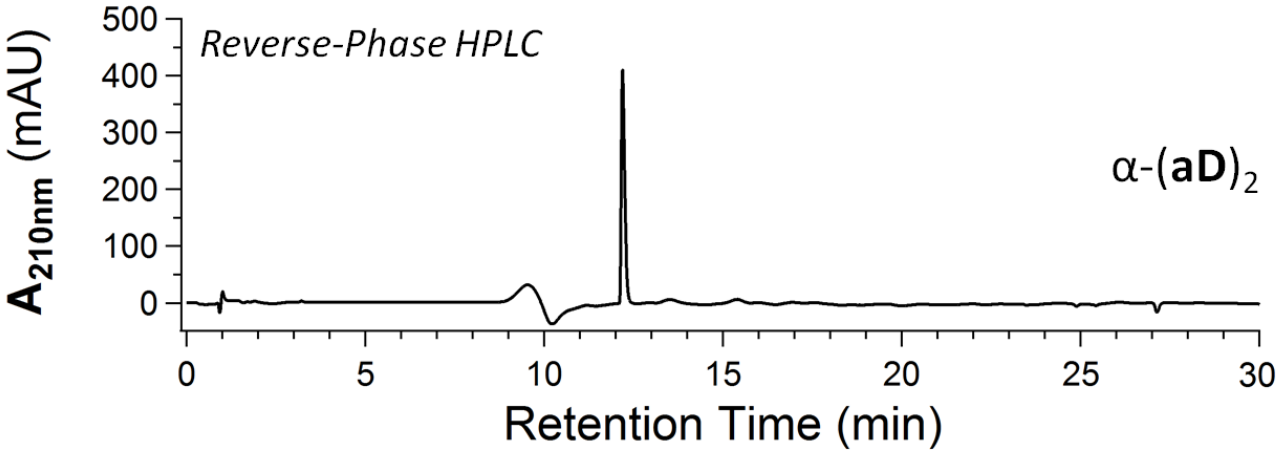

Synthesis of Fmoc-Glu(tBu)-phe-OBn.

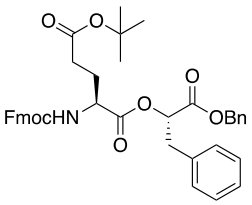

Fmoc-Glu(tBu)-OH (12 mmol, 5.106 g, Aapptec) and benzyl (*S*)-(-)-2-hydroxy-3-phenylpropionate (10 mmol, 2.56 g, Santa Cruz Biotech) were dissolved in dry DCM (25 mL) and chilled in an ice bath. DMAP (2 mmol, 0.24 g) was added to the cold mixture, followed by EDC (13 mmol, 2.49 g). The pale yellow solution was stirred and allowed to warm to room temperature overnight. HPLC analysis indicated the reaction was complete by 24 h. The reaction mixture was diluted with 100 mL DCM and then extracted 4x with saturated $NaHCO_3$, 2x with saturated $KHSO_4$, and 1x with brine. The organic layer was dried over anhydrous $MgSO_4$ and evaporated to a yellow oil. The crude product was purified by flash chromatography using 200 g silica in a 70 cm diameter column, with 25% EtOAc/hexanes as the eluent. A clear oil (5.62 g, 85%) was obtained after evaporation of the solvent. ^{1}H NMR (500 MHz, DMSO-d6): δ 7.91-7.88 (d, 2H), 7.84-7.83 (d, 1H), 7.73-7.70 (m, 2H), 7.44-7.41 (t, 2H), 7.38-7.29 (m, 5H), 7.27-7.19 (m, 7H), 5.29-5.27 (t, 1H), 5.13-5.06 (q, 2H), 4.30-4.15 (m, 4H), 3.17-3.09 (m, 2H), 2.31-2.28 (m, 2H), 2.02-1.95 (m, 1H), 1.81-1.73 (m, 1H), 1.40 (s, 9H). ^{13}C NMR (126 MHz, DMSO-d6): δ 172.08, 171.86, 169.12, 156.48, 144.28, 144.18, 141.21, 135.92, 135.73, 129.86, 128.89, 128.71, 128.67, 128.48, 128.13, 127.53, 127.30, 125.71, 120.61, 80.27, 73.41, 66.87, 66.21, 53.03, 47.07, 36.93, 31.36, 28.21, 26.48. ESI-MS (m/z): $[MH]^+$ calc'd for $C_{40}H_{42}NO_8$, 664.29; found, 664.5

Synthesis of Fmoc-Glu(tBu)-phe-OH.

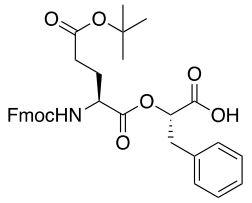

Fmoc-Glu(tBu)-phe-OBn (5.62 g, 8.47 mmol) was dissolved in 50 mL EtOH (200 proof) along with 20 mL EtOAc to aid solubility. Pd/C (0.8 g, 5 wt%, wet support, Degussa E101 NOW, Aldrich) was added. Hydrogen gas was bubbled into the flask from a balloon.

The insoluble starting material dissolved over the course of the reaction, which was completed by 35 min as tracked by TLC (5% MeOH/DCM). To prevent possible removal of the Fmoc group under the conditions of hydrogenation, the reaction was immediately filtered through celite. The solvent was evaporated to yield a white solid (4.74 g, 98%). ^{1}H NMR (500 MHz, DMSO-d6): δ 7.91-7.89 (d, 2H), 7.82-7.80 (d, 1H), 7.74-7.71 (t, 2H), 7.44-7.41 (t, 2H), 7.35-7.19 (m, 7H), 5.12-5.10 (dd, 1H), 4.31-4.21 (m, 3H), 4.17-4.12 (m, 1H), 3.16-3.05 (m, 2H), 2.34-2.29 (m, 2H), 2.05-2.00 (m, 1H), 1.83-1.75 (m, 1H), 1.40 (s, 9H). ^{13}C NMR (126 MHz, DMSO-d6): δ 172.03, 171.96, 170.65, 156.47, 144.31, 144.18, 141.20, 136.69, 129.79, 128.66, 128.12, 127.53, 127.16, 125.74, 120.60, 80.22, 73.50, 66.20, 53.03, 47.08, 36.90, 31.36, 28.22, 26.50. HRMS (m/z): $[MH]^+$ calcd. for $C_{33}H_{36}NO_8$, 574.2441; found, 574.2440

Synthesis of Fmoc-Asp(tBu)-phe-OBn

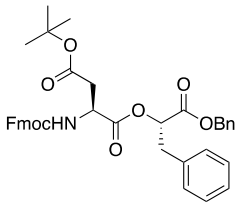

Fmoc-Asp(tBu)-OH (12 mmol, 4.938 g, Aapptec) and benzyl (*S*)-(-)-2-hydroxy-3-phenylpropionate (10 mmol, 2.56 g, Santa Cruz Biotech) were dissolved in dry DCM (25 mL) and chilled in an ice bath. DMAP (2 mmol, 0.24 g) was added to the cold mixture, followed by EDC (13 mmol, 2.49 g). The pale yellow solution was stirred and allowed to warm to room temperature overnight. HPLC analysis indicated the reaction was complete by 24 h. The reaction mixture was diluted with 100 mL EtOAc and then extracted 2x with saturated $NaHCO_3$, 2x with 1 N HCl, and 1x with brine. The organic layer was dried over anhydrous $MgSO_4$ and evaporated to a yellow oil. The crude product was purified by flash chromatography using 200 g silica in a 70 cm diameter column, with 23% EtOAc/hexanes as the eluent. A clear pinkish oil (5.1 g, 78%) was obtained after evaporation of the solvent. ^{1}H NMR (500 MHz, DMSO-d6): δ 7.93-7.89 (m, 3H), 7.71-7.68 (m, 2H), 7.44-7.16 (m, 14H), 5.29-5.26 (m, 1H), 5.14-5.07 (q, 2H), 4.52-4.46 (m, 1H), 4.31-4.30 (d, 2H), 4.24-4.21 (t, 1H), 3.15-3.08 (m, 2H), 2.73-2.69 (dd, 1H), 2.55-2.49 (dd, 1H), 1.38 (s, 9H). ^{13}C NMR (126 MHz, DMSO-d6): δ 171.13, 169.19, 169.02, 156.21, 144.22, 144.16, 141.21, 135.89, 135.71, 129.82, 128.89, 128.70, 128.53, 128.13, 127.53, 127.30, 125.63, 120.61, 81.01, 73.61, 66.95, 66.27, 50.76, 47.03, 37.16, 36.89, 28.10. ESI-MS (m/z): $[MH]^+$ calc'd for $C_{39}H_{40}NO_8$, 650.28; found, 650.2

Synthesis of Fmoc-Asp(tBu)-phe-OH.

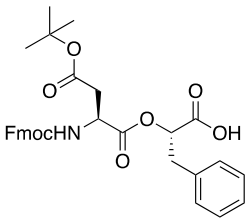

Fmoc-Asp(tBu)-phe-OBn (5.1 g, 7.85 mmol) was dissolved in 30 mL EtOH (200 proof) along with 20 mL EtOAc to aid solubility. Pd/C (0.6 g, 5 wt%, wet support, Degussa E101 NOW, Aldrich) was added. Hydrogen gas was bubbled into the flask from a balloon. The insoluble starting material dissolved over the course of the reaction, which was completed by 55 min as tracked by TLC (5% MeOH/DCM). To prevent possible removal of the Fmoc group under the conditions of hydrogenation, the reaction was immediately filtered through celite. The solvent was evaporated to yield a white solid (4.29 g, 98%). ^{1}H NMR (500 MHz, DMSO-d6): δ 7.90-7.87 (t, 3H), 7.71-7.68 (t, 2H), 7.44-7.40 (m, 2H), 7.34-7.30 (m, 2H), 7.24-7.16 (m, 5H), 5.11-5.09 (m, 1H), 4.49-4.45 (m, 1H), 4.31-4.29 (m, 2H), 4.26-4.21 (m, 1H), 3.14-3.03 (m, 2H), 2.79-2.74 (dd, 1H), 2.56-2.52 (m, 1H), 1.39 (s, 9H). ^{13}C NMR (126 MHz, DMSO-d6): δ 171.12, 170.57, 169.27, 156.19, 144.24, 144.17, 141.21, 136.66, 129.76, 128.65, 128.13, 127.53, 127.15, 125.65, 124.63, 120.61, 120.42, 80.99, 73.72, 66.26, 50.76, 47.03, 37.22, 36.85, 28.11. HRMS (m/z): $[MH]^+$ calc'd for $C_{32}H_{34}NO_8$, 560.2284; found, 560.2285

Syntheses of α-(fD)$_n$ and α-(fE)$_n$ depsipeptides

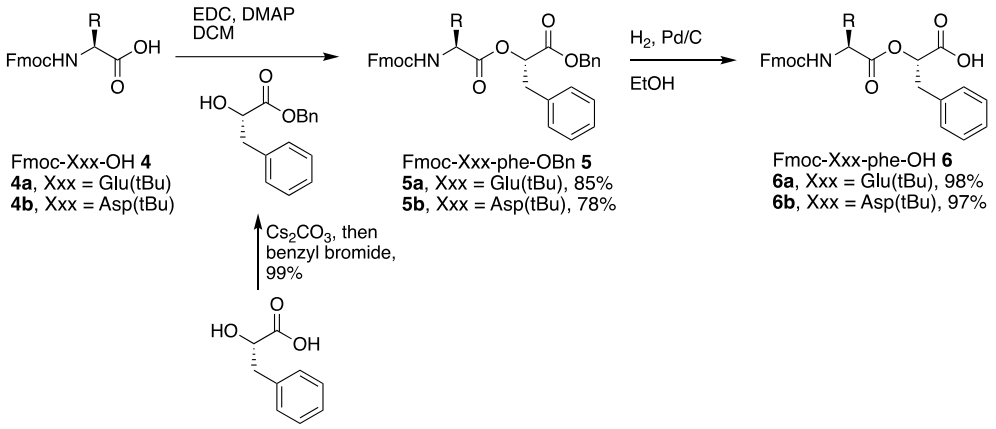

Oligo (phe-Asp)$_n$ and (phe-Glu)$_n$ depsipeptides were synthesized by using standard Fmoc solid-phase procedures on an Advanced Chemtech Apex 396 peptide synthesizer. A typical synthesis was performed on 0.15-mmol scale using Fmoc-Asp(tBu)-Wang or Fmoc-Glu(tBu)-Wang resin (~0.7 mmol/g). Ester bonds were incorporated into the depsipeptides by coupling the Fmoc-didepsipeptide building blocks Fmoc-Glu(tBu)-phe-OH or Fmoc-Asp(tBu)-phe-OH. Chain elongations were carried out using 1,3-diisopropylcarbodiimide (DIC) and ethyl 2-cyano-2-(hydroxyimino)acetate (oxyma) in *N*-methylpyrrolidin-2-one (NMP) with 75-min couplings. Fmoc deprotection was achieved using 2x8 min treatments with 25% 4-methylpiperidine in dimethylformamide (DMF). Washing steps involved 6x1min treatments with DMF. Sequences were cleaved from the resin with concomitant side chain deprotection by agitation in a solution of 95:2.5:2.5 TFA:triethylsilane (TES):water for 3 h. The crude products were lyophilized. Preparative reverse-phase (RP)-HPLC was performed by using a Thermo BioBasic C18 column. Analytical RP-HPLC was performed using a Zorbax 300-SB C-18 column connected to a Hitachi D-7000 HPLC system. Binary gradients of solvent A (99% H_2O, 0.9% acetonitrile, 0.1% TFA) and solvent B (90% acetonitrile, 9.9% H_2O, 0.07% TFA) were employed for HPLC. The products were further purified using an Agilent semi-preparative reverse-phase HPLC system as described in section 21 of the supplementary information. Final purities for each of the polymers was determined by analytical HPLC-UV total integration at 257nm absorbance with blank baselines subtraction: α-(**fD**)$_2$, 99.9% purity (HPLC). ESI-MS (m/z): calc'd for $C_{26}H_{28}N_2O_{11}$ $[M-H]^-$, 543.17, Obs'd, 542.9; α-(**fD**)$_3$, 96.5% purity (HPLC). ESI-MS (m/z): calc'd for $C_{39}H_{41}N_3O_{16}$ $[M-H]^-$, 806.25, Obs'd, 805.8; α-(**fD**)$_4$, 92.8% purity (HPLC). ESI-MS (m/z): calc'd for $C_{52}H_{54}N_4O_{21}$ $[M-H]^-$, 1069.33, Obs'd, 1068.7; α-(**fE**)$_2$, 99.9% purity (HPLC). ESI-MS (m/z): calc'd for $C_{28}H_{32}N_2O_{11}$ $[M-H]^-$, 571.20, Obs'd, 570.9; α-(**fE**)$_3$, 99.9% purity (HPLC). ESI-MS (m/z): calc'd for $C_{42}H_{47}N_3O_{16}$ $[M-H]^-$, 848.30, Obs'd, 847.8; α-(**fE**)$_4$, 91.0% purity (HPLC). ESI-MS (m/z): calc'd for $C_{56}H_{62}N_4O_{21}$ $[M-H]^-$, 1125.39, Obs'd, 1124.7.

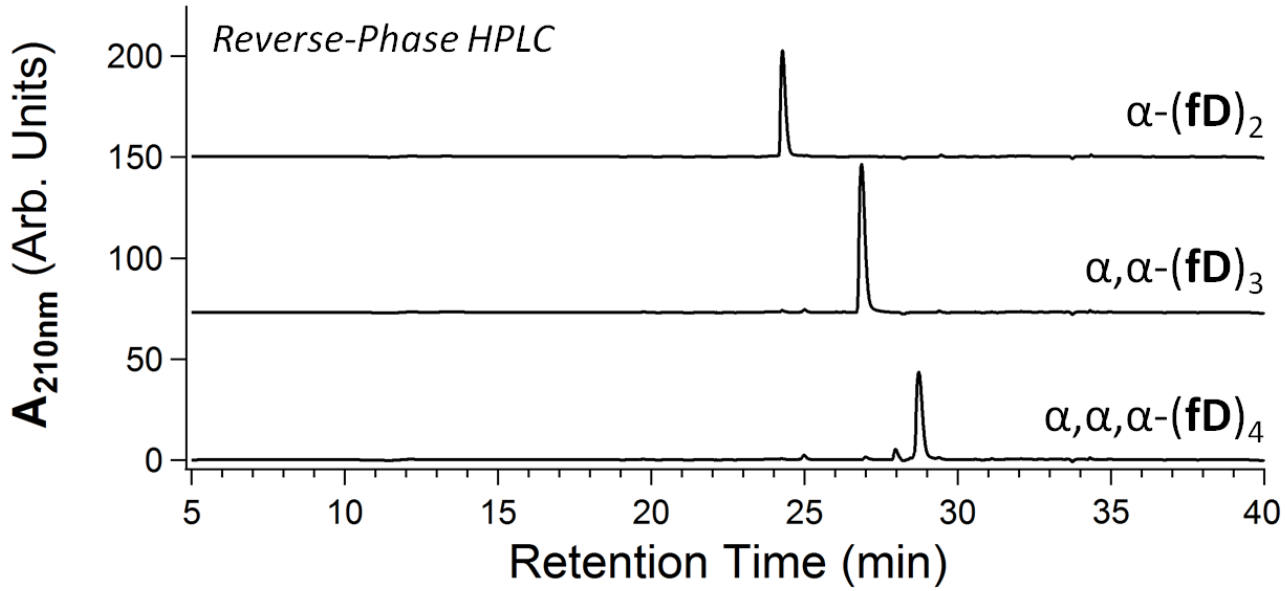

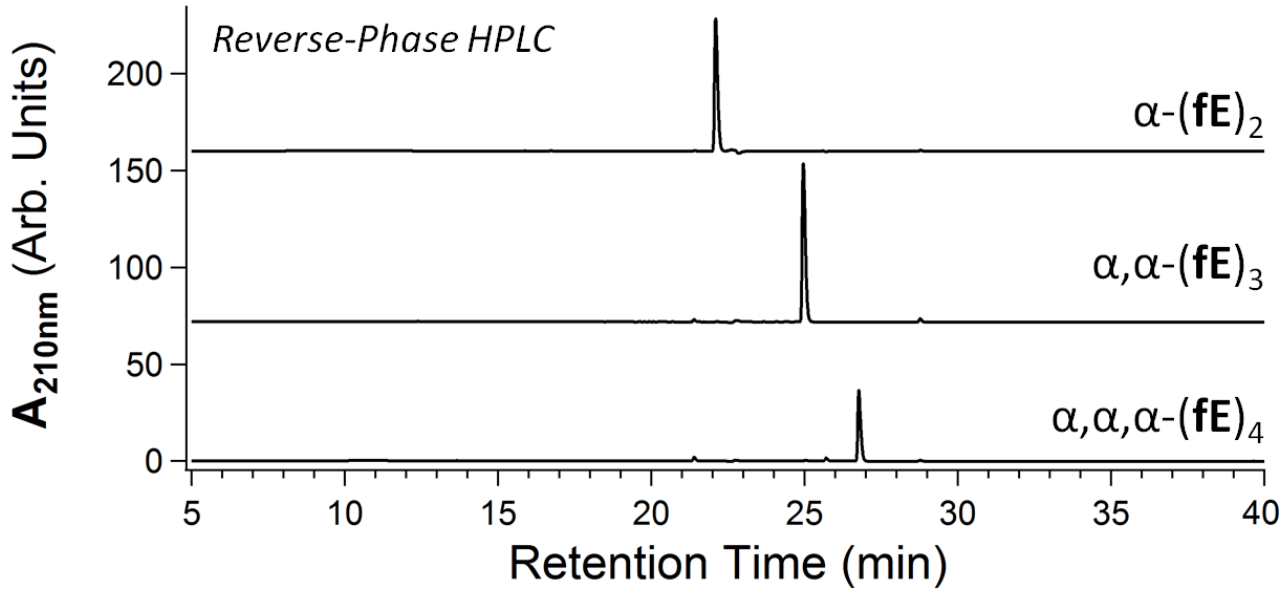

Synthesis of L-phe-L-Glu-OtBu

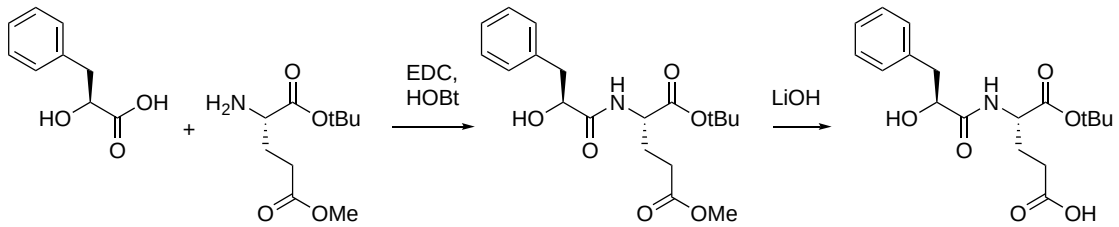

L-phenylactic acid (698 mg, 4.2 mmol, Oakwood) and HOBt hydrate (689 mg, 4.5 mmol) were dissolved in DCM (15 mL) and placed in an ice bath. L-Glu(OMe)-OtBu hydrochloride (989 mg, 3.9 mmol, Combi-Blocks) and triethylamine (840 µL, 6.0 mmol) were added, followed by EDC (863 mg, 4.5 mmol). The clear solution stirred and was allowed to warm to RT overnight. The solvent was diluted with DCM and the organics were washed with saturated $NaHCO_3$ (3x), saturated $KHSO_4$ (3x), and brine. The organic layer

was dried over $MgSO_4$, and the solvent was evaporated to yield 1.40 g (98%) of a clear oil that solidified to a white solid upon standing, which was used without further purification. The methyl ester was removed by dissolving the compound (1.3 g, 3.6 mmol) in MeOH (12 mL) and adding a solution of LiOH monohydrate (755 mg, 18 mmol) in water (12 mL). The cloudy mixture was stirred at RT for 40 min, after with HPLC indicated no remaining starting material. The reaction was acidified using 1 N HCl to pH 2 and was extracted twice with EtOAc. The combined organic layers were washed with brine and dried over $MgSO_4$. Evaporation of the solvent yielded a white solid, which was purified by preparative HPLC using a water/acetonitrile/TFA solvent system. Lyophilization of fractions containing the product yielded 699 mg (55%) of a white crystalline solid. HRMS: Calculated 352.1760 $[M+H]^+$ for $C_{18}H_{25}NO_6$, observed 352.1753. ^{1}H NMR (500 MHz, DMSO-*d6*) δ 12.15 (br s, 1H), 7.84-7.82 (d, 1H), 7.28-7.22 (m, 4H), 7.20-7.17 (m, 1H), 5.62 (br s, 1H), 4.23-4.18 (m, 1H), 4.14-4.11 (m, 1H), 3.00-2.96 (dd, 1H), 2.76-2.71 (dd, 1H), 2.21-2.11 (m, 2H), 1.97-1.90 (m, 1H), 1.84-1.76 (m, 1H), 1.41 (s, 9H). ^{13}C NMR (126 MHz, DMSO-*d6*) δ 174.18, 173.81, 171.23, 138.85, 129.94, 128.37, 126.48, 81.37, 72.40, 51.94, 40.85, 30.25, 28.07, 26.79.

Synthesis of (D)-2-bromo-3-phenylpropionamide-L-Glu(OtBu)-OtBu

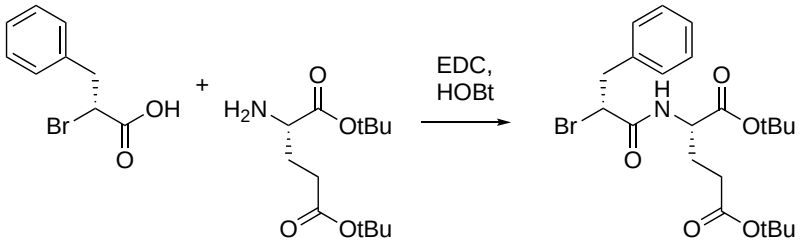

(D)-2-bromo-3-phenylpropionic acid (962 mg, 4.2 mmol, Toronto Research Chemicals) and HOBt hydrate (689 mg, 4.5 mmol) were dissolved in DCM (15 mL) and placed in an ice bath. EDC (863 mg, 4.5 mmol), L-Glu(OtBu)-OtBu hydrochloride (1.24 g, 4.2 mmol, Nova Biochem) and triethylamine (840 µL, 6.0 mmol) were added in that order. The cloudy solution stirred and was allowed to warm to RT overnight, at which point it had become a clear yellow solution. The solvent was diluted with DCM and the organics were washed with saturated $NaHCO_3$ (3x), saturated $KHSO_4$ (3x), and brine. The organic layer was dried over $MgSO_4$, and the solvent was evaporated to yield 2.0 g (98%) of a gummy solid. The product was purified by preparative HPLC using a water/acetonitrile/TFA solvent system. Lyophilization of fractions containing the product yielded 1.4 g (71%) of a clear oil. HRMS: Calculated 492.1362 $[M+H]^+$ for $C_{22}H_{32}BrNO_5$, observed 492.1350. ^{1}H NMR (500 MHz, DMSO-*d6*) δ 8.50-8.48 (d, 1H), 7.30-7.27 (m, 2H), 7.24-7.21 (m, 3H), 4.66-4.63 (dd, 1H), 4.14-4.10 (m, 1H), 3.37-3.32 (dd, 1H), 3.16-3.12 (dd, 1H), 1.98-1.88 (m, 2H), 1.85-1.79 (m, 1H), 1.61-1.54 (m, 1H), 1.40 (s, 18H). ^{13}C NMR (126 MHz, DMSO-*d6*) δ 171.69, 170.74, 168.20, 137.83, 129.60, 128.76, 127.32, 81.39, 80.18, 52.22, 48.33, 40.95, 31.01, 28.20, 28.05, 26.74.

Synthesis of L-phe-L-Glu-γ-(L-phe-L-Glu)-OH (γ-(fE)$_2$).

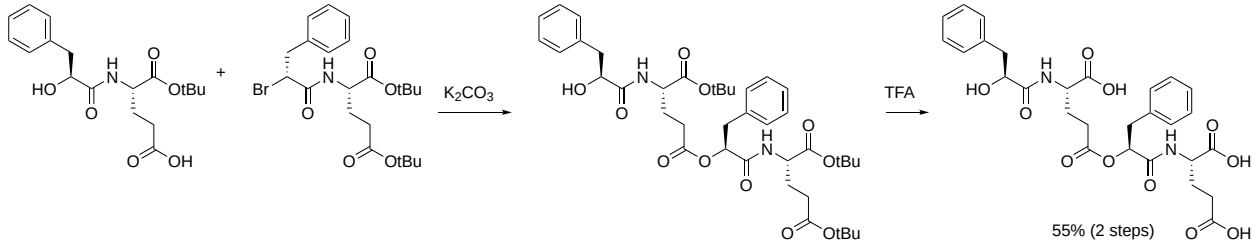

L-phe-L-Glu-OtBu (228 mg, 0.65 mmol) and (D)-2-bromo-3-phenylpropionamide-L-Glu(OtBu)-OtBu (281 mg, 0.60 mmol) were dissolved in DMF (1.7 mL). Potassium carbonate (90 mg, 0.65 mmol) was added, and the reaction was stirred vigorously at 73 °C for 24 h. After this time, the mixture was acidified to pH 3 using 1 N HCl and the solvent was evaporated. The residue was dissolved in 95:5 TFA/triethylsilane (10 mL) and allowed to stand for 2 h. The volatiles were evaporated, and the product was purified by

preparative HPLC using a water/acetonitrile/TFA solvent system. Lyophilization of fractions containing the product yielded 188 mg (55% for 2 steps) of a powdery solid. 90.0% purity (HPLC). ^{1}H NMR (500 MHz, DMSO-*d6*) δ 8.40-8.38 (dd, 1H), 7.78-7.77 (dd, 1H), 7.31-7.26 (m, 4H), 7.23-7.18 (m, 5H), 7.11-7.06 (m, 1H), 5.17-5.15 (dd, 1H), 4.29-4.23 (m, 2H), 4.14-4.12 (dd, 1H), 3.13-3.08 (dd, 1H), 2.99-2.93 (m, 2H), 2.76-2.72 (dd, 1H), 2.28-2.23 (m, 2H), 2.21-2.14 (m, 1H), 2.12-1.98 (m, 2H), 1.95-1.88 (m, 1H), 1.85-1.71 (m, 2H). ^{13}C NMR (126 MHz, DMSO-*d6*) δ 174.21, 173.68, 173.40, 173.29, 172.02, 169.40, 158.97, 158.66, 138.65, 137.25, 130.00, 129.97, 129.73, 128.66, 128.36, 128.33, 127.01, 126.48, 74.12, 72.34, 51.49, 50.97, 40.75, 37.69, 30.44, 30.02, 26.76, 26.62. HRMS: Calculated 573.2084 $[M+H]^+$ for $C_{22}H_{32}BrNO_5$, observed 573.2094.

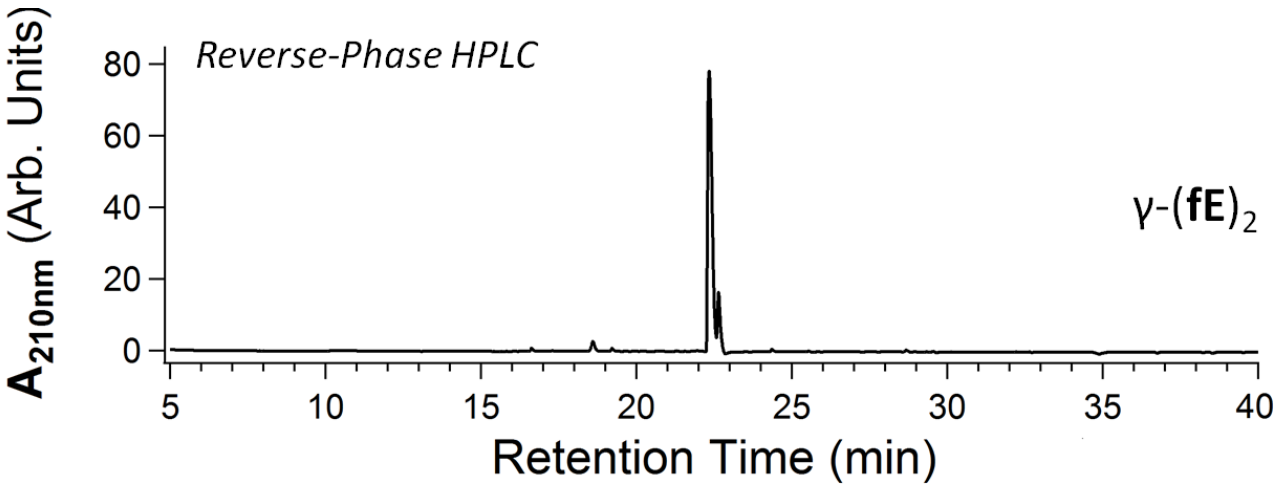

Electrospray Ionization Mass Spectrometry

All depsipeptide peak assignments correspond to $[M-H]^-$ ions, unless otherwise stated. Samples were directly infused into mass spectrometer system using the following parameters: Binary running solvents: 95% H_2O, 5% Acetonitrile. Flow rate was 0.5 mL/min. 5 µL Injection with H2O needle wash. UV detection 210nm or 257 nm. 0.6cm path length. Scanning ±65 - ± 2000 m/z. Equipment: ESI-MS – Agilent 6130 single quad MS (Agilent Technologies, Santa Clara, CA) and with UV detector coupled to Agilent 1260 HPLC. Capillary voltage: 2.0kV. Fragmentor voltage: 70V.

High Resolution Mass Spectrometry

HRMS samples were analyzed on a Thermo Fisher Q-Exactive Orbitrap Mass Spectrometer using nanoElectrospray Ionization with PicoTip Emitters with a mass range of 50-700 m/z. The Q-Exactive MS Tune source voltage was 1.500 kV with a capillary temperature of 150 °C. Sheath Gas was switched off and the S-Lens RF level was held at 30 V.

Liquid Chromatography-Mass Spectrometry-Single Ion Monitoring

LCMS samples were injected through an Agilent 1290 HPLC pump and thermostat with Agilent 1260 Autosampler and DAD UV-vis detector. Path length was 0.6cm. Reverse phase separation apparatus was a Phenomenex Kinetix 2.6mmxB-C_{18}100Å LC column 150x2.1mm. Column temperature was set to 25 °C. 10 µL Injections with needle wash and 100 µL/s Injection speed. Binary solvents: A) 0.1% formic acid in LCMS grade water, B) LCMS grade acetonitrile. Flow rate was 0.3 mL/min. Binary solvent gradient: 5 min 100% A, 0% B; 20 min ramp to 45% A, 55% B; 10 min 0% A, 100% B; 1 min ramp 100% A, 0% B; 9 min 100% A, 0% B. Wavelengths recorded typically 210, and 257 nm, with entire spectrum 180-400 nm detected in 2 nm steps. This system was coupled to our Electrospray Ionization Mass Spectrometry system, an Agilent 6130 single quad MS using parameters: Scanning ±65 - ± 2000 m/z. Capillary voltage: 2.0 kV. Fragmentor voltage: 70 V. Single ion monitoring (SIM) was carried out using the same system and tracking particular of ions for various depsipeptides. Masses detected for a given size of $(\mathbf{gE})_n$ species were first determined using

control samples, and then actual samples were monitored over 7 separate LCMS injections (3 specific ions maximum could be monitored per injection) of dried **gE** material. Masses monitored are annotated as needed in figures. Detection of ions for species larger than 16-mer for **gE** was unsuccessful.

Nuclear Magnetic Resonance Spectroscopy.

NMR samples were dissolved in D_2O or DMSO-*d6*. ^{1}H- and ^{13}C-NMR spectra were recorded using Bruker Avance III-HD-500 and 700 MHz spectrometers. Temperature was 298 K, using a t_1 relaxation delay of 5 seconds, collecting 16 scans. All spectra were processed and plotted using Bruker TopSpin Software. When applicable, internal standards of either Sodium 2,2-Dimethyl-2-silapentane-5-sulfonate-d_6 (DSS) or 3-(Trimethylsilyl)propionic-2,2,3,3-d_4 acid sodium salt (TSP) (Sigma-Aldrich) at either 11.11 mM or 27.78 mM as necessary for quantitative analysis.

Fourier Transform Infrared Spectroscopy

FTIR data was obtained on a Thermo Nicolet 4700 FTIR Spectrometer. Prior to analysis, samples (5 µl, 100 mM) were placed on hydrophilic PVDF Membranes with a pore size of 0.2µm (Pall Laboratory, #66477) and allowed to dry. Dried samples were analyzed in an Attenuated Total Reflectance (ATR) sample chamber. Spectra were background-subtracted from 400 to 4000 cm^{-1} and signal-averaged (16 scans per spectrum).

Data Processing

Wavemetrics IGOR Pro v6.37, Agilent Chemstation and Microsoft Excel packages each with macros written in-house.

Supplementary Figures

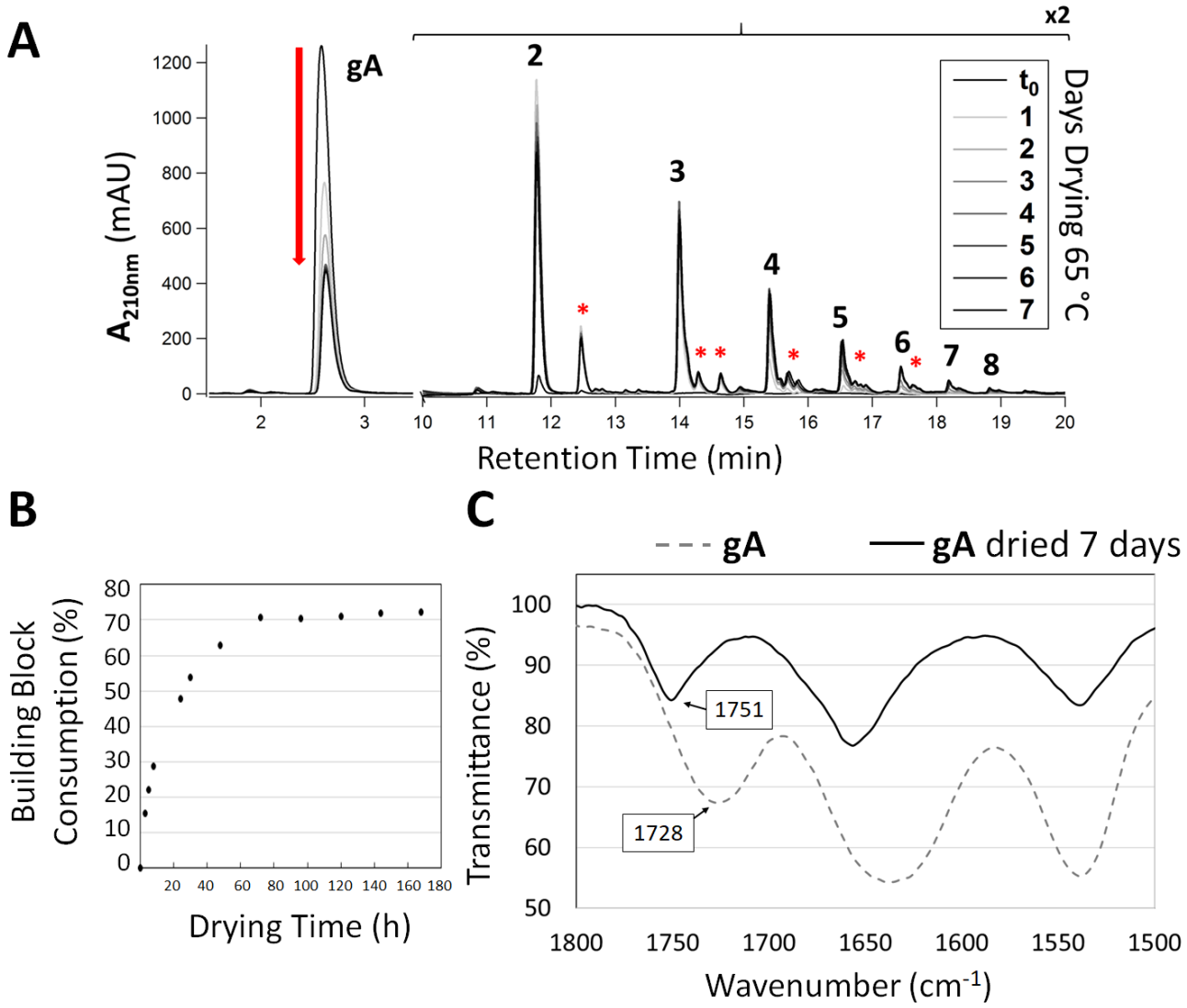

Figure S1. Ester formation between building blocks upon drydown. (A) HPLC chromatograms overlaid for 10 mM **gA** that was dried unbuffered at 65 °C for up to seven days shows a gradual increase in polymer length with concomitant building block consumption (arrow). Red asterisks indicate side products attributed to building block degradation. (B) Integrated areas of **gA** at various time points indicate gradual decrease in building block present, depicted here as consumption or percent conversion. (C) FTIR spectra of a fresh **gA** sample vs. **gA** that was dried at 65 °C for 51 days. The C=O band shifts from a free acid (1728 cm^{-1}) to an ester (1751 cm^{-1}) following dry-heating.

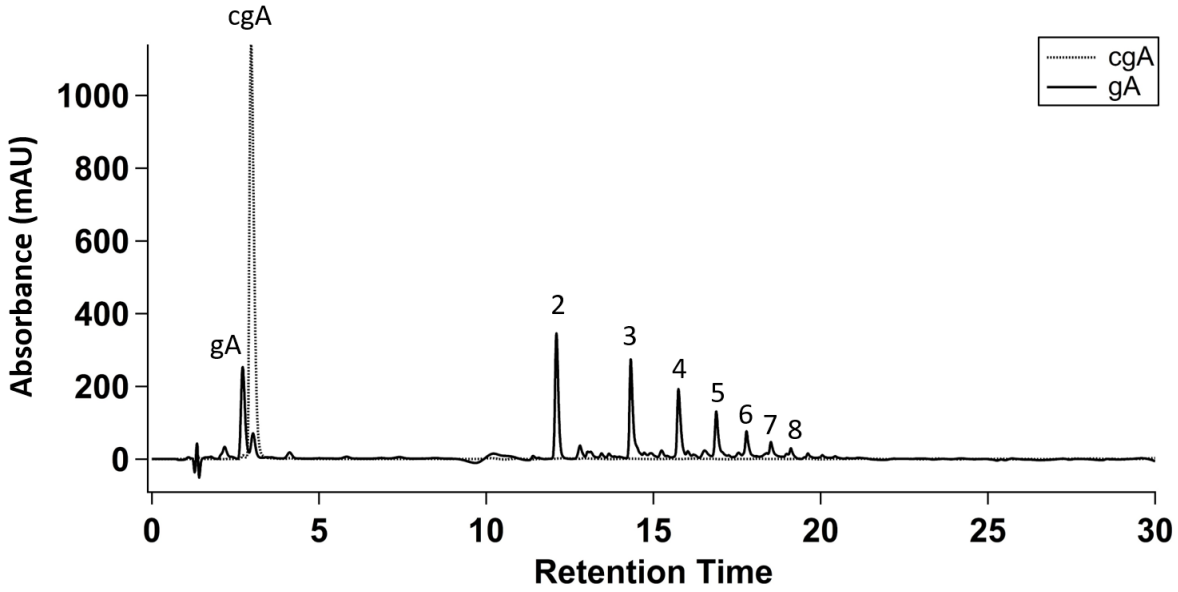

Figure S2. Formation of 2,5-morpholinediones upon drying of building blocks. Overlay between the 3-methyl-2,5-morpholinedione standard (c(**gA**)) (*grey*, dotted) and the products formed during dry-down reactions of **gA** monomers unbuffered for 10 days at 65 °C (*red*). Absorbance values are shown for **gA** at 210nm and for c(**gA**) at 220 nm.

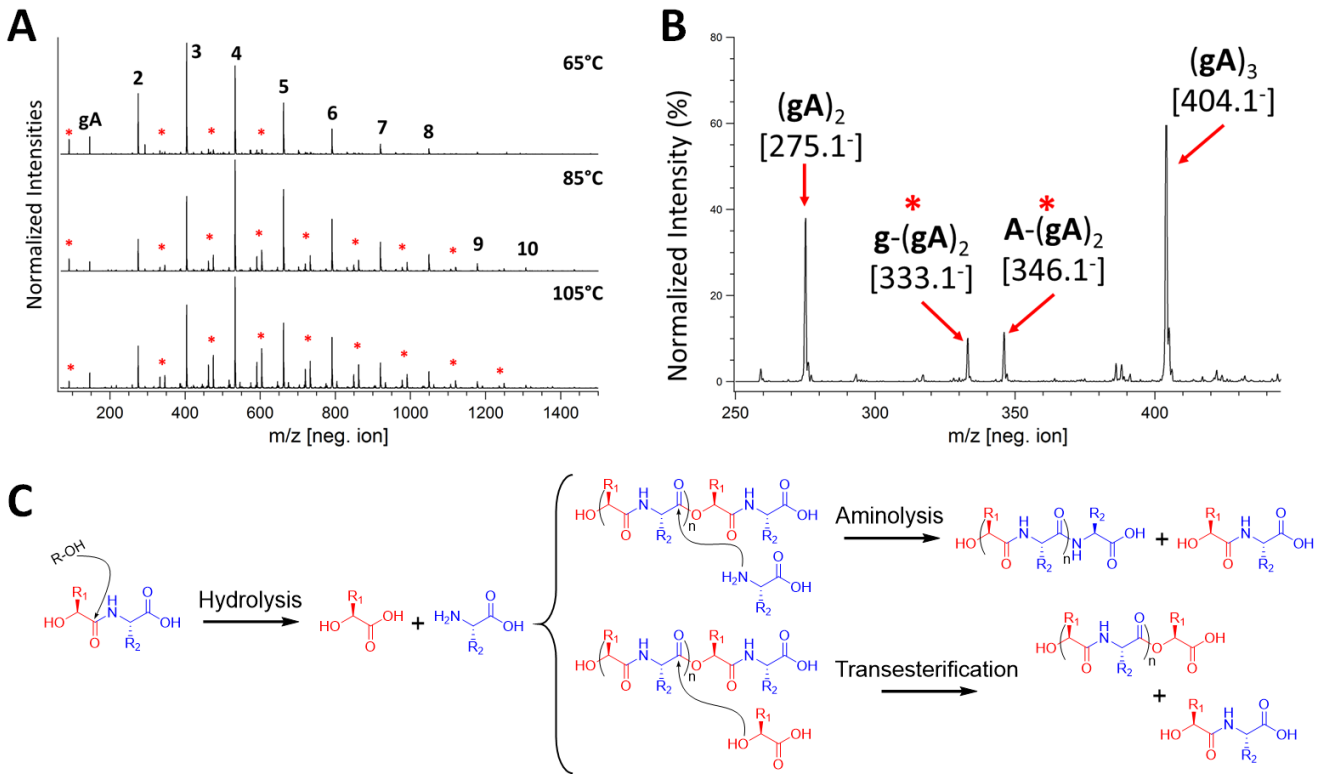

Figure S3. Polymerization and building block degradation rates increase at increased drying temperatures. (A) 10 mM unbuffered **gA** was dried at varying temperatures for 7 days and the products were analyzed via negative mode ESI-MS. Asterisks represent peaks which are a result from building block degradation and subsequent side product formation. (B) Close-up of side product peaks produced at 85 °C, with masses of interest and side product compositions labeled as the observed $[M-H]^-$ ions. Sequences are unknown. (C) Side product polymers form in multiple steps. The first step is building block degradation, which frees an amino and or hydroxy acid. This is then followed by the incorporation of a free amino or hydroxy acid into a growing depsipeptide polymer, giving rise to sequences that differ from those made solely from intact building blocks. Other mechanistic routes are possible.

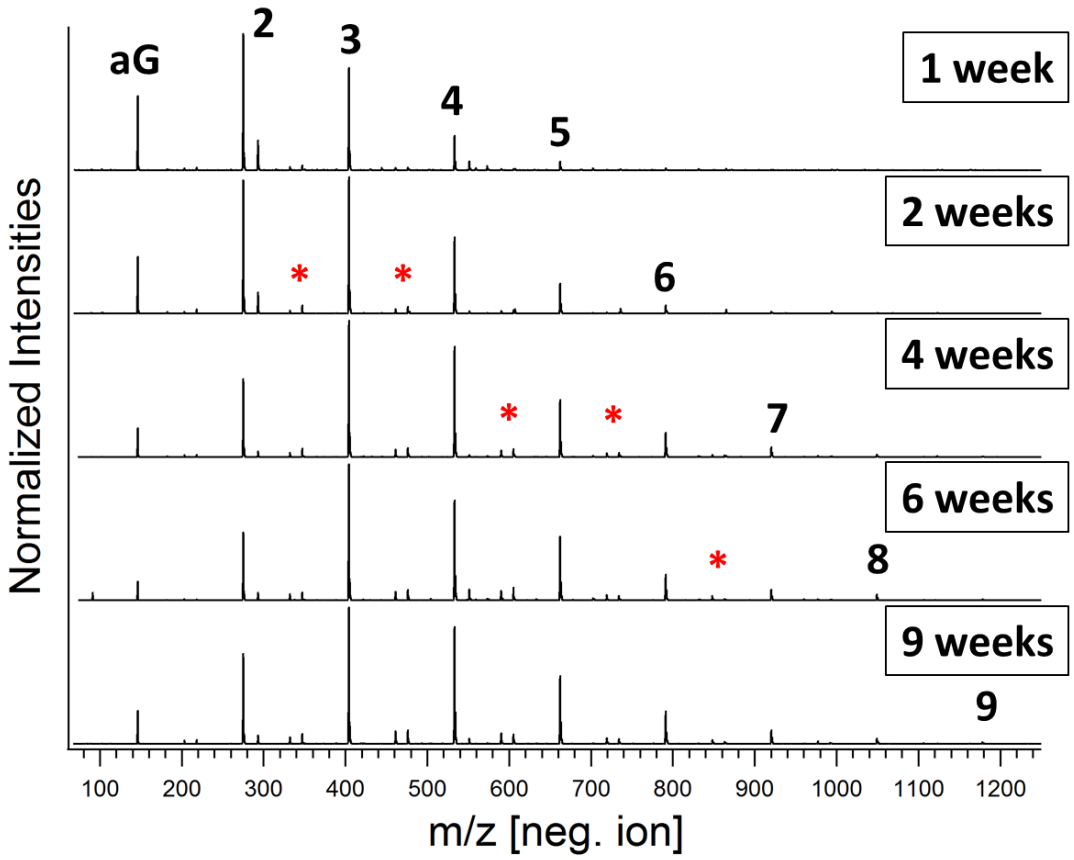

Figure S4. Dry heating duration effects on building block polymerization. ESI-MS analysis for time-dependent drying of 10 mM **aG** building block (unbuffered, pH 3) for up to 9 weeks. Product depsipeptides up to (**aG**)$_9$ are observed with a concomitant increase in side product formation (asterisks).

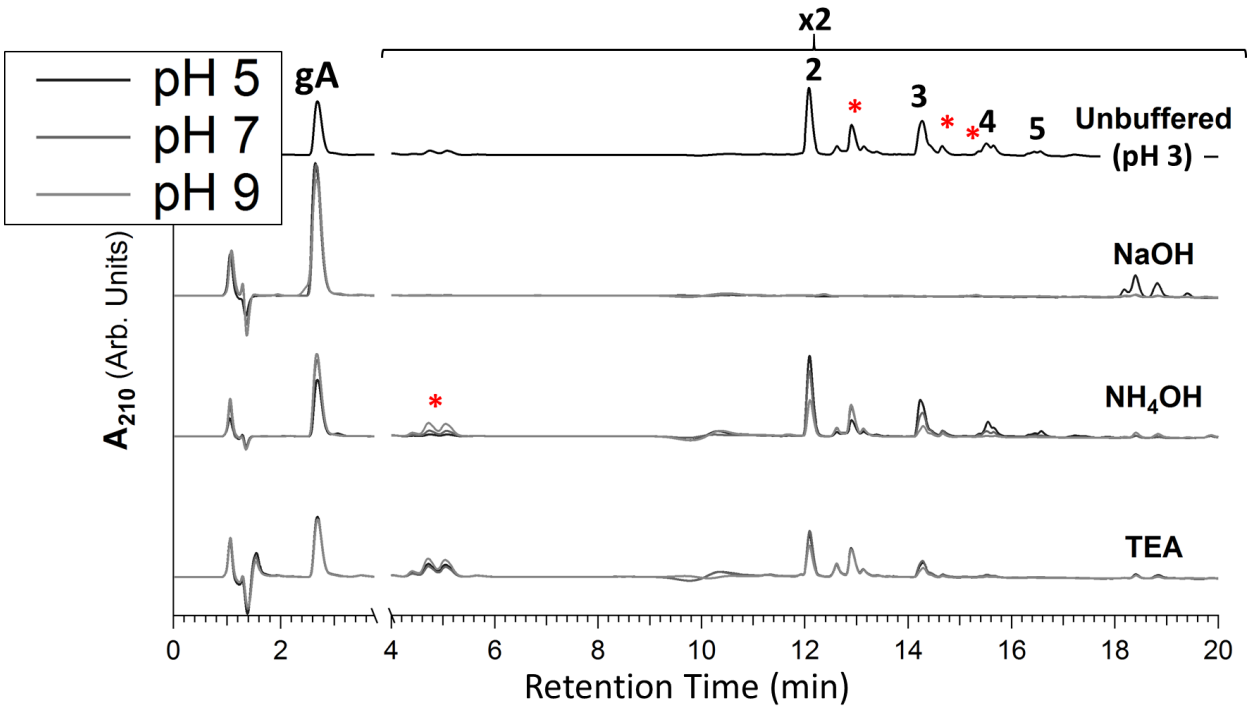

Figure S5. Effect of pH on polymerization of gA. HPLC chromatograms of 10 mM **gA** that was dried under different pH conditions for seven days at 65 °C. Unbuffered **gA** sample in water is acidic (~pH 3). pH was adjusted to 5.0, 7.0 and 9.0 using NH_4OH, triethylamine (TEA) or NaOH solutions. Polymerization of **gA** decreases as the pH increases using the volatile buffers NH_4OH or TEA, while polymerization is halted almost entirely when adjusted using NaOH. We attribute this result to the volatility of NH_3 and TEA, which have boiling points below that of water and are evaporating away prior to the samples reaching the dry state. Asterisks: side products.

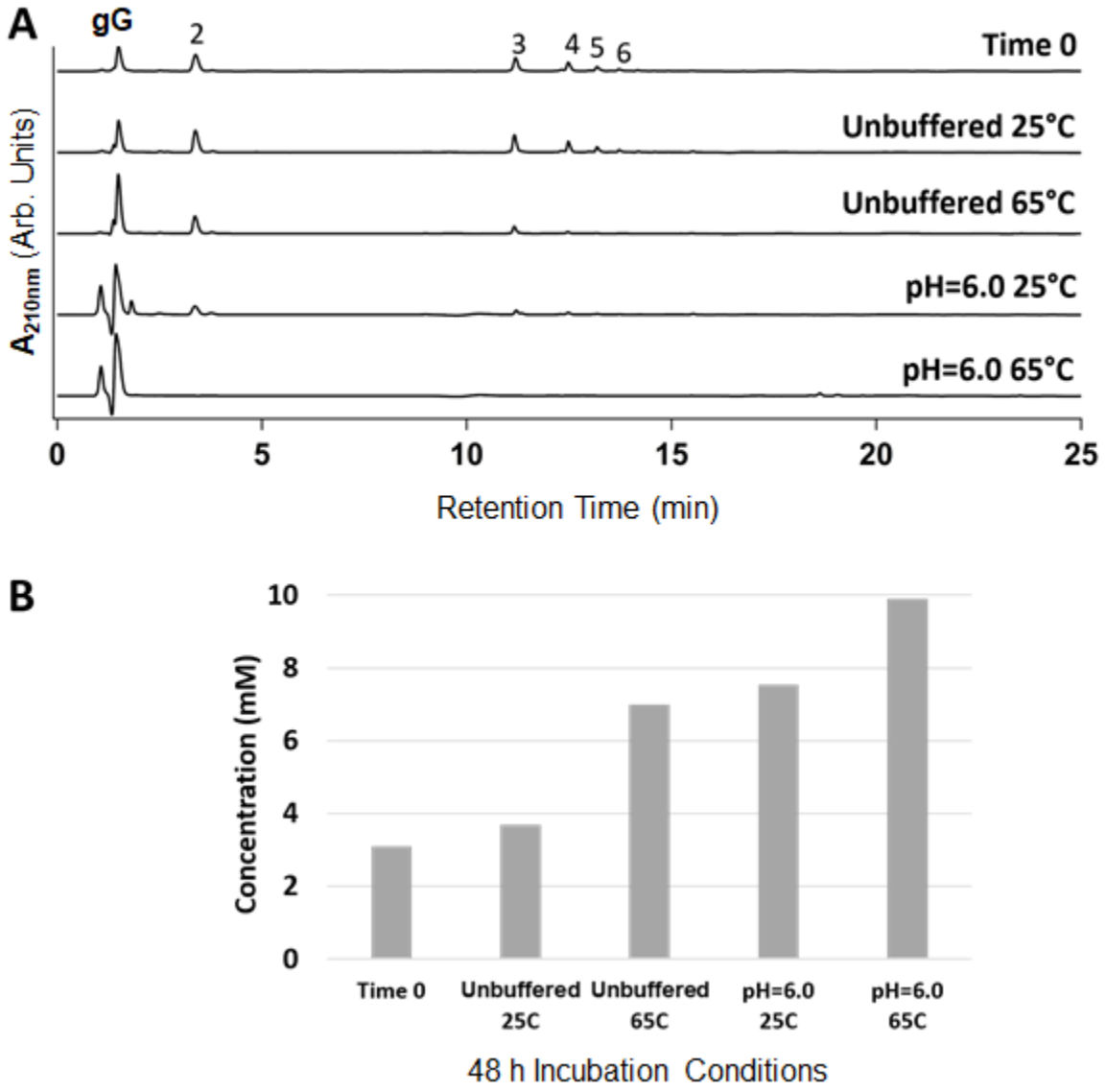

Figure S6. Temperature and pH-dependent degradation of gG oligomers.gG was dried at 65 °C for 23 days and the resulting depsipeptides were subjected to incubation in water (unbuffered, pH 3) or sodium phosphate buffer at pH 6.0 for two days at 25 °C or 65 °C. (A) HPLC spectra showing the degradation of **gG** oligomers and (B) Quantification of **gG** building block recovery following incubation under the different conditions.

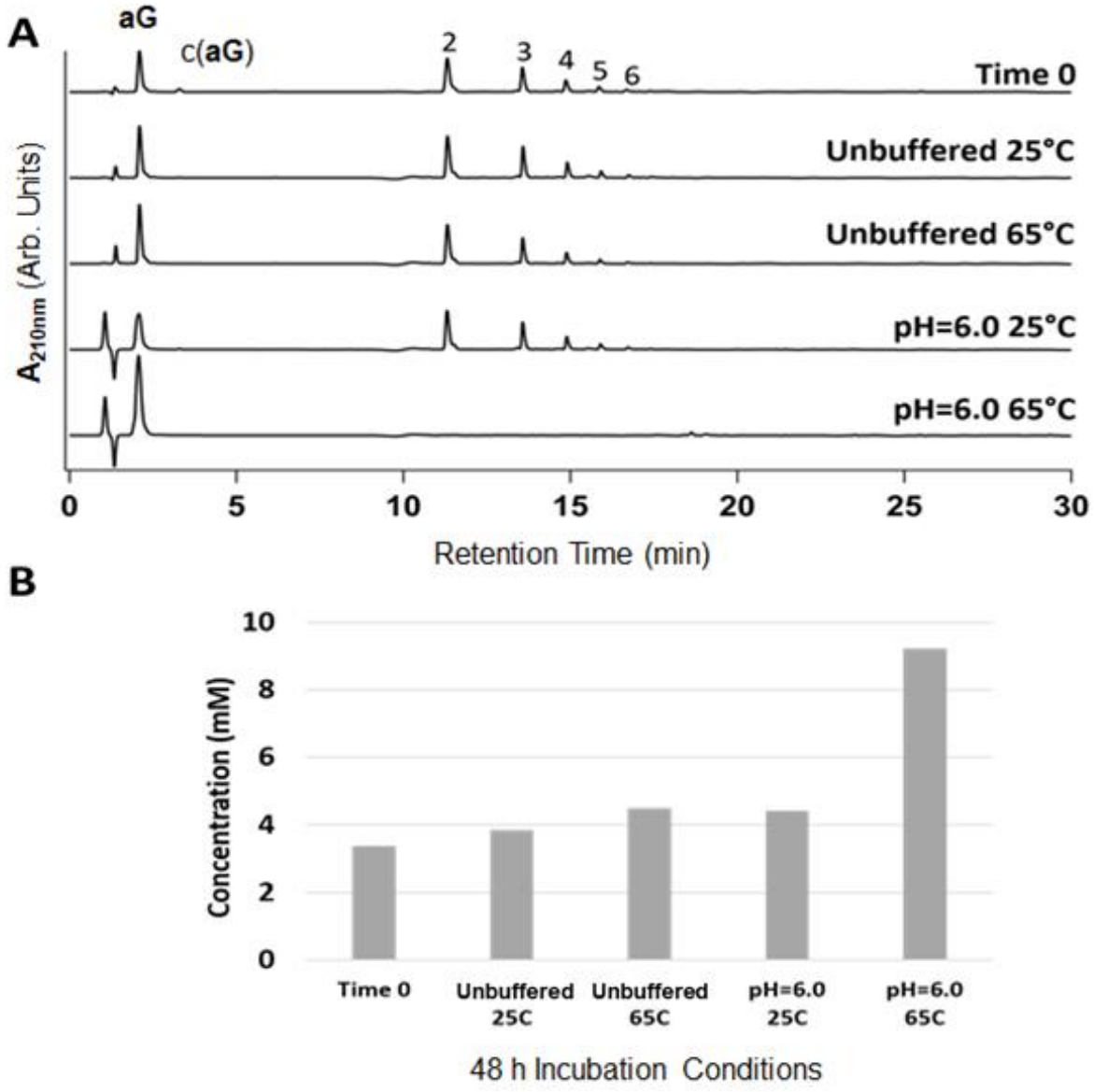

Figure S7. Temperature and pH-dependent degradation of aG oligomers. aG was dried at 65 °C for 23 days and the resulting depsipeptides were subjected to incubation in water (unbuffered, pH 3) or sodium phosphate buffer at pH 6.0 for two days at 25 °C or 65 °C. (A) HPLC spectra showing the degradation of **aG** oligomers and (B) Quantification of **aG** building block recovery following incubation under the different conditions.

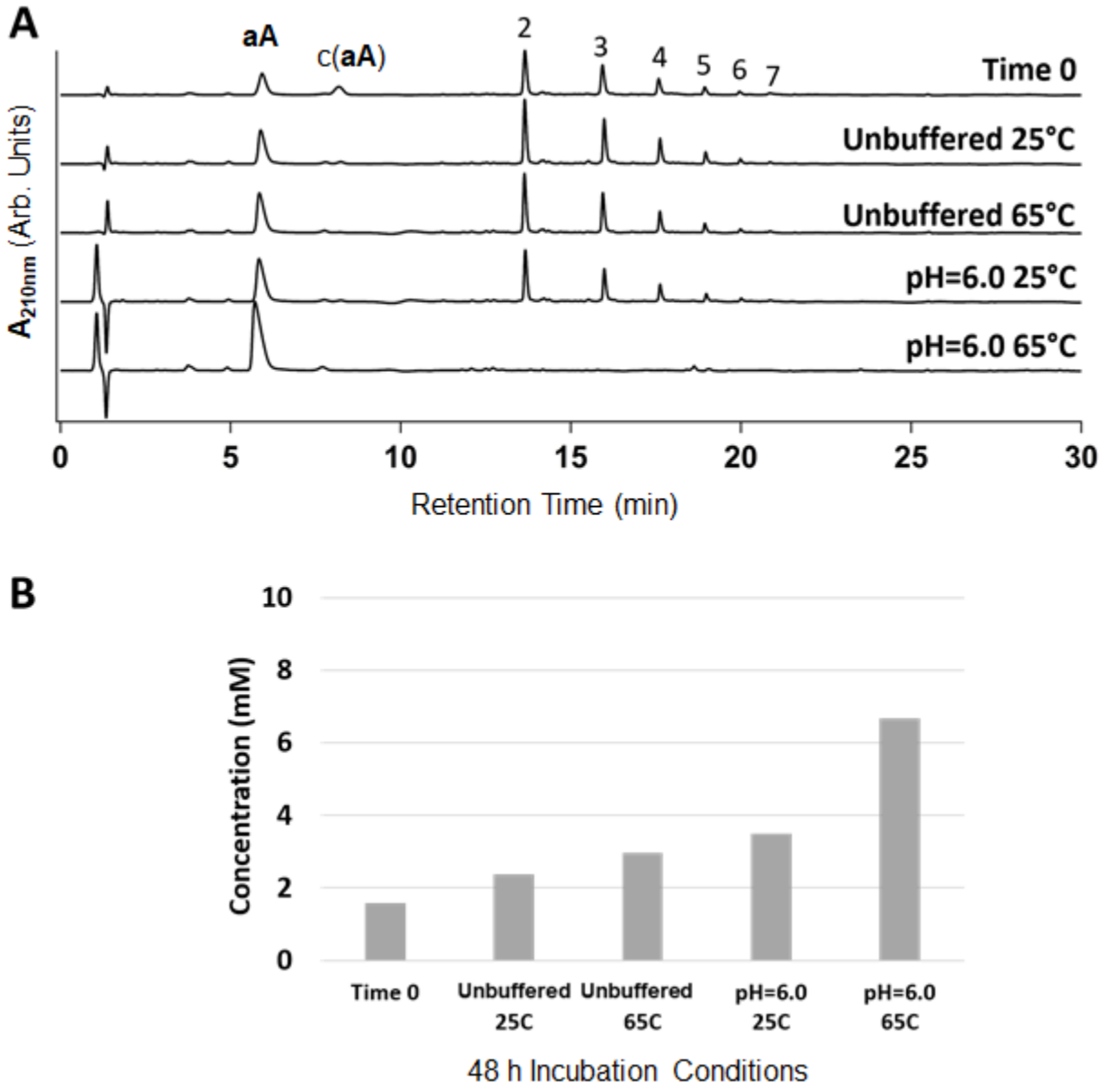

Figure S8. Temperature and pH-dependent degradation of aA oligomers. aA was dried at 65 °C for 23 days and the resulting depsipeptides were subjected to incubation in water (unbuffered, pH 3) or sodium phosphate buffer at pH 6.0 for two days at 25 °C or 65 °C. (A) HPLC spectra showing the degradation of **aA** oligomers and (B) Quantification of **aA** building block recovery following incubation under the different conditions.

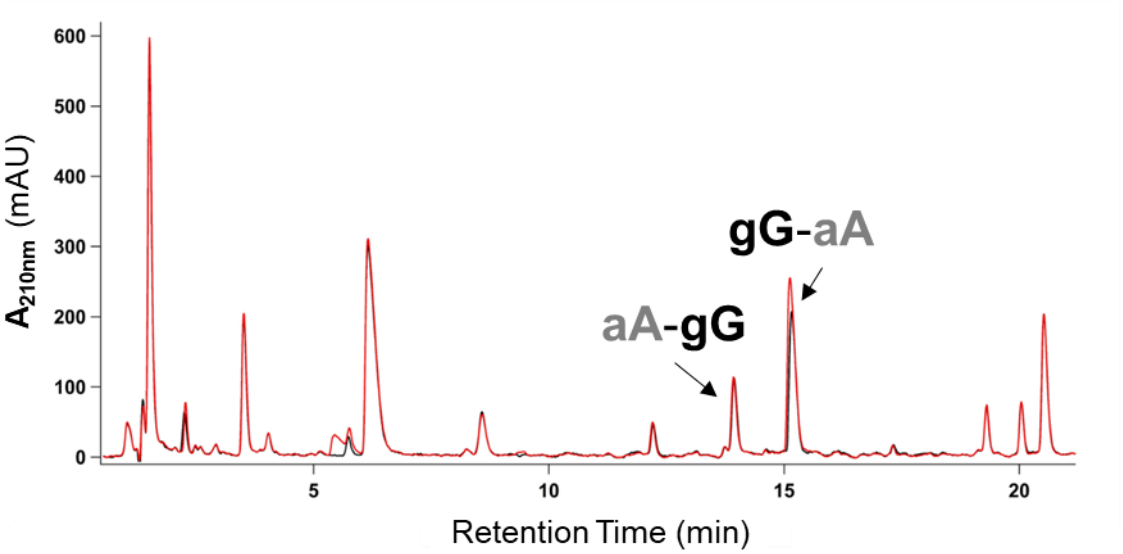

Figure S9. Identification of aAgG with synthetic standard. Co-polymerization of **gG** with **aA** results in four possible 2-mers, amongst myriad other copolymers: **gGaA** and **aAgG**, and the homopolymers $(\mathbf{gG})_2$ and $(\mathbf{aA})_2$. We are able to resolve each of these species by C18 chromatography. Identification of the peaks was done using spiking of the standard **aAgG** to a pre-dried mixture of **gG** and **aA**. The non-spiked mixture trace is colored *black*, whereas a mixture that is spiked with the **aAgG** standard is overlaid in *red*. Note: Identity of the **gGaA** 2-mer is *inferred* as we were unable to prepare a synthetic standard of this molecule.

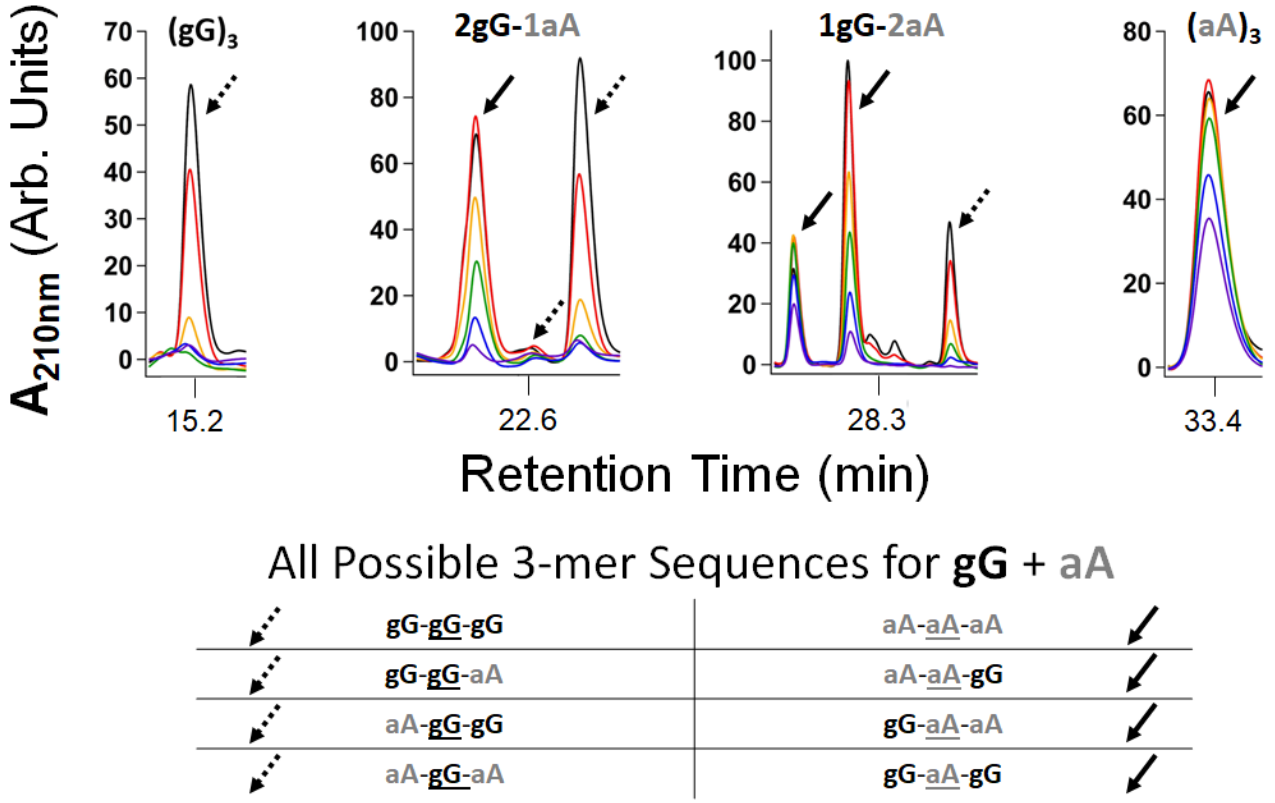

Figure S10. Increased hydrolytic stability for specific depsipeptide 3-mer sequences. An equimolar mixture of **gG** and **aA** was dried for seven days unbuffered at 65 °C and incubated for up to ten days at 65 ˚C in unbuffered solution. The varying aqueous lifetimes are shown for the trimers. Out of the 8 possible trimeric sequences, the **xX-aA-xX** motifs (4 possibilities, see bottom) are the presumptive species labeled with bold arrows that exhibit increased aqueous lifetime over the other relatively labile sequences (**xX-gG-xX**, dashed arrows). The purported labile **xX-gG-xX** species show depletions in abundances by ~5 days of incubation (*green* traces), whereas the **xX-aA-xX** species maintain significantly higher abundances throughout the entire 10 day incubation. Incubation time is depicted by trace color: *black* – time 0 (post-drying), *red* – 1 day, *orange* – 3 days, *green* – 5 days, *blue* – 7 days, and *purple* – 10 days. Bottom: All possible 3-mer sequences for **gG** + **aA** with corresponding dashed or solid markers to guide the eyes.

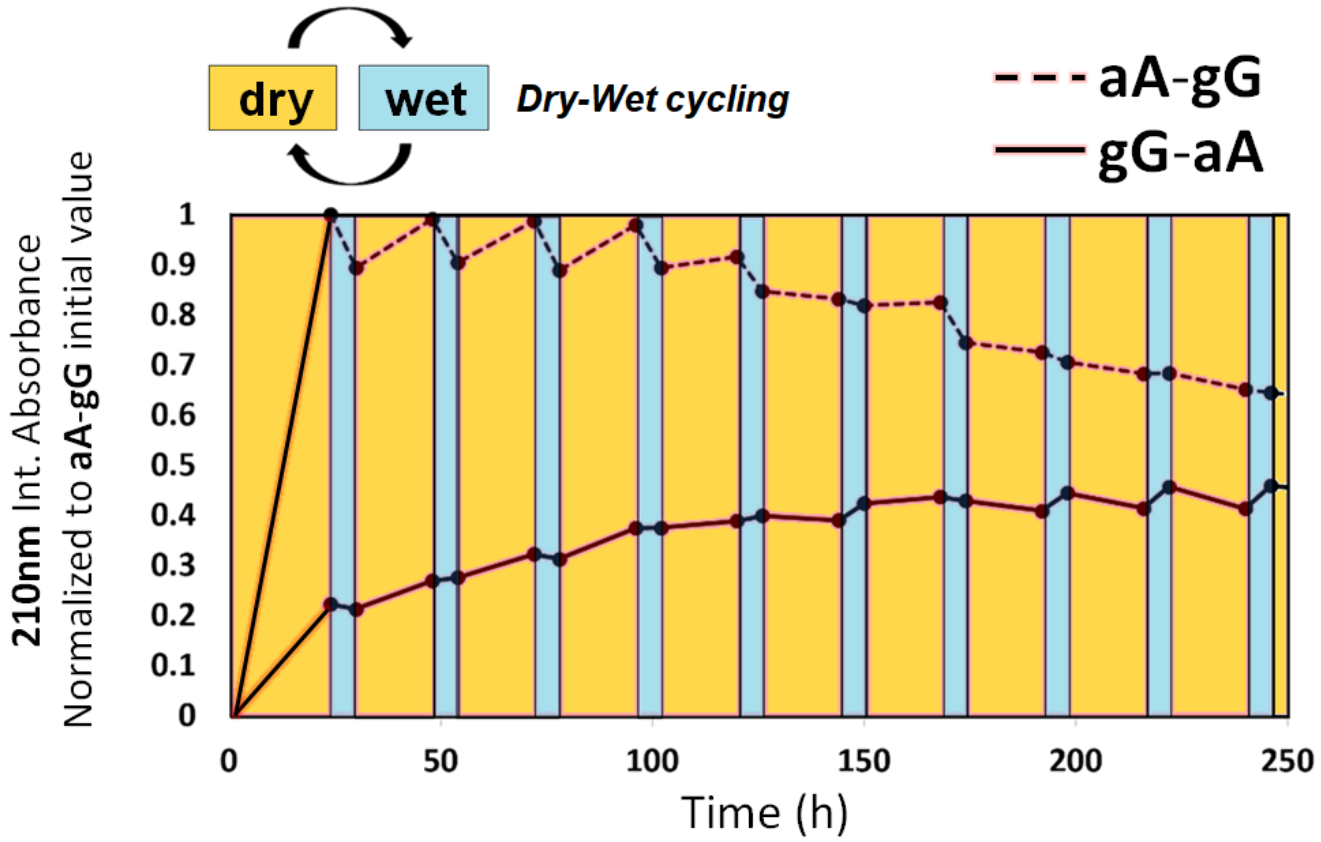

Figure S11. Compositional variation in complex depsipeptide mixtures during dry-wet cycles. A 1:1 mixture of **gG** and **aA** was dried for 24 h before subjected to daily wet-dry cycles at 65 °C, with a 6 h wet phase (in *blue*) and 18 h dry phase (*orange*). Samples were analyzed by HPLC at the end of each phase and the appropriate peaks were integrated. Graph shows relative integrated abundance of the two heterodimers, **gG-aA** to **aA-gG**, normalized to the integration of the **aA-gG** peak after the 1st drying period. The product distribution fluctuates over the course of ten cycles.

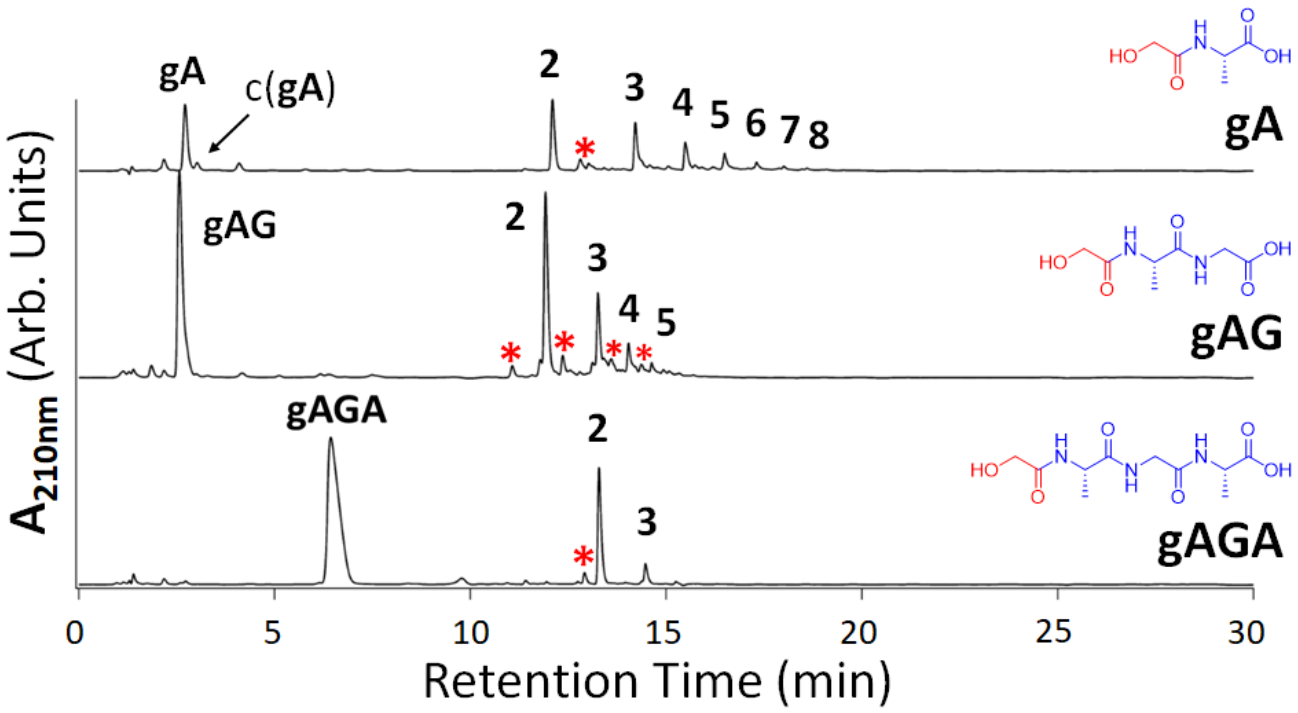

Figure S12. Building block length effect on dry-heating polymerization. HPLC-UV Chromatograms for various sizes of building blocks dried for 29 days at 65 °C. c(**gA**) is the cyclic 2,5-MD of the **gA** building block. Red asterisks are various side products generated from building block degradation in the dry-heating process.

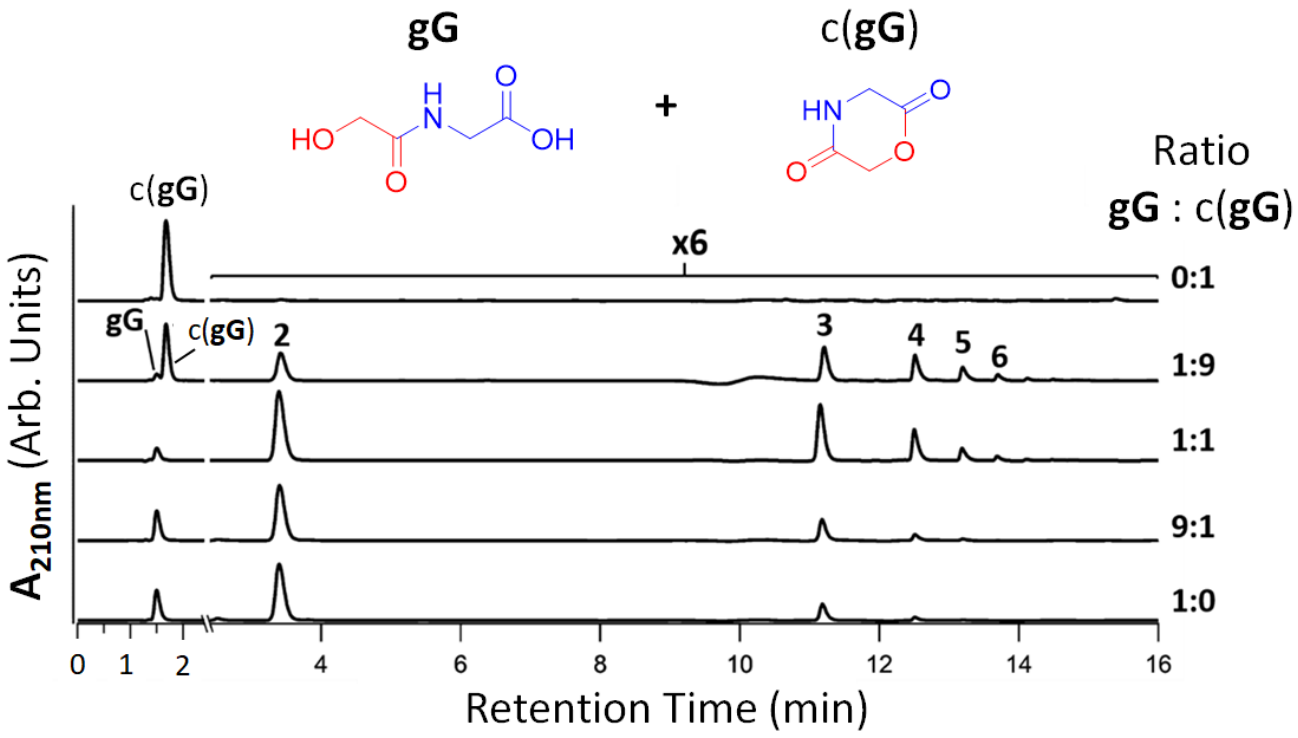

Figure S13. 2,5-morpholinediones catalyze the polymerization of building blocks during dry-heating. Polymerization of various molar ratios of **gG** with c(**gG**) when dried together with the total number of moles held constant. HPLC analysis of the oligomers obtained after drying unbuffered from solid starting material for one day at 65 °C is shown.

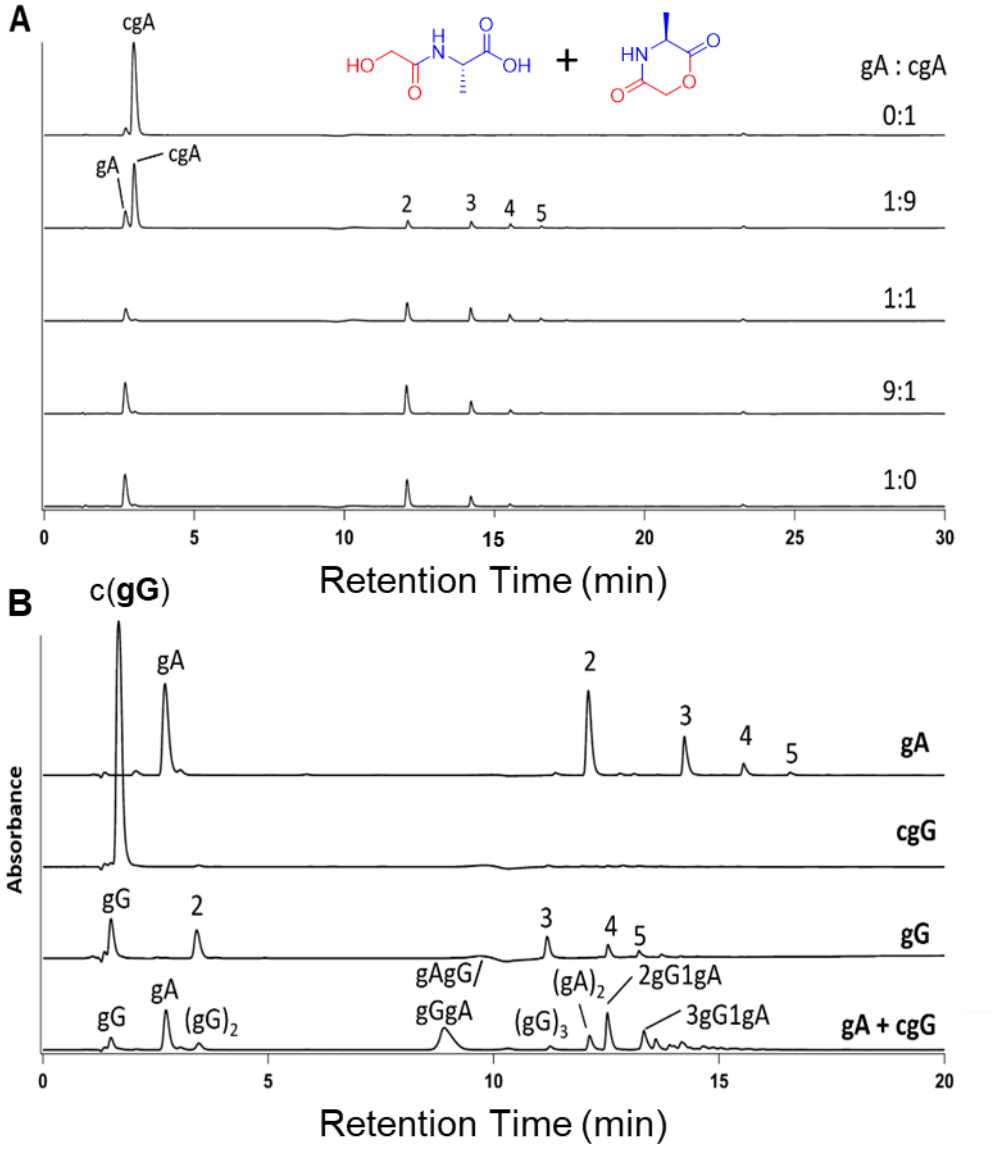

Figure S14. Ring-opening polymerization of linear building blocks and morpholinediones. (A) Polymerization of various molar ratios of **gA** with **c(gA)**. (B) HPLC analysis of copolymerization of **gA** with c(**gG**) after drying the peptides for one day at 65 °C indicates the formation of heteropolymers and verifies that the morpholinediones incorporate into the growing polymers.

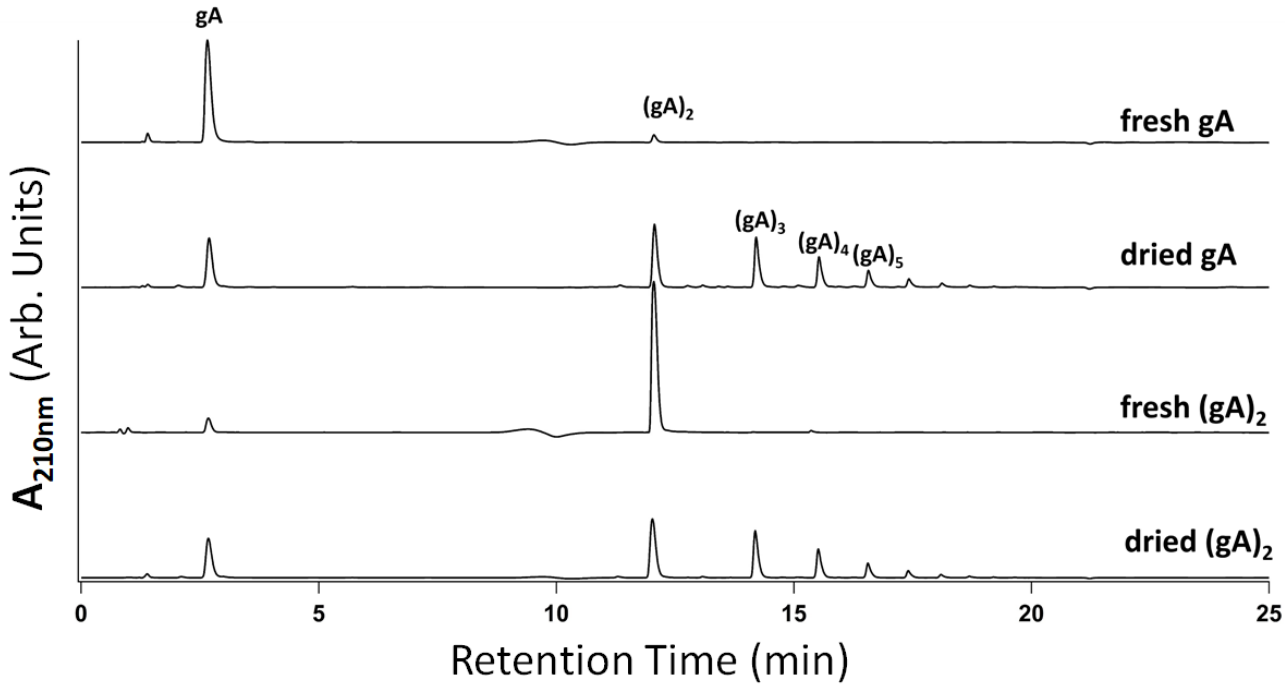

Figure S15. Dynamic polymerization of (gA)$_2$ upon dry-heating. Side-by-side heating and drying of **gA** and (**gA**)$_2$ starting material for 7 days at 65 °C (unbuffered) results in a similar product distribution, indicating the dynamic nature of building block polymerization during the dry-down. The "fresh" traces were recorded using non-dried samples.

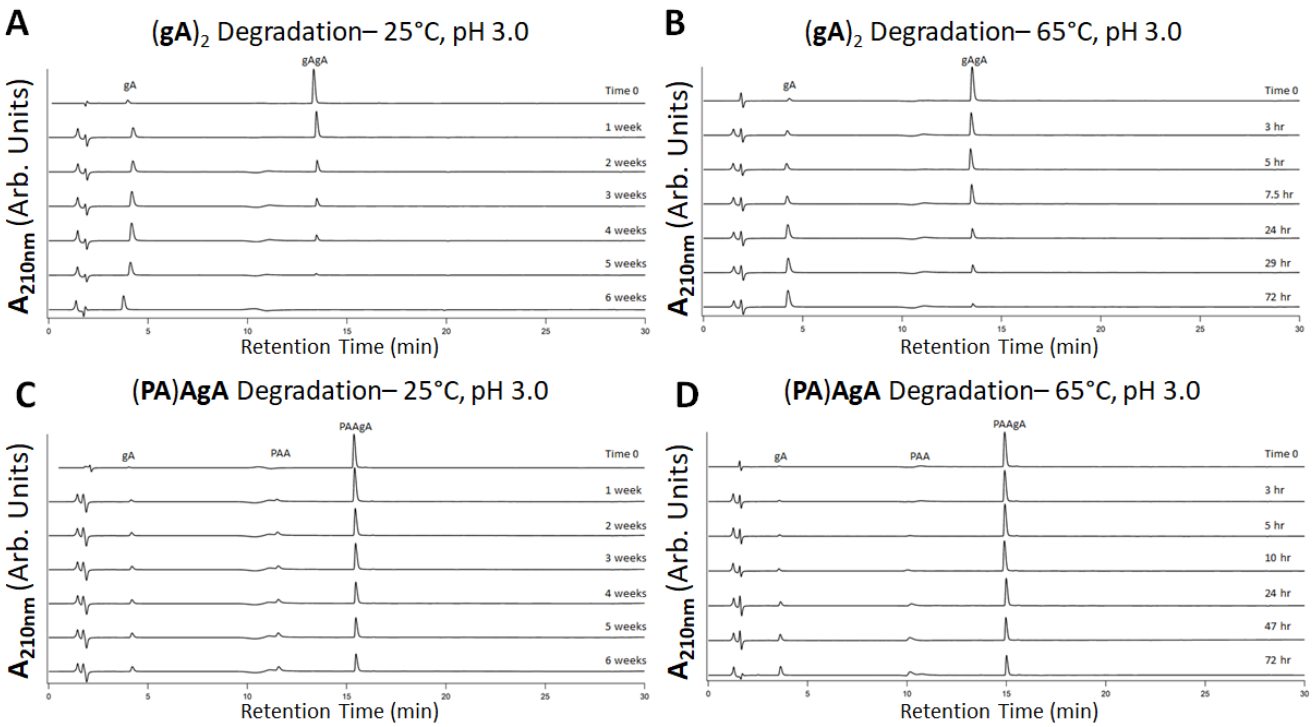

Figure S16. Degradation of (gA)$_2$ and (PA)AgA under acidic conditions indicates differing modes of breakdown. (A,B) 10 mM of (**gA**)$_2$ was incubated at (A) 25 ℃ or (B) 65 ℃ in unbuffered aqueous solutions to monitor degradation rates. (C,D) 10 mM of (**PA)AgA** was incubated at (C) 25 ℃ or (D) 65 ℃ in unbuffered aqueous solutions to monitor degradation rates. HPLC-UV abundances indicate that degradation occurs substantially faster for (**gA**)$_2$ than for (**PA**)**AgA** under similar, mildly acidic conditions.

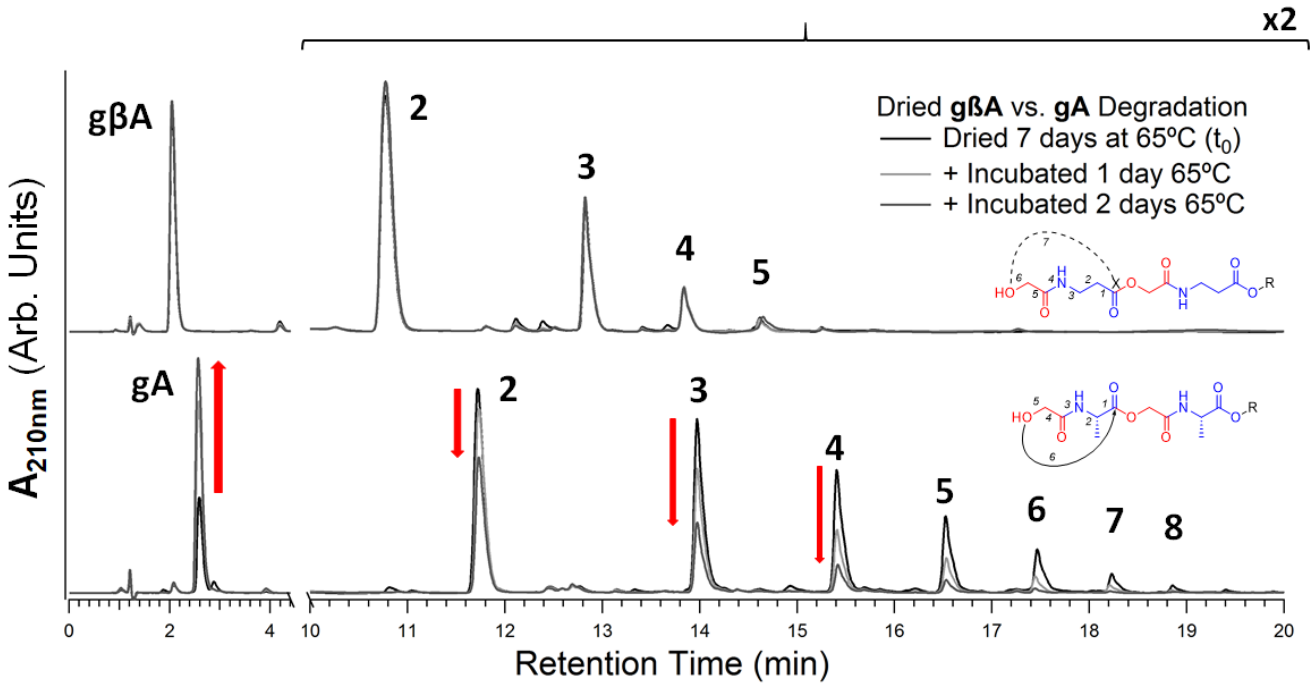

Figure S17. Comparison of gβA and gA depsipeptide degradation. gA and **gβA** were each dried unbuffered at 65 °C for seven days (t_0) and the resulting depsipeptide mixtures were subjected to aqueous degradation conditions. Following unbuffered (pH 3.0) incubation at 65 °C in water, **gβA** depsipeptides show a greatly diminished rate of degradation when compared to the **gA** polymers incubated under identical conditions, likely due to their inability to undergo backbiting degradation (drawings). Red arrows highlight **gA** building block recovery and depsipeptide breakdown.

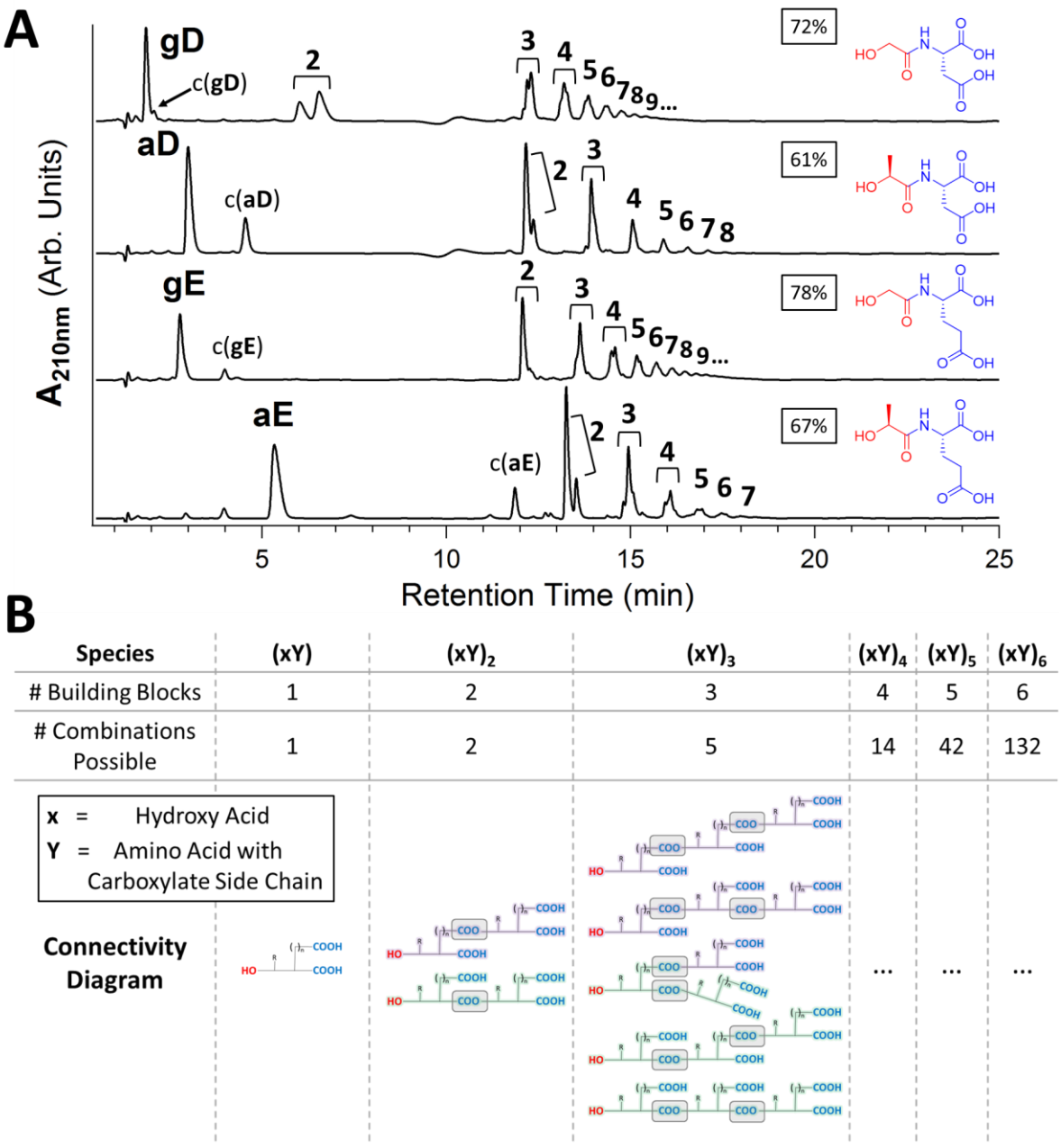

B

Species	(xY)	$(xY)_2$	$(xY)_3$	$(xY)_4$	$(xY)_5$	$(xY)_6$
# Building Blocks	1	2	3	4	5	6
# Combinations Possible	1	2	5	14	42	132

x = Hydroxy Acid
Y = Amino Acid with Carboxylate Side Chain

Connectivity Diagram

Figure S18. Dry-heating of xD and xE building blocks produces depsipeptide isomers of varying regiochemistry. (A) HPLC chromatograms showing unbuffered drying of **gD**, **aD**, **gE**, and **aE** for 7 days at 65 °C. Brackets indicate multiple isomers present, as verified by LCMS. Longer sets of isomers tend to elute more closely in time and overlap, causing apparent peak broadening of longer species. Percent conversions to polymers are given in the boxes above each trace. (B) Scheme indicating possible regioisomers for varying lengths of multifunctional building blocks. Notation: *x* – any hydroxy acid; *Y* – any carboxylate side-chained amino acid. Ester bonds are highlighted in grey. For brevity, only regioisomers up to 3-mers are shown. The number of isomeric combinations possible for a given length of polymer follows the set of numbers from mathematics known as the *Catalan Numbers*. 2-mers and 3-mers highlighted in *green* are able to undergo at least one backbiting degradation event, while those highlighted in *purple* degrade primarily through hydrolysis.

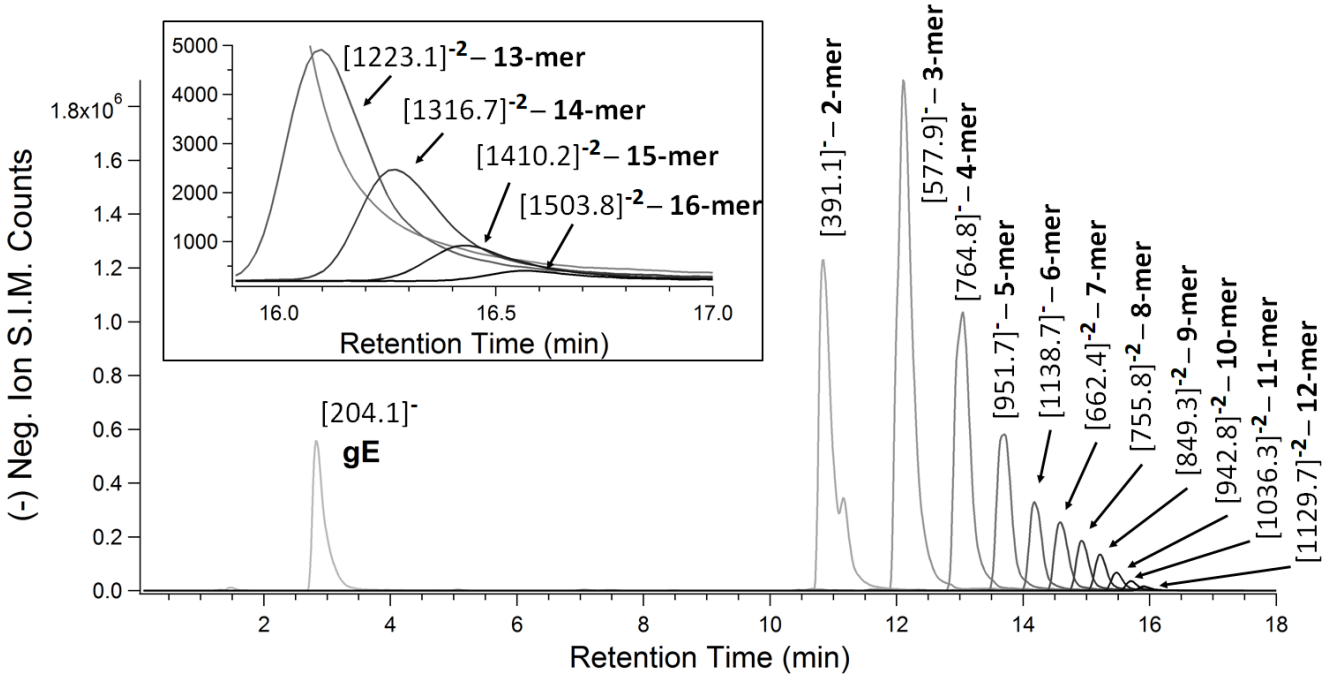

Figure S19. Liquid Chromatography Mass Spectrometry - Single Ion Monitoring (LCMS-SIM) of $(gE)_n$ polymers. 10 mM **gE** was dry-heated unbuffered at 65 °C for 7 days and subsequently analyzed by LCMS-SIM (See Materials and Methods) over several injections. Negative mode SIM traces were obtained and overlaid. Full spectrum with inset zoomed in for a close-up of 13-16-mer SIM traces. Detected/monitored mass to charge ratios as well as charges for each individual isomer are annotated. Note that the larger species ionized most efficiently as doubly charged ions.

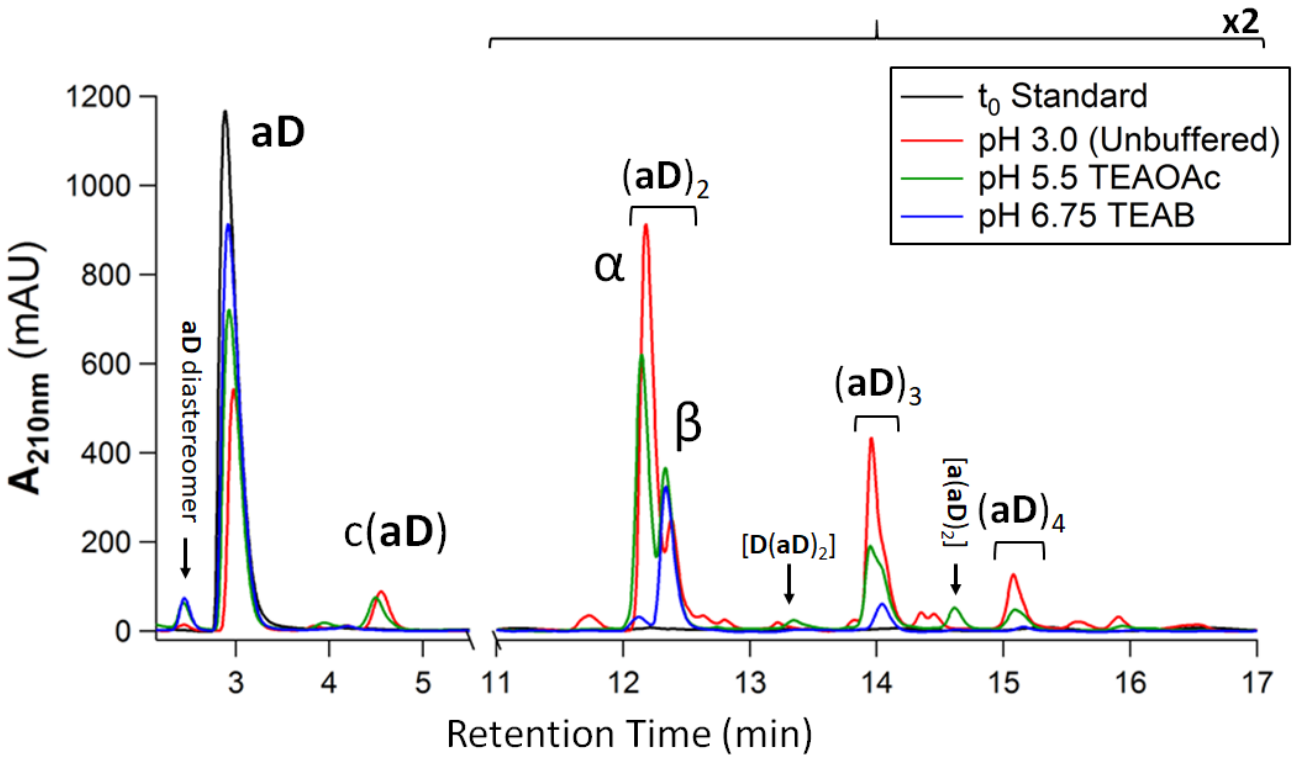

Figure S20. pH-dependent modulation of $(aD)_n$ depsipeptide distribution . HPLC chromatograms overlaid showing 10 mM **aD** dry-heated for 24 hours at 75 °C, at either pH 3 (unbuffered, *red*), pH 5.5 (triethylammonium acetate, *green*), or pH 6.75 (triethylammonium bicarbonate, *blue*). Distribution of depsipeptide isomers shifts with changes in dry-down pH.

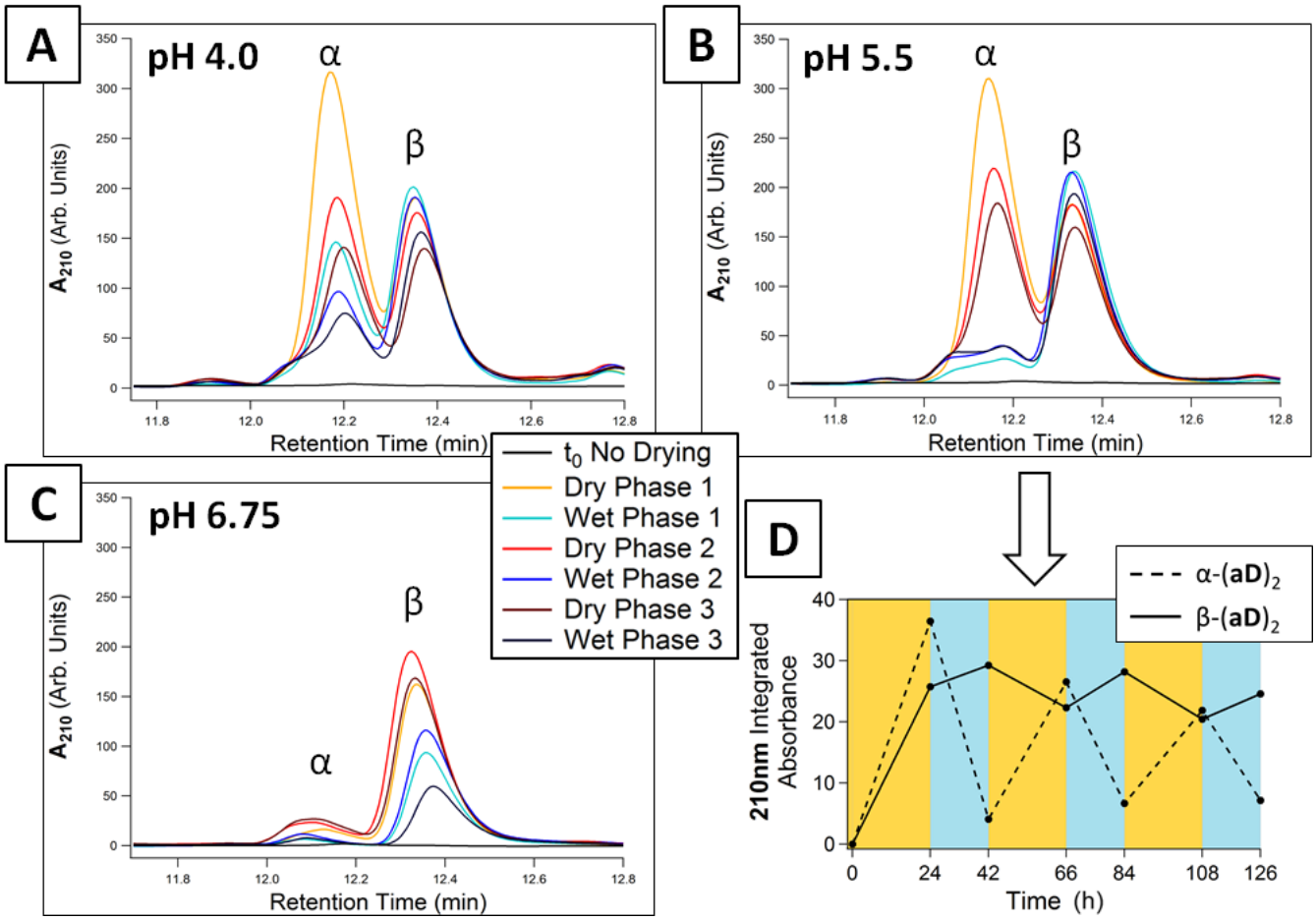

Figure S21. 2-mer Abundances during dry-wet cycling of aD at various pH. HPLC-UV chromatograms. Cycles were 24 hour, 75 °C Heating and drying, followed by 18 hour, 65 °C aqueous incubation each in various buffers, replenished after every dry phase to restore solution pH. Buffers, 10 equivalents for all: pH 4.0 TEAOAc (A), pH 5.5 TEAOAc (B), and pH 6.75 TEA-Bicarbonate (C). α and β peak identities are known based on authentic standards (Main text, Figure 4C). (D) Integrated 2-mer areas from pH 5.5 cycling plotted with respect to cycle time.

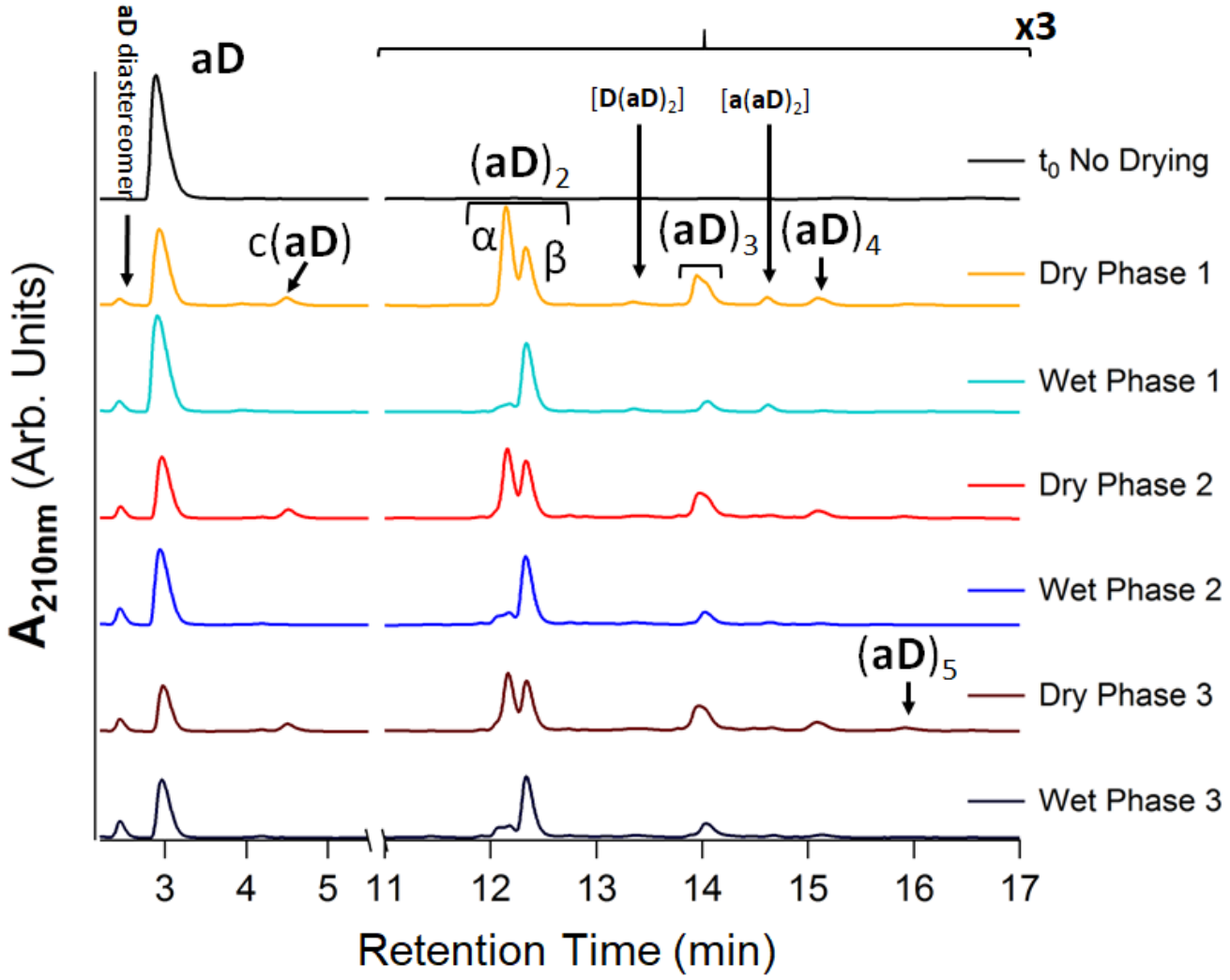

Figure S22. Stack plot of dry-wet cycling aD at pH 5.5. Building block **aD** dry-wet cycled in pH 5.5 TEAOAc showed comparable abundances of both (**aD**)$_2$ isomers formed following 24 hr dry-heating phases (orange traces), and preferential preservation of β-(**aD**)$_2$ following 18 hr wet-phases (blue traces). Peaks labeled [**D**/**a**(**aD**)$_2$] displayed a mass consistent with a dehydration product from **D**/**a** + (**aD**)$_2$. Data and trace coloring are identical to that of Figure 4A in the main text, but the traces are separated along the Y-axis for clarity.

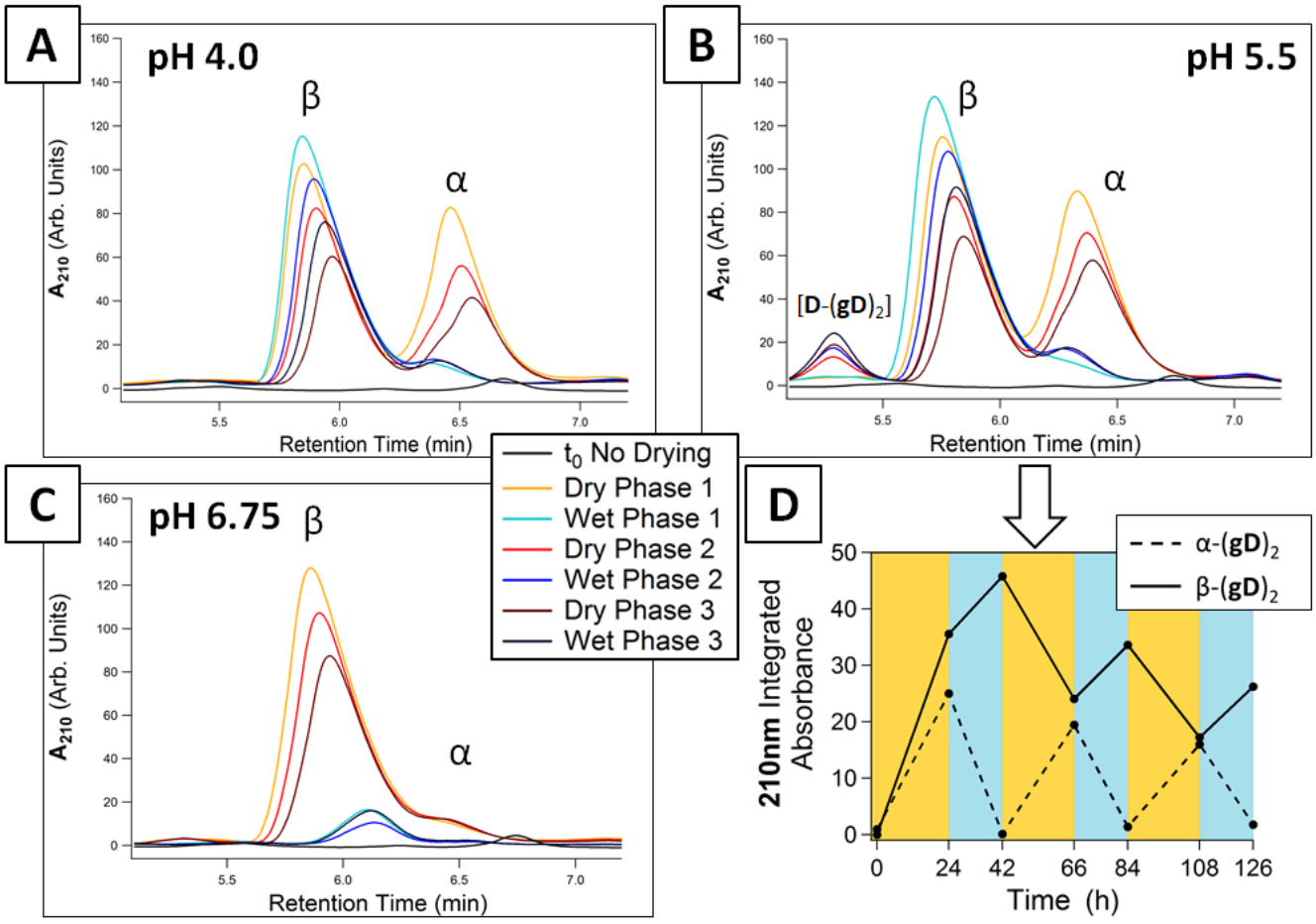

Figure S23. 2-mer Abundances during dry-wet cycling of gD at various pH. HPLC-UV chromatograms monitoring 2-mers of **gD**. Cycles were 24 hour, 75 °C Heating and drying, followed by 18 hour, 65 °C aqueous incubation each in various buffers, replenished after every dry phase to restore solution pH. Buffers, 10 equivalents for all: pH 4.0 TEAOAc (A), pH 5.5 TEAOAc (B), and pH 6.75 TEA-Bicarbonate (C). (D) Integrated 2-mer areas from pH 5.5 cycling plotted with respect to cycle time. The α or β regioisomer identities of the (**gD**)$_2$ species were assigned based on resemblance to degradation profiles of each of the 2-mer (**aD**)$_2$ regioisomers, for which we prepared authentic standards. Briefly: native α-linked 2-mers decay rapidly during wet phases (more so at increased pH, as in (C)), while side chain linked species persist. Lastly, side chain linked 2-mers generally have the highest abundance after dry phases using pH 6.75 buffer (C).

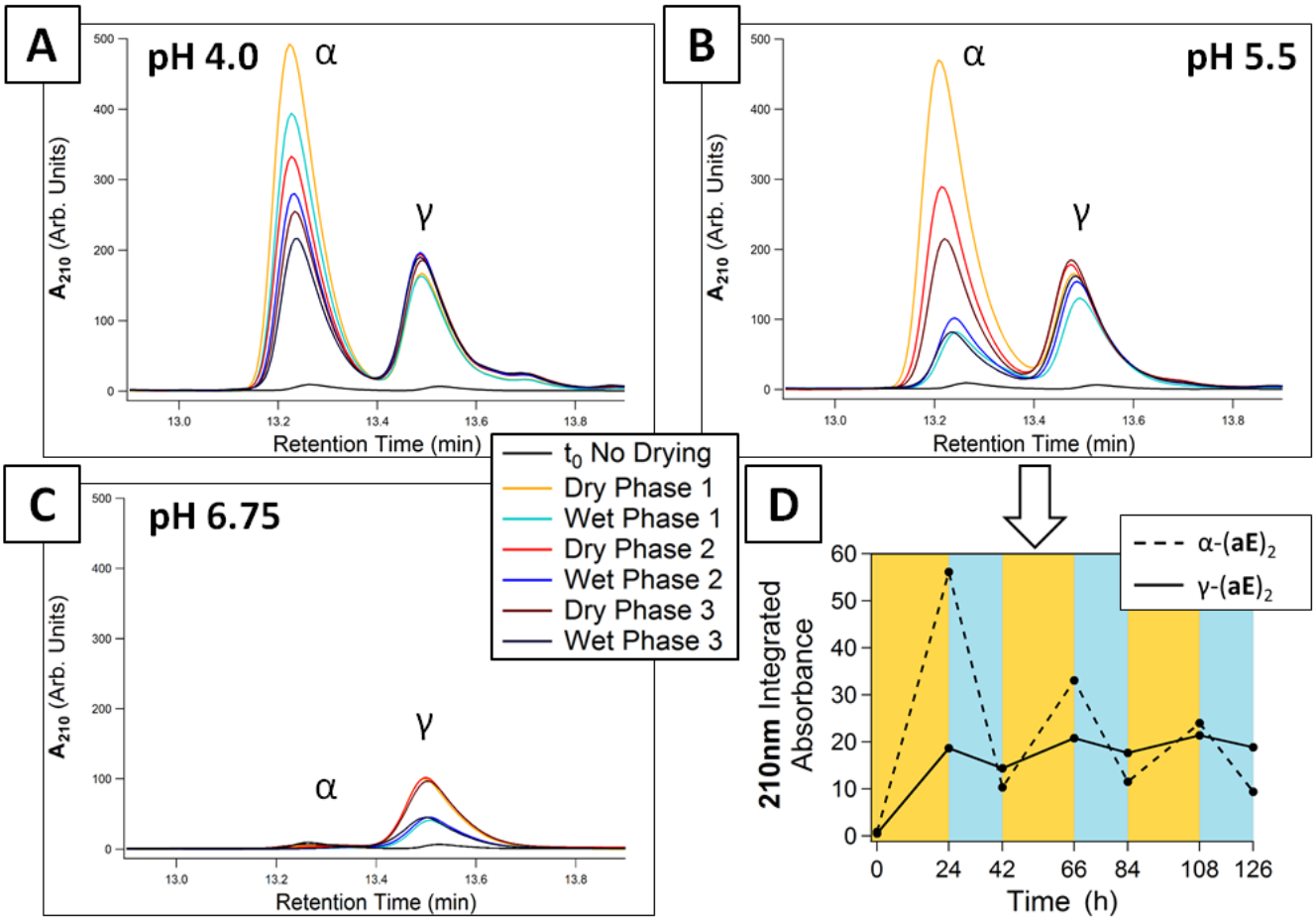

Figure S24. 2-mer Abundances during dry-wet cycling of aE at various pH. HPLC-UV chromatograms monitoring 2-mers of **aE**. Cycles were 24 hour, 75 °C Heating and drying, followed by 18 hour, 65 °C aqueous incubation each in various buffers, replenished after every dry phase to restore solution pH. Buffers, 10 equivalents for all: pH 4.0 TEAOAc (A), pH 5.5 TEAOAc (B), and pH 6.75 TEA-Bicarbonate (C). (D) Integrated 2-mer areas from pH 5.5 cycling plotted with respect to cycle time. The α or γ regioisomer identities of the (**aE**)$_2$ species were assigned based on resemblance to degradation profiles of each of the 2-mer (**aE**)$_2$ regioisomers, for which we prepared authentic standards. Briefly: native α-linked 2-mers decay rapidly during wet phases (more so at increased pH, as in (C)), while side chain linked species persist. Lastly, side chain linked 2-mers generally have the highest abundance after dry phases using pH 6.75 buffer (C).

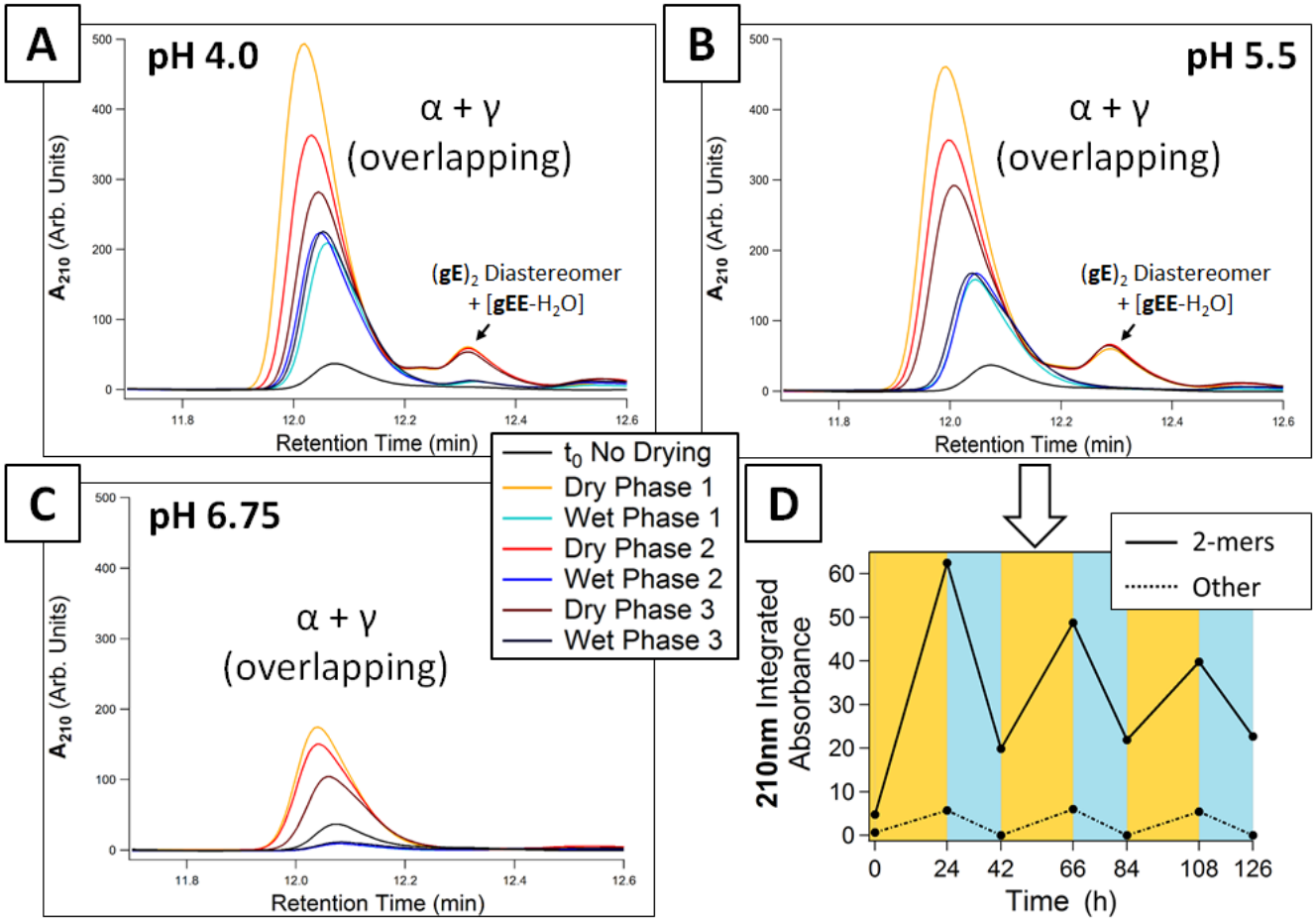

Figure S25. 2-mer Abundances during dry-wet cycling of gE at various pH. HPLC-UV chromatograms monitoring 2-mers of **gE**. Cycles were 24 hour, 75 °C Heating and drying, followed by 18 hour, 65 °C aqueous incubation each in various buffers, replenished after every dry phase to restore solution pH. Buffers, 10 equivalents for all: pH 4.0 TEAOAc (A), pH 5.5 TEAOAc (B), and pH 6.75 TEA-Bicarbonate (C). (D) Integrated major peak areas from pH 5.5 cycling plotted with respect to cycle time, both peaks exhibit sharp drop-offs post wet phases. The α or γ regioisomer identities of the (**gE**)$_2$ species were unable to be assigned due to suspected strong overlap of the two species in the HPLC. Briefly, the native α-linked and side chain linked 2-mers of **aD** form in similar abundances following dry phase 1—slightly favoring the α-species (likely due to ROP, Figure 3A). In the case of (**gE**)$_2$, no such trend is present. Out of caution, we cannot definitively assign distinct regioisomers for (**gE**)$_2$. The closely eluting peak contains masses consistent with a diastereomer of (**gE**)$_2$, as well as a side product (in brackets, sequence not implied).

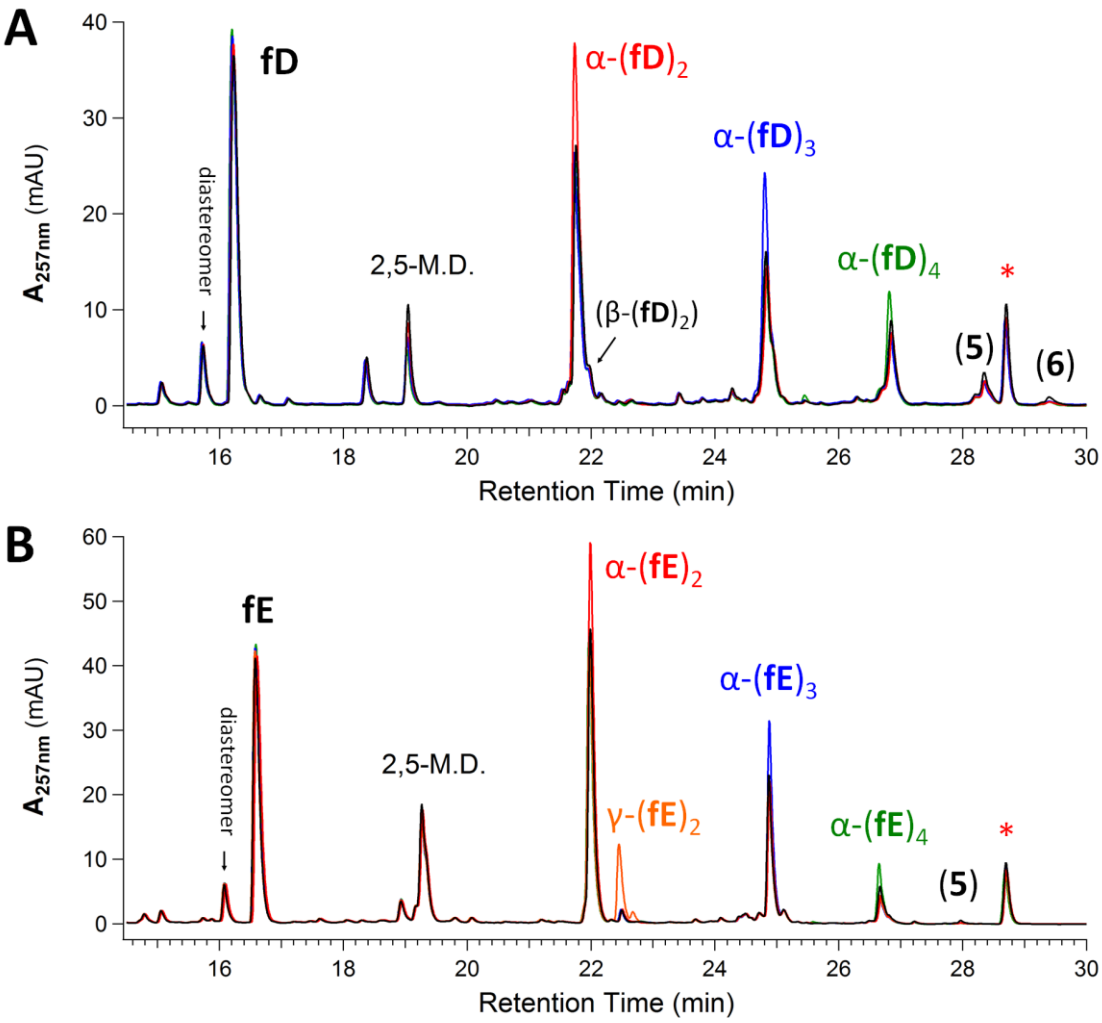

Figure S26. Synthetic standards confirm α-linked depsipeptides dominate product mixtures of dried fD and fE. Black traces: HPLC chromatograms for 10 mM (A) **fD** and (B) **fE** dried for 9 days at 75 °C with 1 equivalent of 2-hydroxypyridine (2HP) to mitigate precipitation as a drydown additive. Colored traces: Synthetic α-linked depsipeptide standards for α-(**fD**)$_n$ and α-(**fE**)$_n$ were spiked into the drydown mixtures and run on HPLC to confirm retention times of native α-linked species. Orange trace in (B) indicates synthetic γ-(**fE**)$_2$ spike, exemplifying the dominance of the native α-ester formation over the side chain ester formation. Species in parentheses were identified using LCMS and no synthetic standards were prepared. Red asterisk indicates PCR tube plasticizer leachate present in all dry-heated samples, consistently eluting at 28.8 minutes using our column and methods.

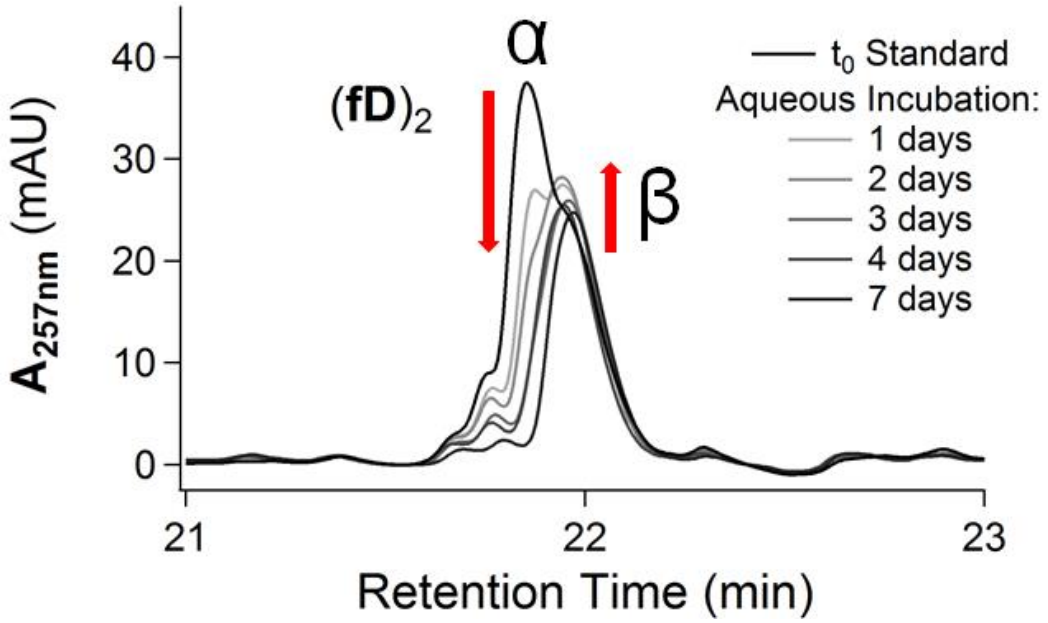

Figure S27. fD 2-mer degradation profile and identification. HPLC chromatogram focused in on the 2-mer region for 10 mM **fD** dried for 9 days at 75 °C with 1 equivalent of 2-hydroxypyridine to prevent precipitation during drydown (Black trace, t_0). Samples then subject to room temperature, pH 7 aqueous incubation for up to 7 days to show degradation profile (Grey-dark grey traces). Native α-linked 2-mer decays rapidly, in agreement with its assignment in Figure S26. β-(**fD**)$_2$ displays the expected brief increase in abundance during incubation (Similar to β-(**aD**)$_2$ in Figure 4B), lending confidence to its regioisomer assignment. Note that these **fD** 2-mers were generated using different conditions than those shown in the main text.

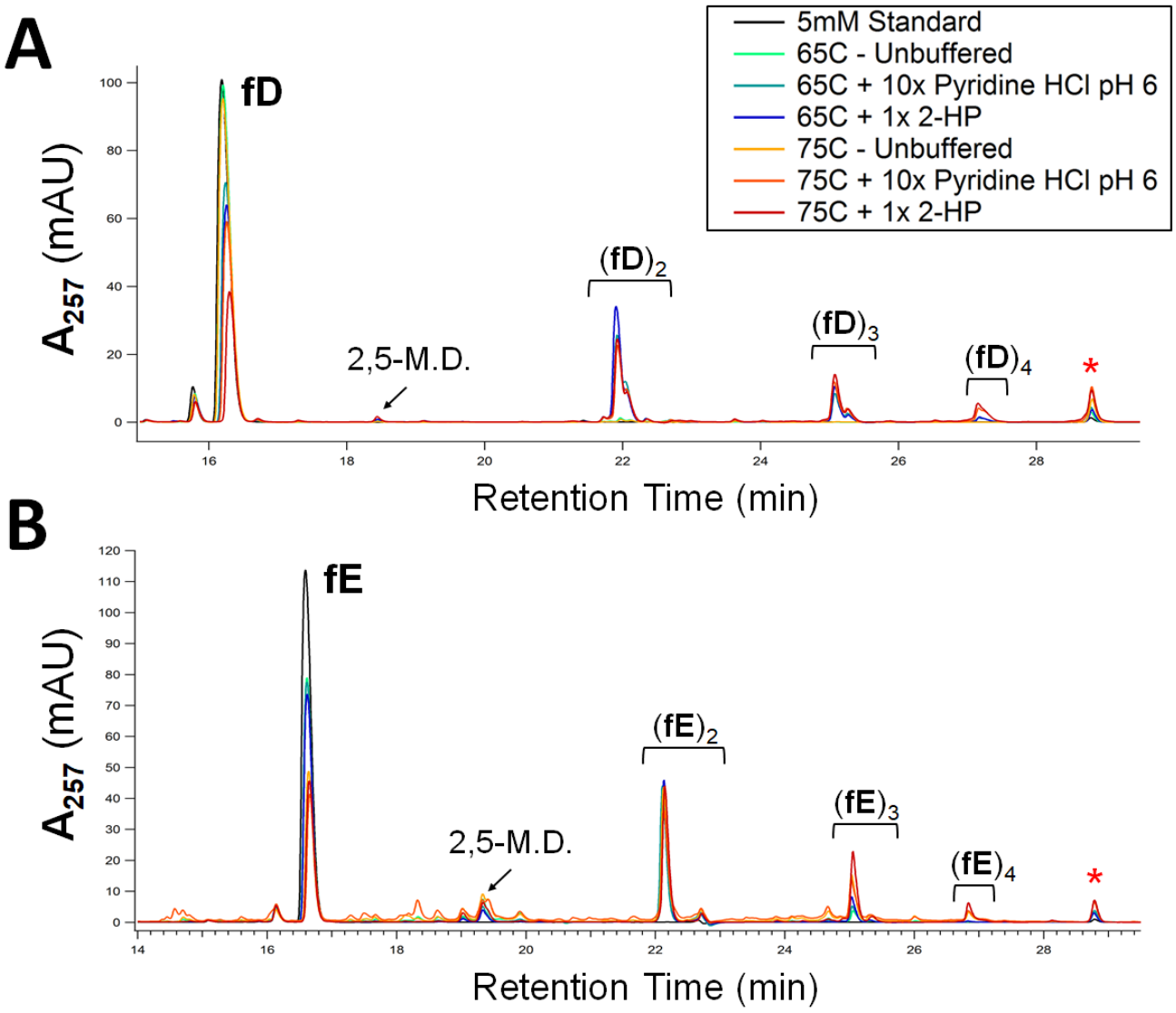

Figure S28. Heterocyclic additives assist dry-heating polymerizations for fD and fE. HPLC chromatograms of 5 mM (A) **fD** and (B) **fE** dried for 7 days at the given temperature, with or without heterocyclic additives pyridine HCl (adjusted to pH 6) or 2-hydroxypyridine (2-HP) added to the solutions prior to dry-heating. In the absence of additives ("unbuffered"), **fD** (A) exhibits almost no polymerization—a condition we ascribed to the sample reaching a solid, semi-crystalline state as the solvent evaporated away. Additives appear to facilitate molecular mobility by imparting a mixed melting point depression, apparently having a lower melting temperature than that of solid **fD** or **fE** themselves. Heavy side product formation for unbuffered and pyridine-buffered **fE** samples (B, raised baselines *e.g.* yellow & orange traces) appears to be mitigated by addition of 2-HP. The specific additives do not appear to alternative or side chain selectivity in depsipeptide formation. Red asterisk indicates PCR tube plasticizer leachate present in all dry-heated samples, consistently eluting at 28.8 minutes using our column and methods.

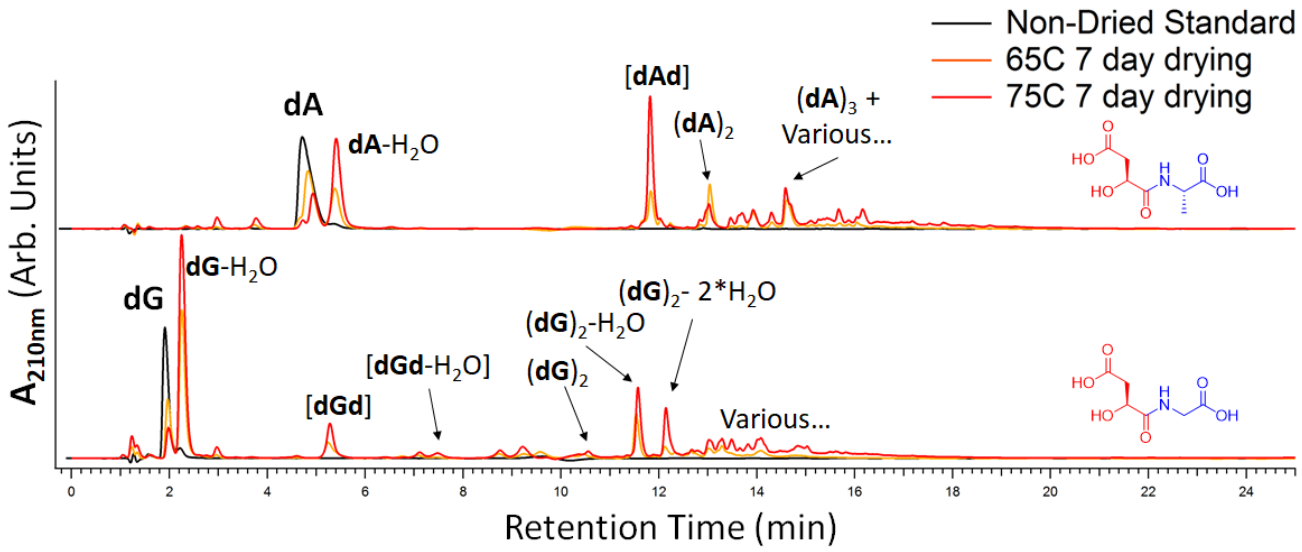

Figure S29. Malic acid in building blocks results in side product accumulation following dry-heating. HPLC-UV traces for unbuffered 7-day heating and drying of building blocks containing **d**: **dA** (top), **dG** (bottom), 10 mM. We observe formation of many overlapping side products with a variety of masses that are difficult to assign by LCMS, and few of the expected polymer products formed. A small number of assignments by mass are shown, with [brackets] indicating the sequence is uncertain, but the found mass matches with the given dehydration polymer. An additional '-H_2O' indicates an additional water loss beyond that which would be expected for the given sequence. Profuse side product formation could be a result of any or more of the following: 1) Intramolecular acyl transfer leading to anhydride formation followed by cleavage of the amide bond.[5] 2) Elimination of the α-hydroxyl group to form an α,β-unsaturated carbonyl: fumaric or maleic acid at the O-terminus.[6, 7] Note that the reverse reaction would racemize the α-stereocenter and lead to more side product formation. 3) Intramolecular succinimide formation, known more commonly as an aspartimide formation.[8]

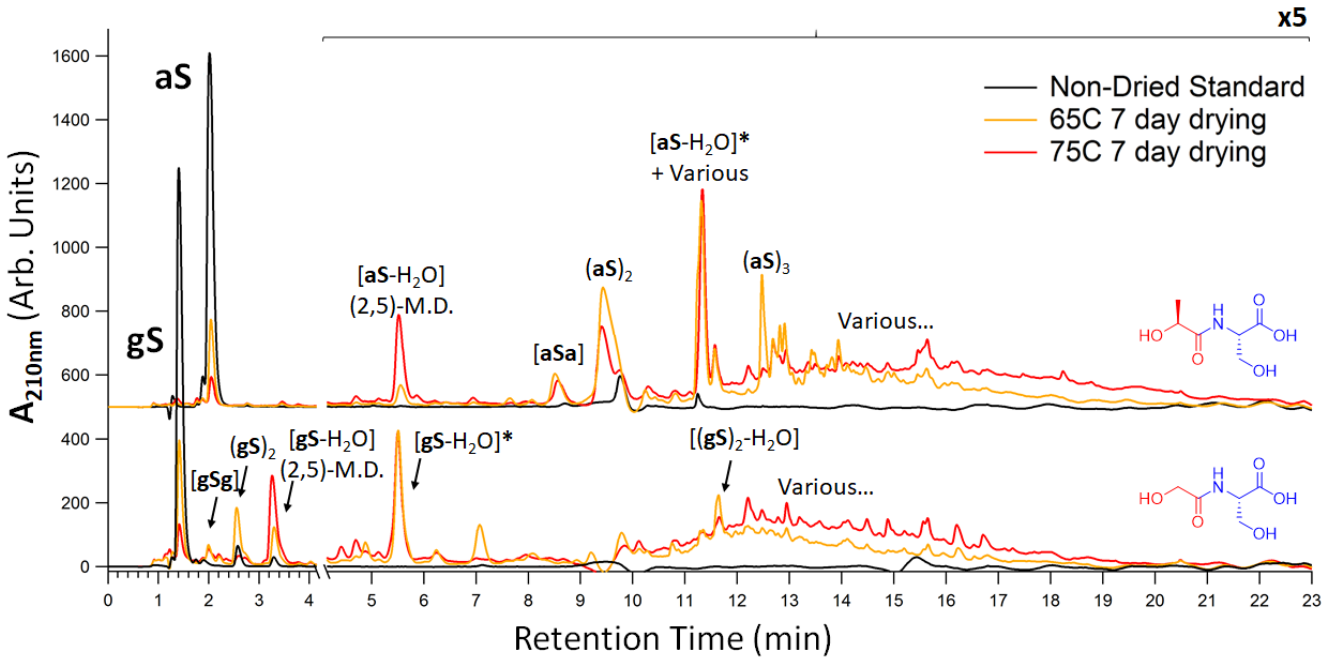

Figure S30. Extensive side product formation when serine is a component in building blocks. HPLC traces for **gS** and **aS** following unbuffered 7-day heating and drying at 10 mM. Many side products are present, with masses difficult to assign by LCMS. A small number of assignments by mass are shown, with [brackets] indicating the sequence is uncertain, but the found mass matches with the given dehydration polymer. An additional '-H_2O' indicates an additional water loss beyond that which would be expected for the given sequence. *Asterisk indicates a building block whose serine β-hydroxyl group may have been eliminated to form dehydroalanine. Profuse side product formation could be a result of any or more of the following: 1) β-elimination of the **S** hydroxyl group to form dehydroalanine (known to occur in biological proteins) and subsequent reactivity of this moiety.[9, 10] 2) the β-hydroxyl group may undergo an *N*,*O*-acyl shift with the neighboring amide, as has been observed in proteins under physiological conditions.[11, 12]

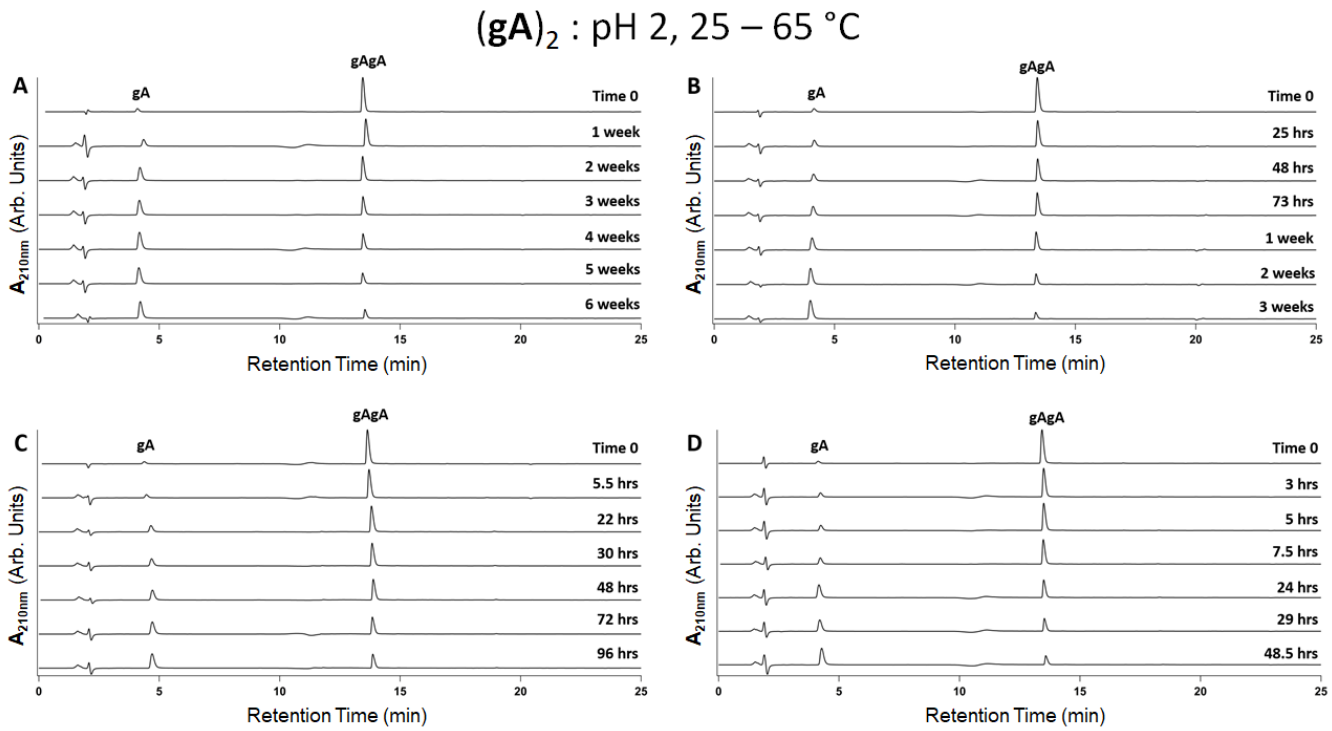

Figure S31. HPLC traces used for integration and depolymerization kinetics. Time-dependent degradation of $(\mathbf{gA})_2$ during prolonged wet phases at pH 2. Temperatures: (A) 25, (B) 37, (C) 50, (D) 65 °C.

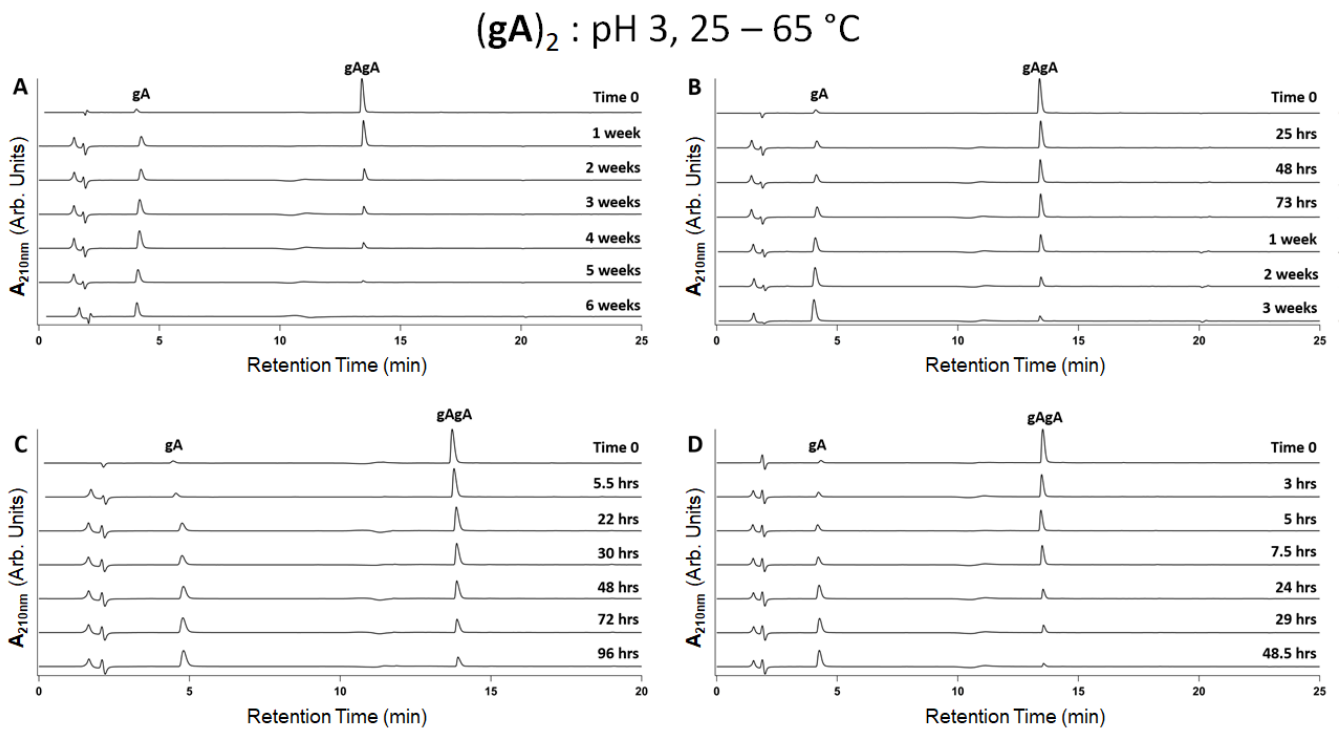

Figure S32. HPLC traces used for integration and depolymerization kinetics. Time-dependent degradation of $(\mathbf{gA})_2$ during prolonged wet phases at pH 3. Temperatures: (A) 25, (B) 37, (C) 50, (D) 65 °C.

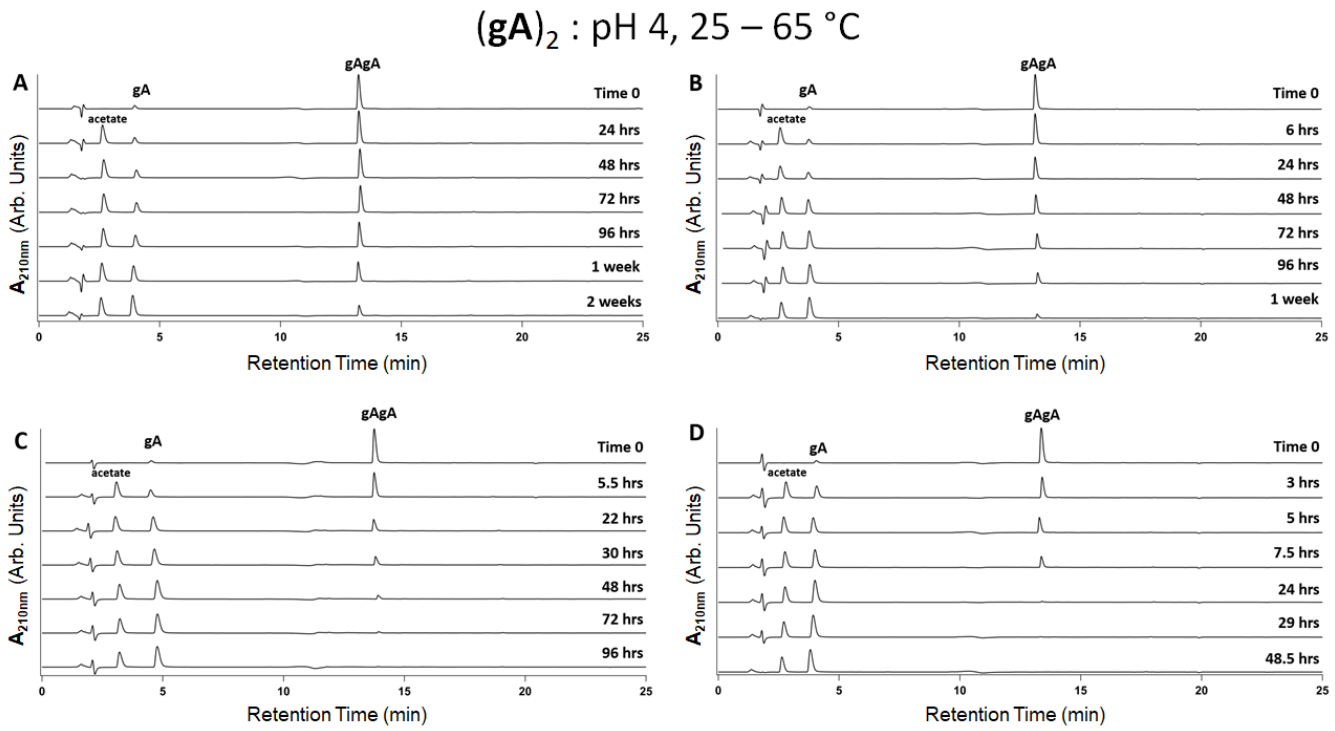

Figure S33. HPLC traces used for integration and depolymerization kinetics. Time-dependent degradation of $(\mathbf{gA})_2$ during prolonged wet phases at pH 4. Temperatures: (A) 25, (B) 37, (C) 50, (D) 65 °C.

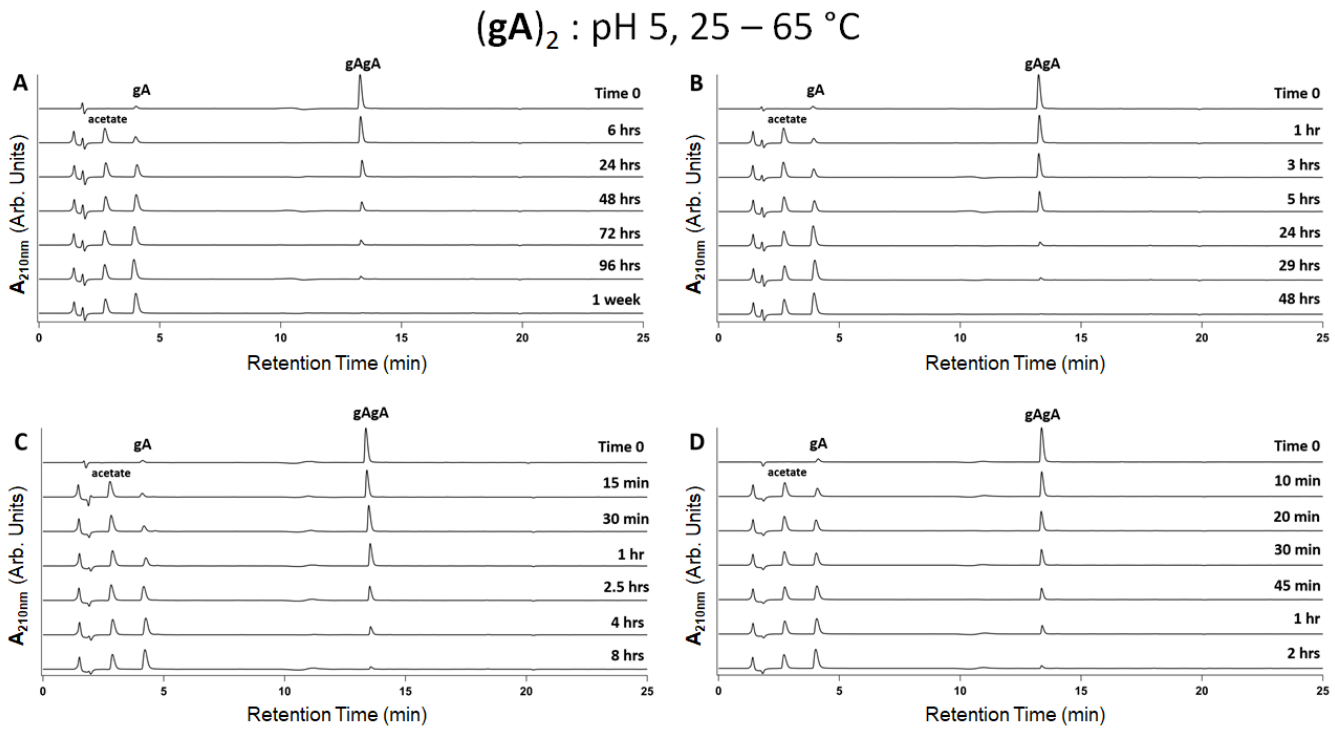

Figure S34. HPLC traces used for integration and depolymerization kinetics. Time-dependent degradation of (**gA**)$_2$ during prolonged wet phases at pH 5. Temperatures: (A) 25, (B) 37, (C) 50, (D) 65 °C.

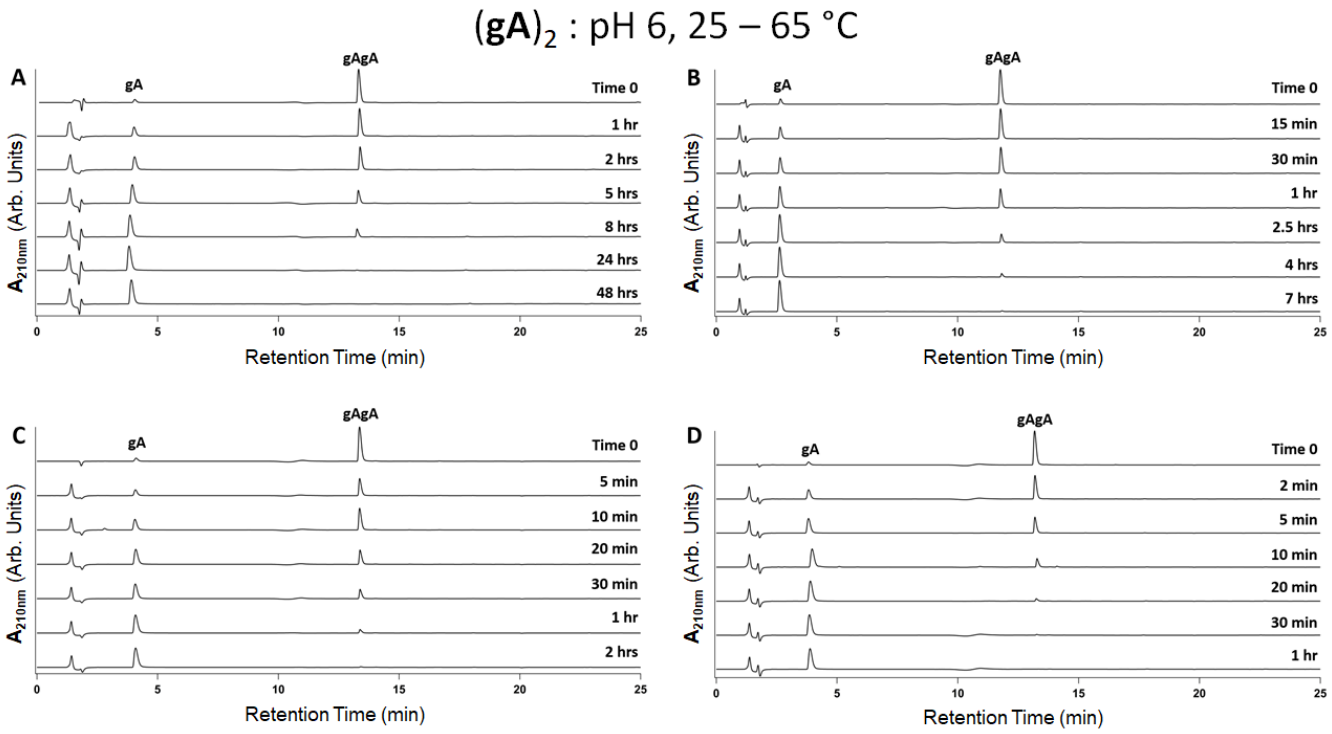

Figure S35. HPLC traces used for integration and depolymerization kinetics. Time-dependent degradation of (**gA**)$_2$ during prolonged wet phases at pH 6. Temperatures: (A) 25, (B) 37, (C) 50, (D) 65 °C.

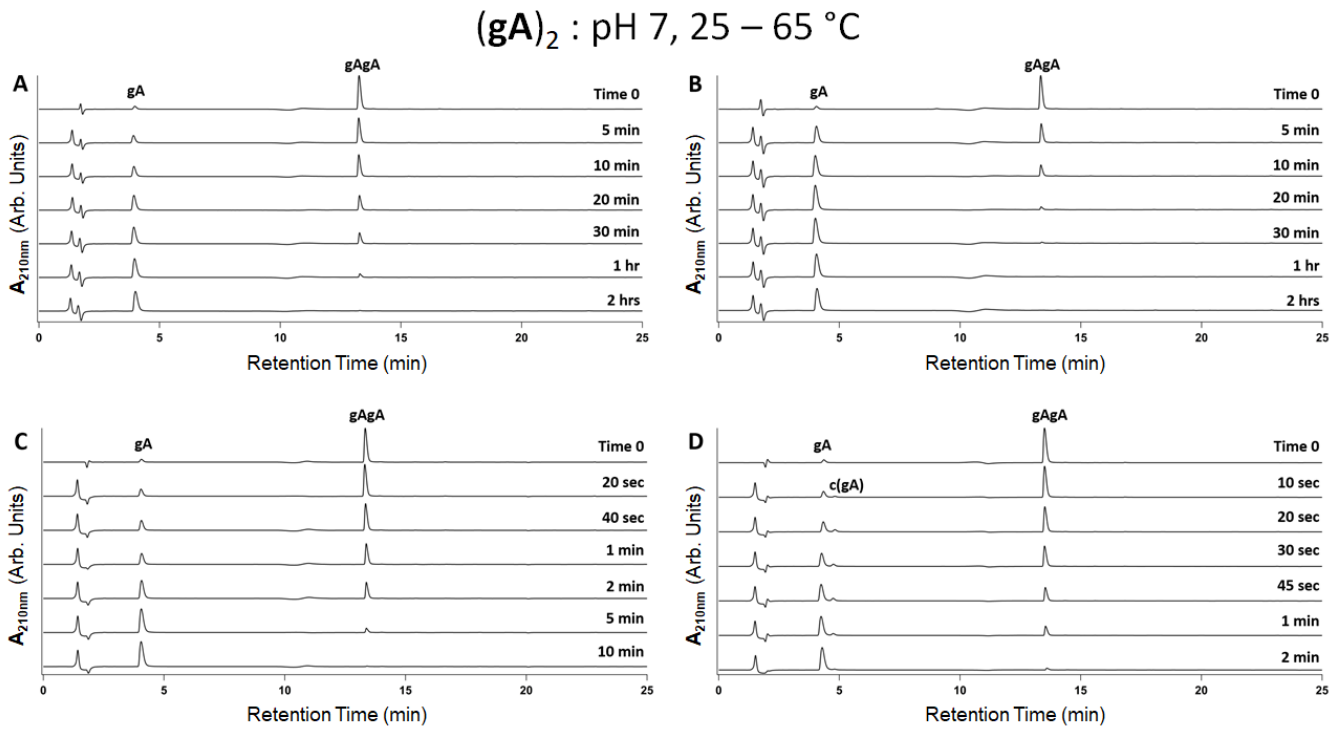

Figure S36. HPLC traces used for integration and depolymerization kinetics. Time-dependent degradation of (**gA**)$_2$ during prolonged wet phases at pH 7. Temperatures: (A) 25, (B) 37, (C) 50, (D) 65 °C.

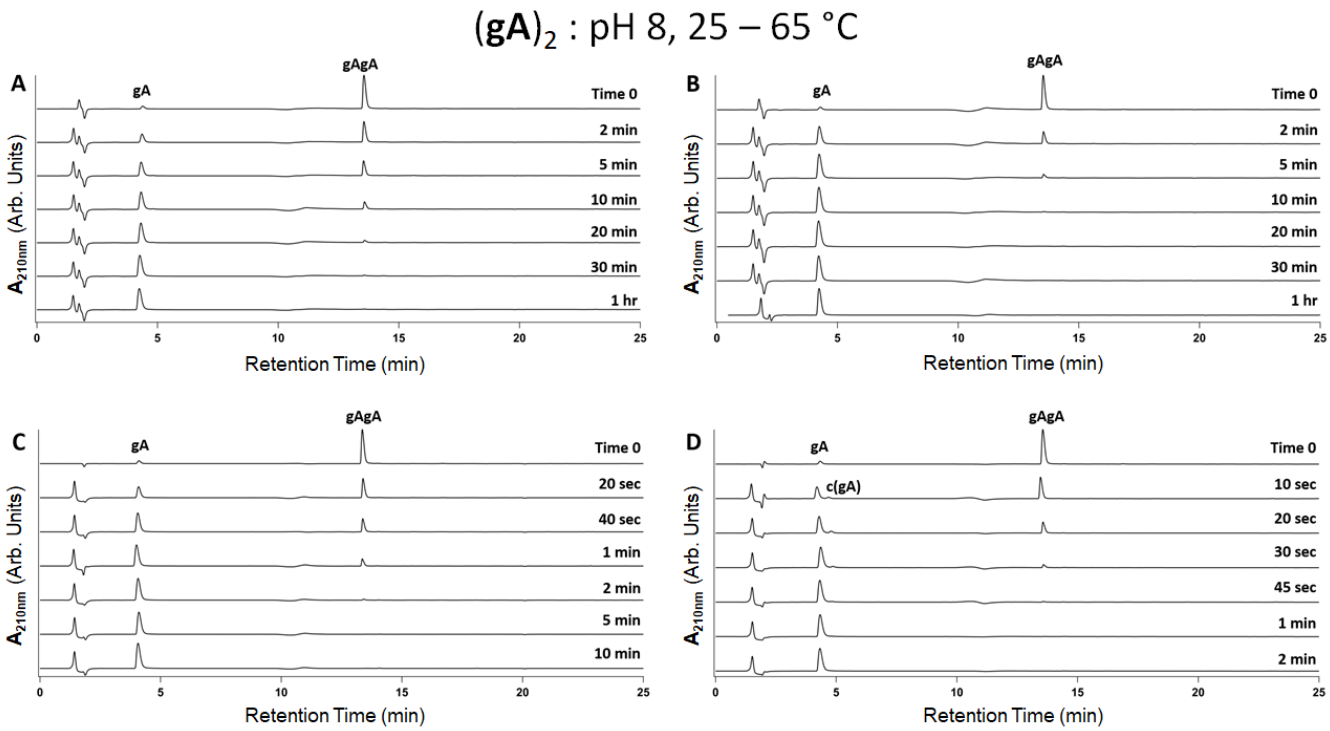

Figure S37. HPLC traces used for integration and depolymerization kinetics. Time-dependent degradation of $(\mathbf{gA})_2$ during prolonged wet phases at pH 8. Temperatures: (A) 25, (B) 37, (C) 50, (D) 65 °C.

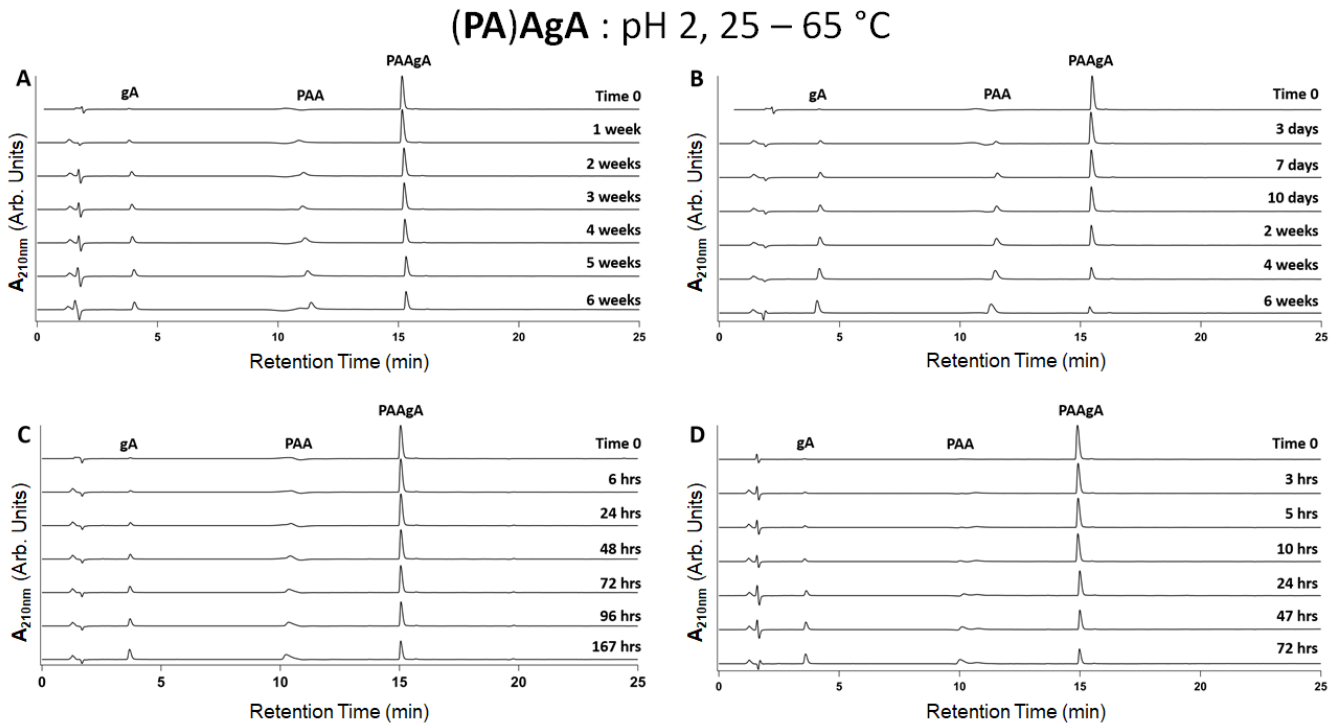

Figure S38. HPLC traces used for integration and depolymerization kinetics. Time-dependent degradation of (**PA**)**AgA** during prolonged wet phases at pH 2. Temperatures: (A) 25, (B) 37, (C) 50, (D) 65 °C.

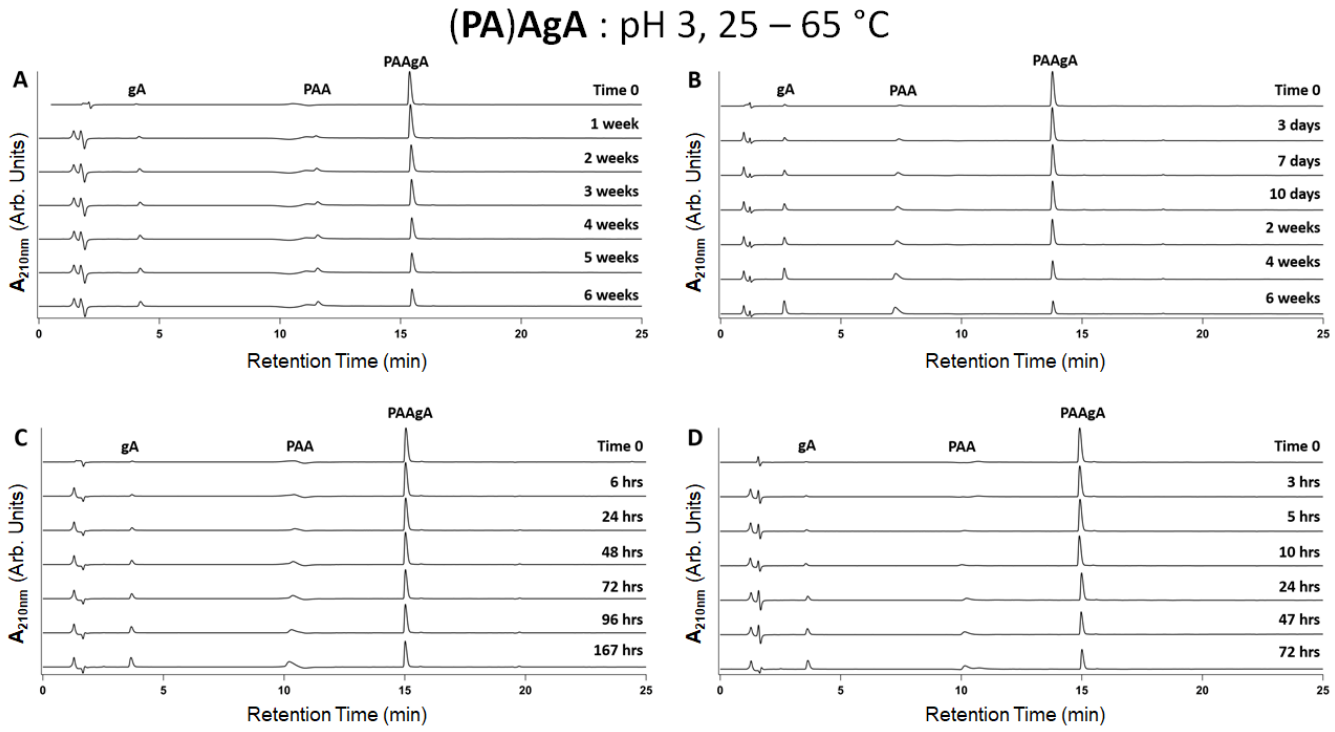

Figure S39. HPLC traces used for integration and depolymerization kinetics. Time-dependent degradation of (**PA**)**AgA** during prolonged wet phases at pH 3. Temperatures: (A) 25, (B) 37, (C) 50, (D) 65 °C.

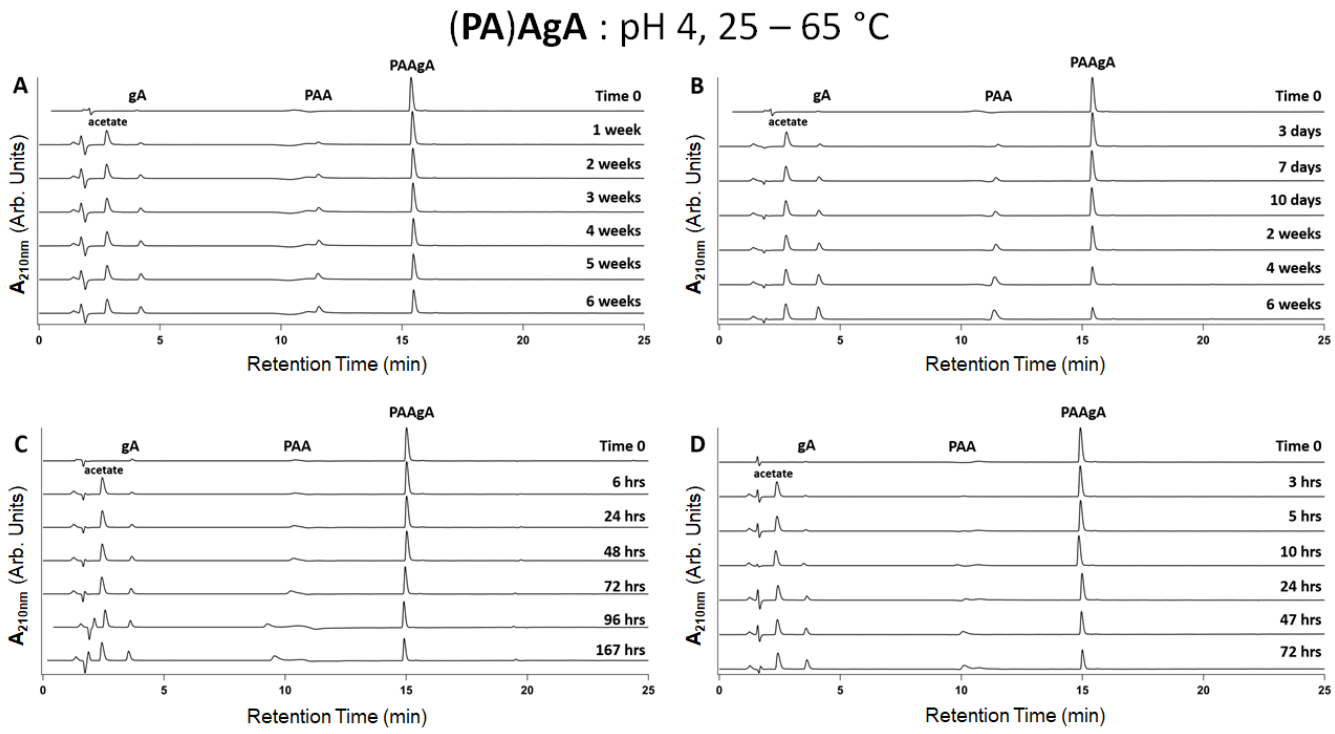

Figure S40. HPLC traces used for integration and depolymerization kinetics. Time-dependent degradation of (**PA**)**AgA** during prolonged wet phases at pH 4. Temperatures: (A) 25, (B) 37, (C) 50, (D) 65 °C.

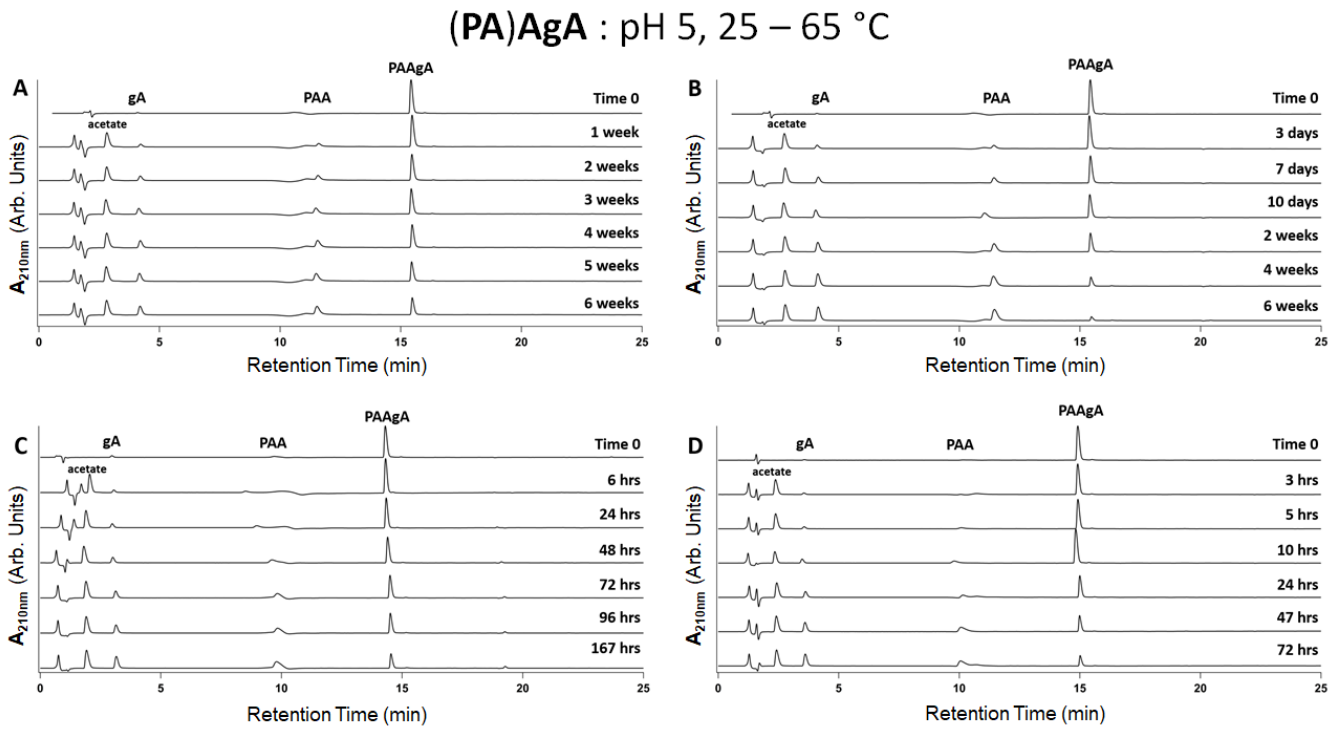

Figure S41. HPLC traces used for integration and depolymerization kinetics. Time-dependent degradation of (**PA**)**AgA** during prolonged wet phases at pH 5. Temperatures: (A) 25, (B) 37, (C) 50, (D) 65 °C.

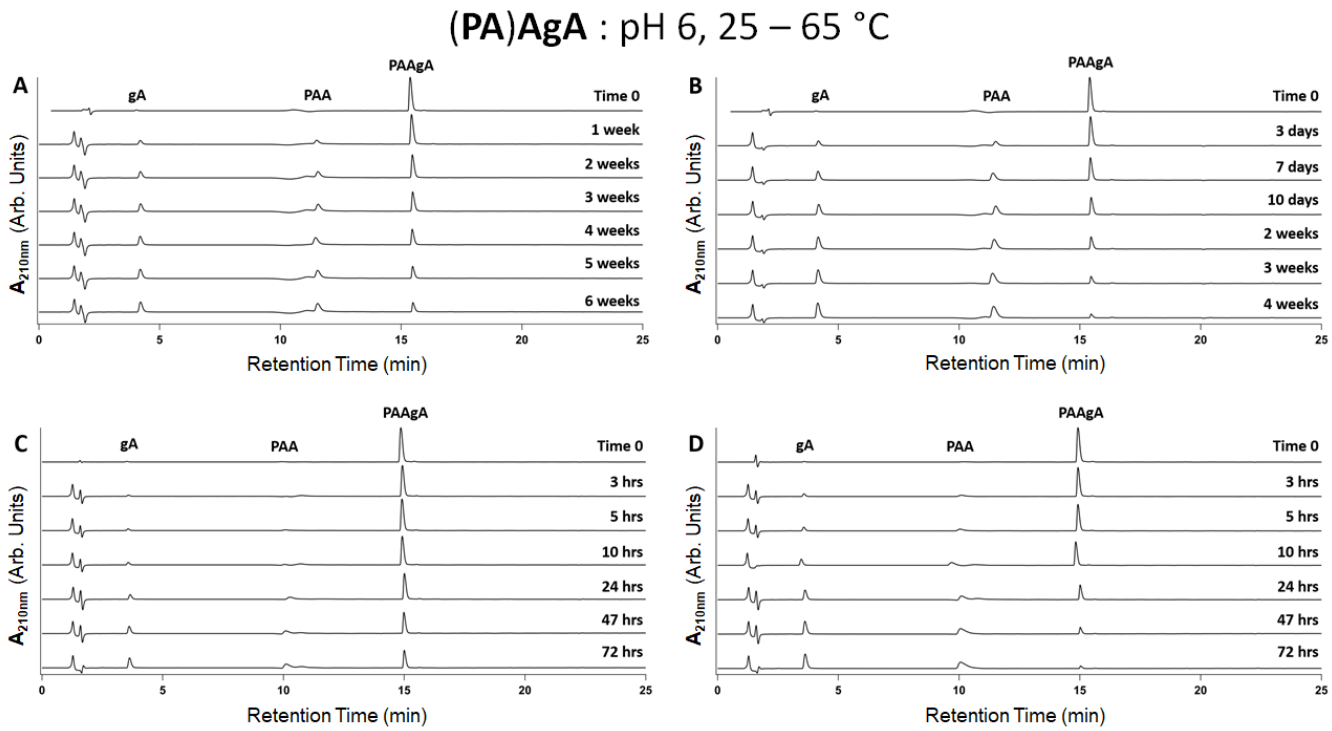

Figure S42. HPLC traces used for integration and depolymerization kinetics. Time-dependent degradation of (**PA**)**AgA** during prolonged wet phases at pH 6. Temperatures: (A) 25, (B) 37, (C) 50, (D) 65 °C.

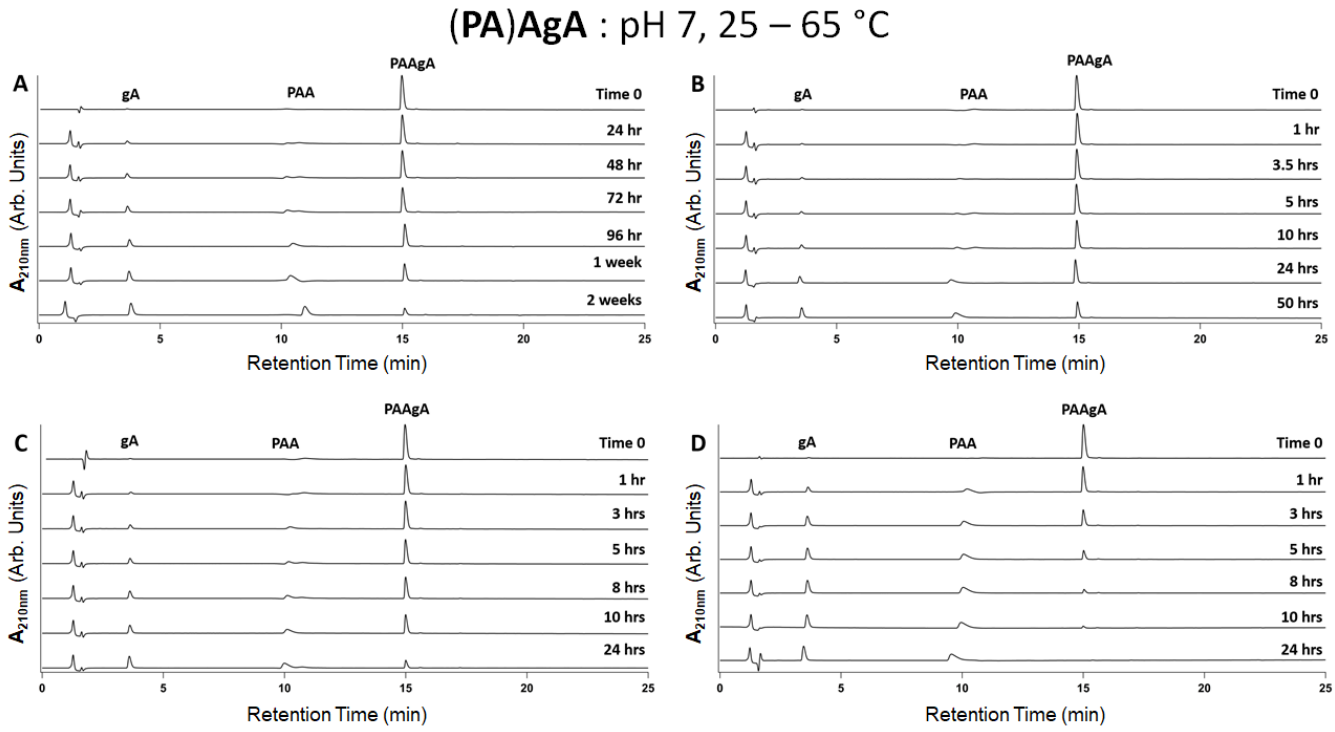

Figure S43. HPLC traces used for integration and depolymerization kinetics. Time-dependent degradation of (**PA**)**AgA** during prolonged wet phases at pH 7. Temperatures: (A) 25, (B) 37, (C) 50, (D) 65 °C.

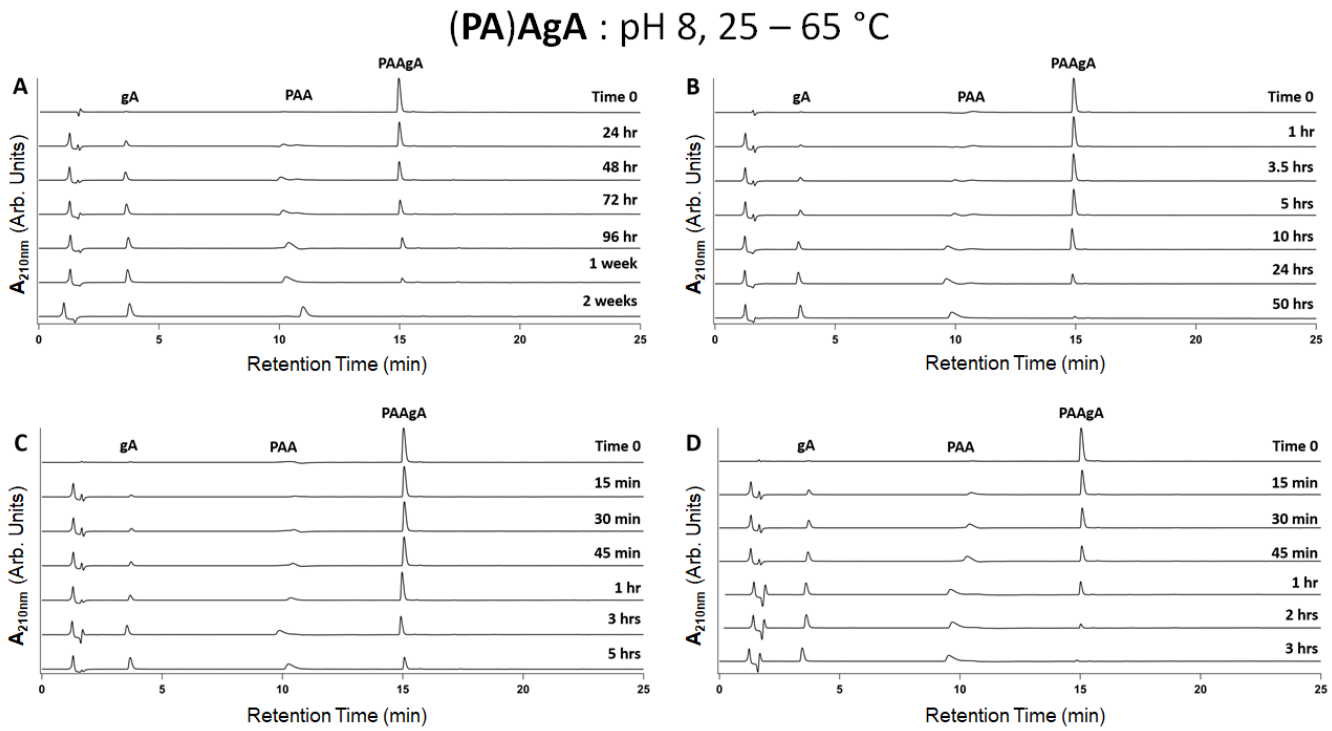

Figure S44. HPLC traces used for integration and depolymerization kinetics. Time-dependent degradation of (**PA**)**AgA** during prolonged wet phases at pH 8. Temperatures: (A) 25, (B) 37, (C) 50, (D) 65 °C.

Kinetic Model for Depolymerization

1.1. Kinetic Modeling Parameters

To elucidate the mechanisms of ester depolymerization, a kinetic model was fit to concentration data for (**gA**)$_2$ and (**PA**)**AgA**, at various temperatures and pH values. The HPLC data were quantified to estimate the concentration at representative time points, by integrating the peak areas with Gaussian fits using Igor Pro v 6.37. The HPLC data can be found in Supplementary Figures S30-S44. These areas are related to concentrations according to the Beer-Lambert Law in Eq. (0).

$$A = \varepsilon bc \tag{0}$$

A is absorbance (which in this case is the integrated peak area); ε is the molar extinction coefficient; b is the path length, and c is the concentration.

The depsipeptide (**gA**)2 can undergo either scission (hydrolysis), with rate constant k_{sc}, or it can undergo intramolecular attack, with backbiting rate constant k_{bb}:

$$\frac{d[(gA)_2]}{dt} = -(k_{sc} + k_{bb})\ [(gA)_2] \tag{1}$$

It is not possible to independently estimate these two rate constants based on the (**gA**)$_2$ data, so experiments were also conducted using (**PA**)**AgA**, which can undergo ester scission but not backbiting. The (**PA**)**AgA** data was fit to the following mathematical model to estimate k_{sc}:

$$\frac{d[(PA)AgA]}{dt} = -k_{sc}\,[(PA)AgA] \tag{2}$$

and then k_{bb} was estimated from the (**gA**)$_2$ data. We used MATLAB's ode15s function to integrate the differential equations, and MATLAB's patternsearch function to calculate the values of the two rate constants that minimize the sum squared error (SSE). Supplementary Table S1 shows the optimized rate constants. Table 1 in the main manuscript presents the corresponding half-lives for (**gA**)$_2$ and (**PA**)**AgA**:

$$t_{1/2}^{(gA)_2} = \frac{\ln(2)}{k_{sc} + k_{bb}} \tag{3}$$

$$t_{1/2}^{(PA)AgA} = \frac{\ln(2)}{k_{sc}} \tag{4}$$

1.2. Experimental Conditions Tested

- pH: 2-8 in 1 unit intervals
- Time Scale: varies depending on the rate of depolymerization
- Temperature (°C): 25, 37, 50, 65
- Experiments performed as described in Experimental methods, using 40 μL volumes and the concentrations were 10 mM in **gA** building block.
- HPLC data taken after each incubation experiment was completed

	k_{bb} ((**gA**)$_2$ Only)						
T (°C)	**pH: 2**	**3**	**4**	**5**	**6**	**7**	**8**
25	0.0005	0.0008	0.0043	0.0154	0.2483	1.101	3.945
37	0.0013	0.0018	0.0102	0.0540	0.5145	5.850	31.05
50	0.0051	0.0100	0.0241	0.2340	0.9060	22.66	66.20
65	0.0128	0.0172	0.1157	0.8295	4.187	62.19	99.32
	k_{sc} (both (**gA**)$_2$ & (**PA**)**AgA**)						
25	0.0005	0.0003	0.0004	0.0007	0.0009	0.0078	0.0154
37	0.0009	0.0005	0.0008	0.0012	0.0016	0.0134	0.0290
50	0.0040	0.0030	0.0025	0.0044	0.0083	0.0492	0.2022
65	0.0074	0.0076	0.0074	0.0139	0.0235	0.1496	0.7919

Table S1. Backbiting and Scission Rate Constants for both (gA)$_2$ and (PA)AgA. Backbiting (bb) and Scission (sc). Units in h^{-1}.

1.3. Sample Model Fits for (PA)AgA

Figure S44 shows the prediction results for depolymerization of (**PA**)**AgA**. Recall that this figure is the best possible fit when optimizing the scission rate constant because scission is the only relevant depolymerization mechanism in (**PA**)**AgA**. Note the half-life of approximately 25-30 hours, which is consistent with the value reported in Table 1.

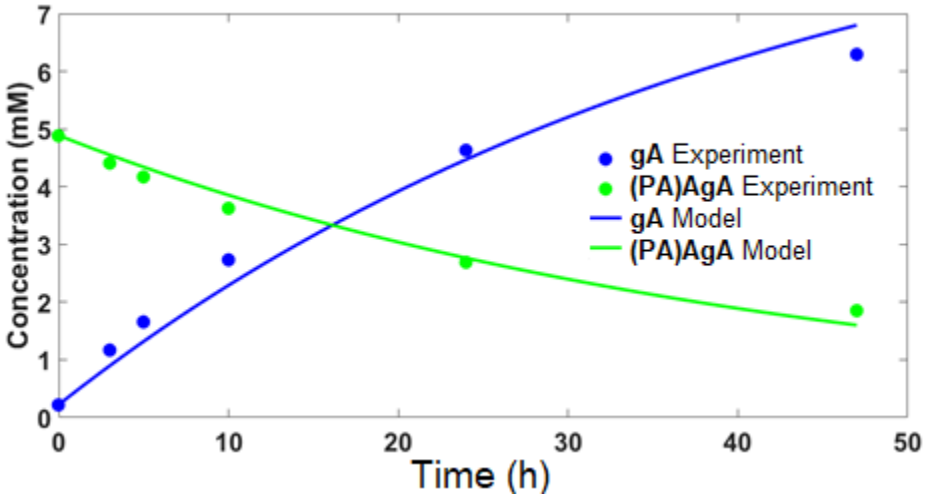

Figure S45. Model fit of (PA)AgA depolymerization at pH 6, 65 °C

The rate constants for both (**gA**)$_2$ and (**PA**)**AgA** depolymerization were plotted and fit to an Arrhenius equation (of the form $y = mx + b$) to demonstrate overarching relationships in pH-dependence for both the backbiting and the random scission processes. These results are displayed in Figure S45.

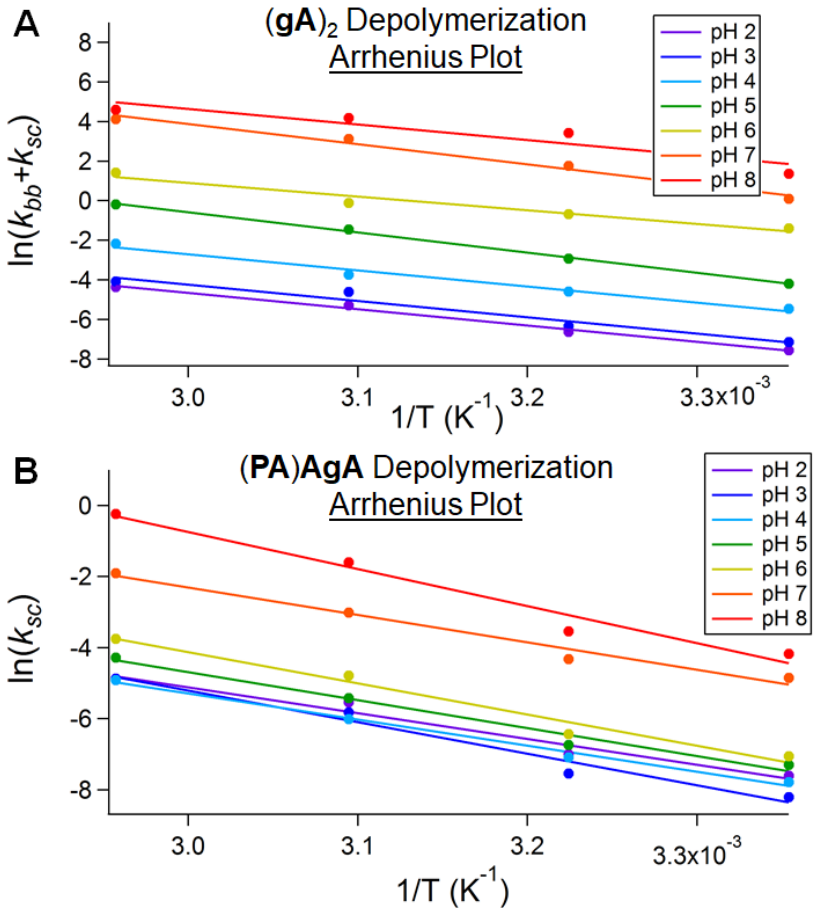

Figure S46. Arrhenius Plots for depolymerization rate constants at various pH values. (A) (**gA**)$_2$ and (B) (**PA**)**AgA** depolymerization. Lines: Arrhenius model fit; points: raw data.

1.4. Percentage Depolymerization of Polymers

This section aims to quantify the percentage of backbiting and random scission of (**gA**)$_2$ at the various temperatures and pH values. Using the depolymerization data obtained above, we can estimate the fraction for each process (backbiting or scission) by comparing the relative proportions of the rate constants compared to their sum, as seen below in Eqs. (5-6):

$$\%\ contribution\ of\ backbiting = \frac{k_{bb}}{k_{sc} + k_{bb}} \tag{5}$$

$$\%\ \text{contribution of scission} = \frac{k_{sc}}{k_{sc} + k_{bb}} \tag{6}$$

where k is the rate constant (either backbiting (k_{bb}) or random scission (k_{sc}) as displayed in Table S1). The results are displayed in Table S2.

Table S2. $(gA)_2$ depolymerization contributions. Contributions from backbiting (top) and scission (bottom). Values calculated from totals in Table S1. Cell color scale depicted below each data set.

Percent Contribution of Backbiting

T (°C)	pH: 2	3	4	5	6	7	8
25	51.7	74.4	91.2	95.8	99.7	99.3	99.6
37	59.4	77.0	92.4	97.8	99.7	99.8	99.9
50	56.2	77.0	90.7	98.1	99.1	99.8	99.7
65	63.2	69.2	94.0	98.4	99.4	99.8	99.2
Scale (%)	50.0	58.0	66.0	75.0	84.0	92.0	100.0

Percent Contribution of Scission (hydrolysis)

T (°C)	pH: 2	3	4	5	6	7	8
25	48.3	25.6	8.83	4.21	0.35	0.71	0.39
37	40.6	23.0	7.59	2.15	0.31	0.23	0.09
50	43.8	23.0	9.30	1.86	0.91	0.22	0.30
65	36.8	30.8	6.00	1.65	0.56	0.24	0.79
Scale (%)	50.0	42.0	34.00	25.00	16.00	8.00	0.00

References

1. Yu, S.-S.; Solano, M. D.; Blanchard, M. K.; Soper-Hopper, M. T.; Krishnamurthy, R.; Fernández, F. M.; Hud, N. V.; Schork, F. J.; Grover, M. A., Elongation of model prebiotic proto-peptides by continuous monomer feeding. *Macromolecules* **2017,** *50* (23), 9286-9294.

2. Zhao, Y.; Li, J.; Yu, H.; Wang, G.; Liu, W., Synthesis and characterization of a novel polydepsipeptide contained tri-block copolymer (mPEG–PLLA–PMMD) as self-assembly micelle delivery system for paclitaxel. *International journal of pharmaceutics* **2012,** *430* (1-2), 282-291.

3. Ohya, Y.; Yamamoto, H.; Nagahama, K.; Ouchi, T., Effects of polydepsipeptide side-chain groups on the temperature sensitivity of triblock copolymers composed of polydepsipeptides and poly (ethylene glycol). *Journal of Polymer Science Part A: Polymer Chemistry* **2009,** *47* (15), 3892-3903.

4. Blake, J. F.; Chicarelli, M. J.; Garrey, R. F.; Gaudino, J.; Grina, J.; Moreno, D. A.; Mohr, P. J.; Ren, L.; Schwarz, J.; Chen, H., Serine/Threonine Kinase Inhibitors. Google Patents: 2017.

5. Joshi, A. B.; Sawai, M.; Kearney, W. R.; Kirsch, L. E., Studies on the mechanism of aspartic acid cleavage and glutamine deamidation in the acidic degradation of glucagon. *Journal of Pharmaceutical Sciences* **2005,** *94* (9), 1912-1927.

6. Kajiyama, T.; Kobayashi, H.; Taguchi, T.; Kataoka, K.; Tanaka, J., Improved synthesis with high yield and increased molecular weight of poly (α, β-malic acid) by direct polycondensation. *Biomacromolecules* **2004,** *5* (1), 169-174.

7. Mamajanov, I.; MacDonald, P. J.; Ying, J.; Duncanson, D. M.; Dowdy, G. R.; Walker, C. A.; Engelhart, A. E.; Fernández, F. M.; Grover, M. A.; Hud, N. V., Ester formation and hydrolysis during wet–dry cycles: generation of far-from-equilibrium polymers in a model prebiotic reaction. *Macromolecules* **2014,** *47* (4), 1334-1343.

8. Bodanszky, M.; Natarajan, S., Side reactions in peptide synthesis. II. Formation of succinimide derivatives from aspartyl residues. *The Journal of Organic Chemistry* **1975,** *40* (17), 2495-2499.

9. Samuel, D.; Silver, B. L., 46. Elimination reactions and hydrolysis of serine phosphate. *Journal of the Chemical Society (Resumed)* **1963**, 289-296.

10. Sen, L. C.; Gonzalez-Flores, E.; Feeney, R. E.; Whitaker, J. R., Reactions of phosphoproteins in alkaline solutions. *Journal of Agricultural and Food Chemistry* **1977,** *25* (3), 632-638.

11. Noren, C. J.; Wang, J.; Perler, F. B., Dissecting the chemistry of protein splicing and its applications. *Angewandte Chemie International Edition* **2000,** *39* (3), 450-466.

12. Lyons, B.; Jamie, J.; Truscott, R. J., Spontaneous cleavage of proteins at serine residues. *International Journal of Peptide Research and Therapeutics* **2011,** *17* (2), 131-135.